2019

Oxytocin, Dopamine, and the Neuromodulation of Mating Behavior in C. Elegans

Meghan Aileen Lockard

OXYTOCIN, DOPAMINE, AND THE NEUROMODULATION OF MATING BEHAVIOR IN *C. ELEGANS*

A Thesis Presented to the Faculty of

The Rockefeller University

in Partial Fulfillment of the Requirements for

the degree of Doctor of Philosophy

by

Meghan Aileen Lockard

June 2019

OXYTOCIN, DOPAMINE, AND THE NEUROMODULATION OF MATING BEHAVIOR IN *C. ELEGANS*

Meghan Aileen Lockard, Ph.D.

The Rockefeller University 2019

FORWARD: *This is Water*[1].

"What a chimera then is man! What a novelty!
What a monster, what a chaos, what a contradiction, what a prodigy!
Judge of all things, imbecile worm of the earth;
depositary of truth, a sewer of uncertainty and error;
the pride and garbage of the universe!"
-Blaise Pascal, Pensees #434

The plot arc of Thomas Mann's *The Magic Mountain*[2] mirrors the writing process of its author. Hans Castrop, the novel's protagonist, is a perfectly healthy man at the beginning of the book. He plans to visit his cousin in a tuberculosis sanitarium for 3 weeks…and ends up staying 7 years. By the end of his stay, Castrop is fever-stricken and has a spot on his lung, perhaps real and perhaps imaginary. Thomas Mann himself first set out to write a short story. By the end of *The Magic Mountain,* he ended up writing a sprawling tome of more than 1,200 pages.

I often think of Castrop when I ask myself, why would someone with no academic ambitions spend more than 7 years at a high-powered research institute working toward a Ph.D. in Neural Circuits and Behavior? Why did someone without tuberculosis spend 7 years in a sanitarium? Like Castrop, I did so because I fell in love. Castrop falls in love

[1] The subtitle of this section is borrowed from David Foster Wallace's last commencement "Howdy boys! How's the Water?" After he departs, the two younger fish look at each other, while one asks, "What is Water?" I love that joke. I love that speech.
[2] Mann, T. *The Magic Mountain.* Tr. H. T. Lowe-Porter. Victoria, BC., Canada : Dead Authors Society, 2016, 1924.

with a pair of "Kirghiz- shaped eyes" belonging to the estranged wife of a Russian officer. I fell in love with the Ethologist's eye: the viewpoint that our innate instincts, motivations, and drives, are both common in mechanism between ourselves and other animals generally, and that they are primal to everything we feel, think, say, and do.

Also, like Castrop, this love was not a recent development, but was prefigured during my early school years by a chance encounter. For him, it was an attractive Russian schoolmate who once handed him a pencil. For me it was Helen Keller's memoir *The Story of My Life*[3]. At the age of ten, my father gave it to me because I was trying out for the role of Helen in the local community theatre's production of *The Miracle Worker*[4]. I didn't get the part (small town politics), but what I did receive from Helen's story awakened something in "…my soul, gave it light, hope, joy, set it free!"

For those who are not familiar with her story, Helen goes deaf and blind as an infant after contracting scarlet fever. In Chapter 4, she describes the moment her teacher Anne Sullivan led her to the "wellspring of language." They were out walking by a stream when Anne reaches one of Helen's hands into the waters and signs W-A-T-E-R into the other. In this moment for the first time Helen connects the word "water" as signifying the substance she is feeling. She describes it "…as if Anne had shown [her] the location of a spring within herself out of which flowed a stream… that nourished the flowers…" of a well-cultivated inner life on its banks. If you follow this internal spring, as Helen describes, it becomes larger. The spring becomes a creek, the creek a stream, the stream a river, and as the flow grows larger, you get places where the water becomes placid and calm. In these

---

[3] Keller, H. and Sullivan, A. *The Story of My Life.* Garden City, New York : Doubleday & Company, Inc., 1954.
[4] Gibson, W. *The Miracle Worker.* New York : Scribner, 2008. ©1988

pools, according to Helen, the river reflects the surroundings of itself, abstract ideas and concepts such as love, pity, courage, compassion, sacrifice, etc.

Helen knew what water was, and I wanted to know, too. Through my idiosyncratic career path from a Classics major in college, to a wilderness adventure guide, to a National Laboratory technical staff member, and now as a single mother neurobiology graduate student at Rockefeller, this has been the central question of my life: what exactly is this spring within us that Helen describes?

I had something of an epiphany with regard to this when I joined the Bargmann lab in September 2012. Cori lent me her copy of *The Study of Instinct* by Nikolaas Tinbergen, required reading for newly minted members of the lab. In it, Tinbergen illustrates the properties of what ethologists refer to as *releasers* and the *innate releasing mechanism*, postulated to be the formal mechanism by which ritualistic instinctual behaviors (such as mating, courtship, nesting, grooming, animal contests, etc.) are organized and governed. *Releasers* are spontaneous. They are "unlocked" by very specific and simple *sign stimuli*, sensory cues found in the natural environment of the animal and associated with the specific context of the behavior released. Today, in a world post-behavioral genetics, *releasers* are not merely *a priori* hypotheticals but material truths: neuromodulators, that is, the "non-classical" neurotransmitters and neuropeptides whose action is not restricted to their local synapse, but can act over larger distances and longer time-spans.

Helen's internal spring may be the *innate releasing mechanism* that the classical ethologists describe. It trickles spontaneously, but Helen's awareness of it, her ability to follow it and unlock her inner world of language and intellect, needed to be released by a

particular constellation of *sign stimuli*: the stream, her hand, the bond between her and Ann.

One of the more infamous *releasers* is the neuropeptide oxytocin. Known to medical research since the early 20th century for inducing labor contractions, oxytocin leapt into the forefront of our collective psyche in the 1990s, after Thomas Insel's group at the NIH showed it to be a modulator of pair bonding in two closely related species of voles. At long last, here was the "love molecule," the "elixir of love," the venom on the tip of cupid's arrow.

It is seductive to revert to these mythological archetypes. Yet, anyone who has carefully reflected on either the evidence of the Insel group's experiments or their own experience of love would come to the conclusion that "love" could not possibly be a molecule, that in fact the concept of a "love potion" only captures the spontaneous nature of love, and not the activity of love: love as the participle, "loving," "love-making," the way "love grows where my Rosemary goes…"[5]

Love is a behavior. Behavior emerges at the circuit level, not the molecular. It carries out a work cycle. It feeds back, feeds forward, modulates and changes over time. Oxytocin is a *releaser* for that behavior. But, is all oxytocin-released behavior, "love"? That is to ask, is it all of the same kind? Or is the behavior "bonding?" Is Helen's spring oxytocin? If so, it would make sense then that her next words, as reported in her memoir later that day, were *mother, father, sister, teacher.* Is Helen's spring even a *releaser* in the ethological sense at all, this source of why we learn and laugh and love and create? Or is

[5] From the chorus of "Love Grows" by Edison Lighthouse, Album: On the Rocks. Released 1981.

Helen's spring and Tinbergen's *releasers* something more primal that subtends all of these? Is it the very water we swim in? Is it because of this water, this moisture, that I now have this damn spot on my lung?

While these are clearly philosophical questions that I am unprepared to definitively answer, one of the most profound notions we inherit from the classical ethologists is that we do not really know to what extent philosophical questions can be scientifically tractable, so we might as well try. This thesis is an attempt to begin to investigate broader questions about our experience of the innate and motional and the role oxytocin plays in our experience of the world by investigating oxytocin's fundamental relationship to its behavioral circuit in the spirit of the ethologists. In the four modalities of analysis that Tinbergen describes: mechanistic, ontological, functional, and phylogenetic, I look at both the "how" and the "why" of oxytocin as a releaser of reproductive behavior. To do so, I take the wide view across 600 million years of metazoan evolution, focusing on the oxytocin-mediated mating behavior and physiology of the often-overlooked invertebrates. By looking to these simpler animals with both smaller, paired-down nervous systems and more diverse sets of mating strategies, I elucidate some of the basic and general principles of the oxytocin circuit (**Chapter I**). In **Chapter II**, I give a survey of the ethology of *Caenorhabditis* (nematode roundworms) mating behavior, before I delve into the experimental investigation of the oxytocin-mediated mating circuit of *Caenorhabditis elegans*. The compact, fully anatomically diagrammed nervous system of this organism makes it an ideal model for this study, as do the multitude of genetic, molecular, pharmacogenic, optogenetic, and imaging tools available for *C. elegans*. The singular most critical feature of this animal this study exploits, however, is that I can constitutively knock

out the gene for its oxytocin homolog, nematocin, without compromising the health, development, or general locomotion of the animal.

In **Chapter III**, I show that the main source of nematocin in the male's copulatory apparatus (his tail), the interneuron DVA, has activity during mating that is critical for carrying it out competently. I do this by acutely silencing DVA with a heterologous histamine-gated chloride channel and its ligand just prior to mating, then by restoring mating by letting the males recover off histamine. The experiment is repeated in the nematocin-deficient males, to identify which of the behavioral phenotypes are nematocin-mediated, and which are not. Next, I discuss a genetic candidate screen to look for a mechanism of nematocin action (**Chapter IV**). I find that nematocin mutants are epistatic to dopamine mutants, implicating them in the same circuit. The classical interpretation of the genetic result suggests that the severe defect in dopamine deficient animals is due to a dysregulation of nematocin. I then rescue mating in dopamine-deficient males by acutely silencing DVA to corroborate this.

In **Chapter V** I investigate the activity of DVA during mating with the fluorescent calcium indicator GCaMP. I describe an activity pattern for DVA that coordinates calcium signal rises and falls with specific sub-behaviors within the mating behavior. I then look at DVA in nematocin deficient and dopamine-deficient males, and find that DVA activity breaks down at behavioral junctures consistent with the genetic behavioral data.

In **Chapter VI** I identify 2 dopamine receptors responsible for communicating the dopamine signal to DVA, one of which is a D1-like receptor (cAMP activating) and the other of which is a D2-like receptor (cAMP suppressing), and demonstrate their reciprocal effects on mating behavior. In **Chapter VII**, I summarize the experimental results,

contextualize the main implications, and generally discuss oxytocin and dopamine's deep phylogenetic connection in modulating reproductive behavior.

Early in his stay on the Magic Mountain, Hans Castrop attends a lecture called "Love as a Pathogenic Force." The entire audience is diagnosed as the victims of love. "Symptoms of disease are nothing but a disguised manifestation of the power of love; and all disease is only love transformed." Castrop is convinced of the truth in this. Madly in love, he stays at the sanitarium for even the possibility that he might see the object of his desire at mealtimes. I am less convinced. I think *The Magic Mountain* is a story about "situatedness" and how we respond to it. It is about how some things, like falling in love… or motherhood… … or trauma …or world wars … or grad school… just happen and there is no way to predict or intellectualize them. But they change everything, and we have to respond to. This is my response.

This is Water.

DEDICATION AND ACKNOWLEDGEMENTS

This thesis is dedicated to the only two people I have ever truly loved.

To my daughter, Willa Catherine Lockard, who taught me more about oxytocin than all of my studies combined, and who sacrificed a large part of her early childhood without consent so her mom could do this batshit crazy thing that meant a lot to me. You took care of me more than I took care of you these past few years, and I promise to make it up to you.

And, to my life-long mentor and best friend, Michael Rawn, the Leopold Bloom to my Stephen Dedalus. I know you will hate that analogy, but it couldn't be more apt, for ours is a relationship where spiritual paternity has also superseded consubstantial paternity, both mine and Willa's, with all its Judeo-Christian implications! Thank you for always being there, for always sharing yourself, your time, your wisdom, and for being a constant reminder that life is a gift no matter what.

I would also like to take this opportunity to thank a number of people in the Rockefeller Community who had their hands on my back for the duration of this race:

My mentor, Cori Bargmann, for giving this girl from "behind the steel curtain" a chance to see what high level research looks, sounds, feels, but especially smells, and tastes like.

My committee members, Gaby Maimon, Shai Shaham, and Leslie Vosshall, for enduring all those extra meetings in the service of helping me finish.

My external examiner Maureen Barr.

Nina Papavasiliou, for her enduring support of me and my work. For sharing her family with me. For her friendship.

My students Ama Kyerewaa and Katya Naphtali for the brainpower and brainspirit you gave to help bring this thesis to fruition.

Former and current postdocs in the Bargmann lab, especially Jennifer Garrison, Andrew Gordus, Navin Pokala, Sagi Levy, and Phil Kidd for their patience, expertise, and mentorship.

Margaret Ebert, my alter ego in so many ways, who's work and life have eerily paralleled my own, and who took on the project of oxytocin, wifehood, motherhood, divorcehood, and single motherhood alongside me.

All Bargmann lab students past and present.

To the staff of the Bargmann lab, Priscilla Kong, Hernan Jaramillo, Holly Hunnicut, and "Mama" Manoush Arizivan, who was more reliable than a scale in telling me when I was getting chubby and needed to lay off the carbs. Thank you for all your professional and personal support.

Dr. Torsten Wiesel, for his early morning talks over the NY Times and coffee, for letting me use his office as a nursery for the first ten months of my daughter's life, when I didn't have childcare, and for allowing me to pump breast milk in there for 8 months thereafter. For being a longstanding champion of families in our scientific community.

Jennifer Jones and Cricket Powell, may I raise a child with ¼ the brilliance, strength and character that you have done so.

Ms. Virginia Huffman, for being the guardian and protectorate of the Child and Family Center, and for keeping Rockefeller the kind of place where children's school is the first thing you see when you enter campus.

All of my daughter's primary care teachers over the years, especially Oi Hu who shares a special bond with her.

Rockefeller Security Director James Rogers and Asst. Director Michael Murphy, for handling my case with professionalism and taking the security of my daughter and me seriously.

Assistant District Attorney Paul Mezan, and 19th Precinct Officers Edward Raniola and Rosie Olivio, for their service to our city and their personal dedication to their vocations.

The Dean's Office, Sid Strickland, Emily Harms, Kristen Cullen, Marta Delgado, Cris Rosario, Stephanie Fernandez, and Courtney McBride for all of your administrative and moral support over these 7 years. And a special thank you to Andrea Morris, for your career mentorship, your candor, and your friendship.

Rockefeller housing staff Marnel Herbert, Mike Akins, and Anthony Jermott, for loving my family and helping to make our apartment a home.

Rockefeller Outreach Director Jeanne Garbarino and her staff, for all their light and grace.

Former and current Parents Association Board Members Christina Akala, Disan Davis, Ainhoa Perez, Fatimah Madari, Xiangwu Ju, Gist Croft, and Michelle Itano, for your dedication to this unique community of parent scientists.

WISeR Board Members past and present, including Emily Dennis, Sarah Stern, Alison Ehrlich, Linda Molla, Ilana Zucker-Sharff, Stephanie Marcus, Margo Herre, and Elena De Obaldia.

Friends Priya and Sethu Rajasethupathy, Michelle Kowanda and Michal Wiesczorek, Amma Asare and Amir Jaima, Sofia and Conrad Axelrod, Andreia Estrella and Marcello Gehara, Victor Bustos and Maria Paulina, Bryce and Leah Carey, Dan and Tia Gareau, Hila and Yotam Bar-On, Alexey Soshnev and Lacy Barton, Simona Giunta and Alistair Field, and Lorena Buitrago, and Nezih Antakli, for loving my kid and letting me love yours.

Finally, my family lawyer and dear friend Jill Zuccardy, for giving me these last 3 years of her life to save mine.

TABLE OF CONTENTS

LIST OF FIGURES

LIST OF TABLES

CHAPTER I: OXYTOCIN MEDIATED BEHAVIOR IN INVERTEBRATES, AN EVOLUTIONARY PERSPECTIVE

Introduction

The observation that instinctive behaviors evolve together with morphological traits is as old as the theory of evolution itself. In his chapter "Instinct" in *On the Origin of Species*, Charles Darwin wrote, "The canon of '*Natura non facit saltum*' ['Nature does not make leaps'] applies with almost equal force to instincts as to bodily organs (Darwin, 1871)." About a century later, the naturalist Wolfgang von de Wall demonstrated with dabbling duck hybrids that innate behaviors sometimes follow the laws of inheritance. He reported that the F_1 progeny resulting from the cross of two compatible but distinct duck species demonstrated courtship behavior patterns that appeared either intermediate between those of the two parental species, or related to ancestral courtship behaviors not seen in either parental species (Von de Wall, 1963). Today, it is widely accepted that many animal species have innate feeding, foraging, quiescence, and reproductive behaviors that result from genetic programs, resembling each other across species or showing stereotypy within a species (Konopka and Benzer, 1971). Despite being "hard-wired" into the genome, many of these behaviors also show a tremendous amount of plasticity, in some cases changing dramatically within a species in different environmental contexts (Tinbergen, 1951), and also between closely related species (Winslow et al., 1993). Both the stereotypy and the plasticity of behavior can be viewed from the standpoint of evolutionary biology, in which new biological functions arise by modifying existing functional systems. What, then, are the genes that provide the raw material for the rich, variable, and essential behaviors that promote animal survival and reproduction?

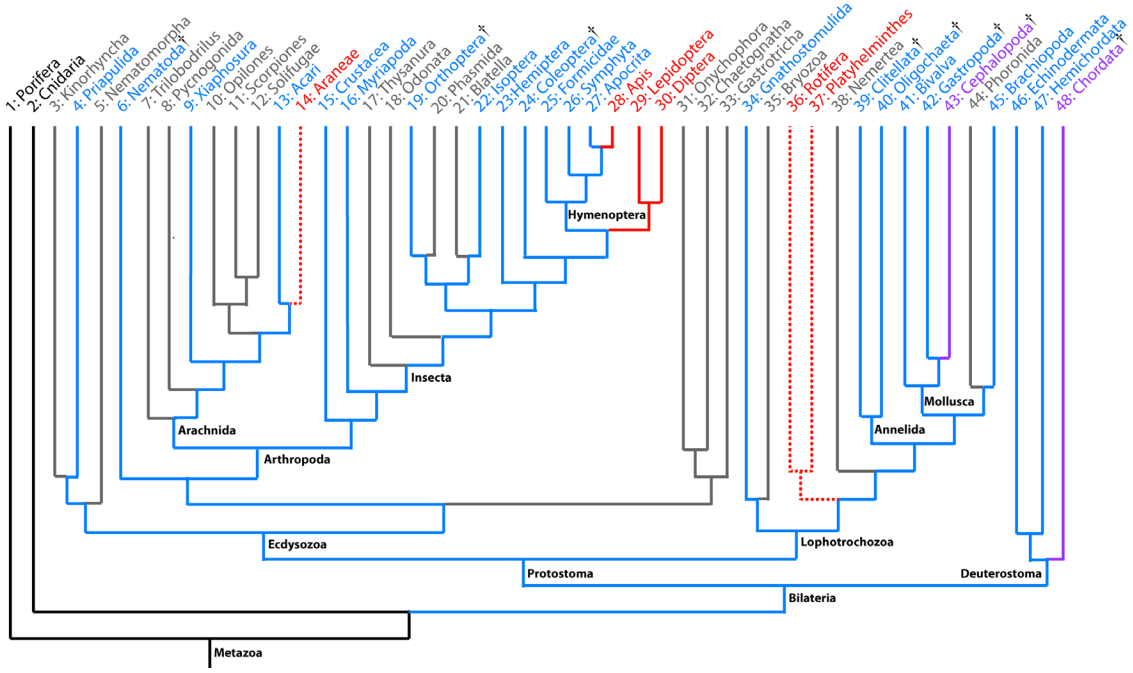

Figure 1.1: Phylogenetic tree for oxytocin-related peptides in metazoans. *Top*: Animal lineage names. Reference numbers are provided for ease of identifying lineages discussed in the manuscript. † indicates lineages represented in **Table 1.** Colors indicate the presence or absence of oxytocin-related peptide(s) in the lineages. *Black* lineages may precede the initial appearance of oxytocin-related peptides. *Red* lineages have high-confidence secondary loss of the peptide, where the absence of a homologous peptide has been experimentally validated and previously published. *Dotted red lines* mark lineages that are newly-inferred candidates for secondary loss of the oxytocin peptide gene; they are high-quality, thoroughly annotated genomes that yielded no homologous peptides in BLAST searches. *Gray* lineages yielded no homologous peptides in a BLAST search, but are composed of genomes of unknown quality. *Blue* lineages represent those where the existence of a single oxytocin-related peptide sequence has been validated. *Purple* marks lineages in which the oxytocin homolog has undergone a duplication event. Landmark clades are labeled in *black* font.

Some of the strongest insights into conservation and plasticity in behavioral genetics have emerged from studies of the oxytocin/arginine-vasopressin neuromodulatory system. Peptides related to oxytocin and vasopressin (henceforth, "oxytocin-related peptides") are encoded in the genomes of animal species separated by 600 million years of evolution (Gwee et al., 2009), including invertebrate nematodes (Beets et al., 2012; Garrison et al., 2012), insects (Egekwu et al., 2014; Gruber and Muttenthaler, 2012; Proux et al., 1987; Stafflinger et al., 2008), annelids (Fujino et al., 1999; Oumi et al., 1996; Wagenaar et al., 2010), and molluscs (Bardou et al., 2009; Takuwa-Kuroda et al., 2003; Van Kesteren et al., 1995a); as well as vertebrate fish (Godwin and Thompson, 2012), amphibians (Searcy et al., 2011), reptiles (Kabelik and Magruder, 2014; Kawazu et al., 2014), birds (Kelly and Goodson, 2014), and mammals (Donaldson and Young, 2008; Stoop, 2014) (**Figure 1.1**). In almost all species in which they have been studied, oxytocin-related peptides have been implicated in behaviors related to reproduction, such as mate selection (Insel et al., 1998; Wagenaar et al., 2010), copulation (De Boer et al., 1997; Garrison et al., 2012; Melis and Argiolas, 2011), and provisioning for offspring (Marlin et al., 2015). In a few cases, oxytocin-related peptides are also implicated in learning and memory (Bardou et al., 2010a; Beets et al., 2012; Oettl et al., 2016; Sarnyai and Kovacs, 2014) and in other non-reproductive behaviors (Dutertre et al., 2008; Martinez-Padron et al., 1992) (**Table 1**). Oxytocin's role in reproductive behavior across a variety of species with diverse reproductive strategies implies that the system can be remodeled by relatively small genetic changes while maintaining a core function. The study of oxytocin's genetic and functional conservation provides a unique opportunity to explore how ancient, slowly evolving genes can generate rapidly evolving behaviors.

Table 1. Oxytocin-mediated behavioral functions in invertebrates. Species name, peptide name, peptide sequence, behavior, evidence, and reference are provided for all invertebrate species with a known oxytocin mediated behavior. *Homo sapiens* provided at the bottom for reference. * in the peptide sequences indicates C-terminal amidation.

Species	Peptide	Sequence	Behavior	Evidence	Reference
Caenorhabditis elegans (Nematode)	Nematocin	CFLNSCPYRRY*	male mating modulation; gustatory learning	genetic knockout, fluorescent reporter determination of cellular expression, single cell knockout	*Garrison, et. al., Beets et. al. 2012*
Hirudo verbana (Medicinal Leech)	Hiruditocin	CFIRNCPKG*	mating: partner exploration, body twisting, oviposition, and cocoon deposition	fictive behavior induction by peptide injection, body wall kinematics, electrophysiology, spectral analysis	*Wagenaar, et. al. 2010*
Lymnaea stagnalis (Large Pond Snail)	Conopressin-G	CFIRNCPKG*	male mating: penile eversion, retraction, *vas deferens* muscle contraction	fictive behavior induction by peptide injection, *in situ* hybridization and immunohistochemistry of neurons and processes, electrophysiology	*van Kestern, et. al. 1995; van Golen et. al. 1995; de Boer, et. al. 1997; de Lange, et. al. 1998 (2); van Soest, et. al. 2000*
Whitmania pigra (Medicinal Leech)	Annetocin	CFVRNCPTG*	oviposition and cocoon deposition	fictive behavior induction by peptide injection	*Fujino, et. al. 1999*
Eisenia foetida (Earthworm)	Annetocin	CFVRNCPTG*	oviposition and cocoon deposition	fictive and authentic behavior induction by peptide injection	*Oumi, et. al. 1996*
Sepia officinalis (Common Cuttlefish)	Sepiatocin, pro-Sepiatocin	CFWTTCPIG* CFFRNCPPG*	reproduction; feeding; communication; learning and memory	passive avoidance task training; immunohistochemistry; tissue specific RT-PCR	*Bardou, et. al. 2009 (2), 2010; Henry, et.al. 2013*
Aplysia californica (Sea Hare)	Conopressin-G	CFIRNCPKG*	suppression of GWR and increase in SGM	superfusion in an *in vitro* preparation	*Martinez-Padron, et. al. 1992*
Locusta migratoria (Locust)	Inotocin	CLIVNCPRG*	CNS function	qPCR in head vs. body, larva vs. adults	*Proux, et. al. 1987; Stafflinger, et. al. 2008*
Tribolium castaneum (Red Flour Beetle)	Inotocin	CLIVNCPRG*	CNS function	qPCR in head vs. body, larva vs. adults	*Stafflinger, et. al. 2008*
Octopus vulgaris (Common Octopus)	Cephalatocin, Octopressin	CYFRNCPIG* CFWTSCPIG*	CNS function	RT-PCR expression in neuronal vs. peripheral tissues	*Kanda, et. al. 2003, 2005*
Conus tulipa (Cone Snail)	Conopressin-T	CFIRNCPKT*	prey capture	isolated from venom	*Dutertre, et. al. 2008*
Homo sapiens (Humans)	Oxytocin, arg- Vasopressin	CYIQNCPLG* CYFQNCPRG*	childbirth, lactation, suckling response, trust, social fear, generosity, pair bonding, parental care.	isolated from pituitary extract, urine excretions, GWAS, intra-nasal application, comparative animal studies	*Dale, 1909; Nickerson, 1954; Insel, et. al 1995; Francis, et. al. 2000; Kirsch, et. al. 2005; Kosfeld et. al. 2005; Zak, et. al. 2007; Baumgartner, et. al. 2008; Hatton et. al. 2008; Schaller et. al. 2010; Wrobel et. al. 2010*

In this chapter we focus on oxytocin-related peptides in invertebrate animals (Gruber, 2014). The relatively short lifespans, rapid reproductive cycles, and compact nervous systems of many invertebrates provide experimental advantages that have been exploited since the dawn of neuroscience (Hodgkin and Huxley, 1990). Invertebrates also use an impressive diversity of breeding systems. While only a few vertebrate species deviate from dioecious (male-female) sexual reproduction (Senior et al., 2012), invertebrates draw broadly from reproductive strategies such as hermaphroditism (ter Maat, 1992), androdioecy (Chasnov, 2010), parthenogenesis (Whitfield and Evans, 1983),

and dedicated reproductive castes (Wilson and Holldobler, 2005). Observing the roles of oxytocin-related peptides in these different contexts reveals both flexibility and constraints on this ancient neuromodulatory system.

Peptide Expression

In **Figure 1.1**, we summarize the current understanding of animal lineages with peptides homologous to oxytocin. Oxytocin-related peptides are only 9-13 amino acids long, but can be reliably recognized in genomic sequences based on the presence of several features: two cyclizing cysteines at positions 1 and 6 of the translated peptide (Gruber, 2014); and an adjacent, highly conserved, cysteine-rich neurophysin domain that is thought to assist in folding, processing, and peptide localization to the dense core vesicles (de Bree, 2000). *Semmens et al.* have suggested that oxytocin/vasopressin peptides are part of a much larger family, including the vertebrate neuropeptide-S (NPS) and crustacean cardio-active peptide (CCAP), where the CCAP-like peptide found in protostomes lost the neurophysin domain, and the NPS-like peptides in deuterstomes lost the 1,6 cysteine disulfide bond first and later, after the divergence of *Echinodermata*, also lost the neurophysin domain (Elphick and Rowe, 2009; Semmens et al., 2015). In many lineages, both the presence of an oxytocin-related peptide in the genome and the expression of a mature peptide have been experimentally validated via transcriptional analysis (Egekwu et al., 2014), immunostaining (Bardou et al., 2009), genetics, and/or proteomics (Beets et al., 2012; Garrison et al., 2012). In others, we identified homologs by iterative NCBI BLAST searches. While the presence of the peptide's gene in the genome does not necessarily mean that a cyclized, mature peptide with functional receptors is made by the organism, peptide

sequence homology serves as the best available proxy for determining which lineages have the oxytocin neuromodulatory system, defined as a functional, mature peptide with one or more functional receptors.

We used BLAST sequence homology to the oxytocin-related peptide annetocin from the earthworm *Eisenia foetida* (Oumi et al., 1996) (**Table 1**) to identify a peptide homolog in the ecdysozoan Atlantic horseshoe crab *Limulus polyphemus* (**Figure 1.1:** *#9*) and in the lophotrochozan brachiopod *Lingua anatina* (**Figure 1.1:** *#45*). Both of these organisms can be considered "living fossils" in the sense that they have slowly evolving genomes (Luo et al., 2015; Nossa et al., 2014), which makes their gene sequences useful as queries for invertebrate-wide BLAST searches. Animal lineages labeled in *blue* in **Figure 1.1** have a single gene that shows the hallmarks of an oxytocin-related peptide. Labeled in *gray* are lineages with incomplete genomes, where we were unable to determine whether an oxytocin-related peptide was present or absent. Labeled in *red* (high confidence) and *red dotted lines* (lower confidence) are lineages with well-annotated genomes that appear to have secondarily lost oxytocin-related peptides that were present in their ancestors.

Oxytocin-related peptides emerged around the same time as bilateral symmetry in body plans: they are present across modern *Lophotrochozoa* (Fujino et al., 1999; Henry et al., 2013; Oumi et al., 1996; Takuwa-Kuroda et al., 2003; Wagenaar et al., 2010) (**Figure 1.1:** *#34-45*), *Ecdysozoa* (Beets et al., 2012; Egekwu et al., 2014; Garrison et al., 2012; Gruber, 2014; Gruber and Muttenthaler, 2012; Proux et al., 1987; Stafflinger et al., 2008) (**Figure 1.1:** *#3-30*), and *Deuterostomia* (Elphick, 2012; Kawada et al., 2008; Semmens et al., 2015; Semmens et al., 2016) (**Figure 1.1:** *#46-48*). Neither the peptide nor its receptors

appear to be present in the earlier animal branches of *Porifera* and *Cnidaria* (Gruber, 2014) (**Figure 1.1:** *#1-2*), labelled *black*, or in any non-metazoan.

Peptide Duplication

Gene expansion and contraction are common themes affecting oxytocin-related peptides and other neuropeptide families. The duplication of a single peptide to generate the oxytocin and vasopressin systems present in most vertebrates is thought to have occurred early in chordate history, after the emergence of jawless fishes (Gwee et al., 2009) (**Figure 1.1:** *#48*). It appears that one peptide gene was lost in the teleost fish lineage, and then a secondary duplication recreated two paralogs within the lineage, with selective receptors (Venkatesh and Brenner, 1995). In the *Cephalapoda* lineage of molluscs, a dual peptide system also emerged independently of these vertebrate duplications (**Figure 1.1:** *#43*). Both the common octopus *Octopus vulgaris* and the cuttlefish *Sepia officinalis* have two different oxytocin homologs: in octopus, cephalatocin and octopressin (Takuwa-Kuroda et al., 2003); and, in cuttlefish, sepiatocin and pro-sepiatocin (Henry, *et al.* 2013) (**Table 1**). As in the vertebrates, the two peptides present in these cephalopod species appear to be non-redundant, having preferential receptors (Kanda et al., 2005; Kanda et al., 2003) and different expression patterns (Bardou et al., 2009; Bardou et al., 2010b). Most interestingly, the peptides seem to have distinct functions from one another within the animal. In *O. vulgaris,* octopressin perfusion causes contractions in the peripheral tissues such as the oviduct, aorta, rectum, efferent branchial vessel, and spermatophoric gland, whereas cephalatocin had no effect on these tissues (Takuwa-Kuroda et al., 2003). Contractile activity on non-neuronal tissue is also a prominent feature of vertebrate

oxytocin (*e.g.* uterine contraction, milk let-down response) (Coria-Avila et al., 2014) and vasopressin (*e.g.* blood vessel contraction) (Wang et al., 2000). Similarly, in *S. officinalis*, sepiatocin induced contractile activity in tissues from the oviduct, accessory sex glands of females, penis, vena cava, gills, and rectum, while pro-sepiatocin conferred no such activity (Henry et al., 2013). Cephalopods have rapidly expanding genomes and the largest nervous systems in invertebrates (Albertin et al., 2015). Considering evidence that cephalotocin enhances long-term memory in the *S. officinalis* (see below), we speculate that duplication and diversification of the oxytocin neuromodulatory system and other neuronal genes in cephalopods may have contributed to the evolution of impressive cognitive abilities that rival those of many vertebrates (Hochner, 2010; Zarrella et al., 2015).

Secondary Peptide Losses

The instances where the oxytocin peptide was lost from a lineage are as interesting as those in which it was retained or duplicated, and raise just as many questions. In flatworms and rotifers, it appears that oxytocin loss accompanied a global reduction in complexity of these animals (Riddiford and Olson, 2011). Oxytocin-related peptides appear to be absent from the genomes of Platyhelminthes (flatworms, *e.g. Schmidtea mediterranea*) and Rotifers ("wheel animals," *e.g. Brachionus manjavacas*) (**Figure 1.1:** *red dotted line #36-37*). These lineages have a reduced dependence on mating for reproduction. Bdelloid rotifers have lost the ability to reproduce sexually (Stelzer et al., 2010). Other species of rotifers reproduce sexually under certain environmental conditions, though parthenogenesis is much more common (Gladyshev and Arkhipova, 2010). Planarian flatworms such as *S. mediterranea* are simultaneous hermaphrodites, possessing

both male and female genitalia, and are capable of both sexual reproduction and parthenogenesis. Some natural variants are known to be parthenogenetic exclusively, and others switch to an outcrossing strategy with some frequency (D'Souza and Michiels, 2008; Lazaro et al., 2011).

Retaining sexual reproduction and the behavioral requisites for successful mating, however, cannot be the sole guiding principle governing the retention of the oxytocin-related peptides. Androdioecious (hermaphrodites and rare males) nematode species such as *Caenorhabditis elegans* have retained an oxytocin-related peptide with functional receptors (Beets et al., 2012; Garrison et al., 2012) (**Figure 1.1:** *#6*) while relying on self-fertilization as their primary reproductive strategy (Anderson et al., 2010; Morran et al., 2009). Conversely, arthropods have some of the most intricate and complex courtship behaviors among invertebrates (Herberstein et al., 2014; Yamamoto and Koganezawa, 2013), and yet there have been several instances of secondary loss of the oxytocin peptide in these lineages (Stafflinger et al., 2008) (**Figure 1.1:** *red*). In arachnids, oxytocin-related peptides are present in the Atlantic horseshoe crab *Limulus polyphemus* (mentioned above), and the *Acari* lineage (**Figure 1.1:** *#13*), which includes ticks and mites (Egekwu et al., 2014). However, the peptide is apparently absent in the well-annotated social velvet spider (*Stegodyphus mimosarum*) genome and the less well-annotated white knee tarantula (*Acanthoscurria geniculate*) genome (Sanggaard et al., 2014), both in the *Araneae* lineage (**Figure 1.1:** *red dotted line, #14*). In insects, oxytocin-related peptides are present in the orthopteran *Locust migratoria* (Proux et al., 1987) (**Figure 1.1:** *#19*), in isopterans (termites) (**Figure 1.1:** *#22*), and in the coleopteran red flour beetle *Tribolium castaneum* (Stafflinger et al., 2008) (**Figure 1.1:** *#24*, **Table 1**), but no homologous peptide is present

in any of the 12 species of *Drosophila* with annotated genomes (*Diptera*), in the mosquito species *Anopheles gambiae* and *Aedes aegypti* (also *Diptera*), or the silk moth *Bombyx mori* (*Lepidoptera*) (Stafflinger et al., 2008), suggesting that the peptide was lost before the divergence of *Lepidoptera* and *Diptera* classes (**Figure 1.1:** *red, #29-30*). Another secondary loss among the holometabolous insects occurred in the lineage of the eusocial honeybee *Apis mellifera* (**Figure 1.1:** *red, #28*) after it diverged from the solitary wasps such as *Nasonia vitripennis* (Stafflinger et al., 2008) (**Figure 1.1:** *blue, #27*). The absence of oxytocin in eusocial bees may be the most counterintuitive loss in animals, given the complexity of their social behavior. Oxytocin is present, however, in other eusocial species within the lineage *Formicidae*, including the leaf-cutter ant *Atta cephalotes*, the carpenter ant *Camponotus floridanus*, and the basal ant *Harpegnathos saltator* (Gruber and Muttenthaler, 2012) (**Figure 1.1:** *#25*).

Why the repeated loss of oxytocin-related peptides within a relatively constrained set of insect lineages, in the absence of behavioral simplification? This evolutionary pattern suggests the existence of a second parallel system with overlapping functions to oxytocin, whose presence in this lineage allows the loss of an otherwise conserved oxytocin pathway. The second pathway may act as a pre-adaptation to oxytocin loss. It is possible that another peptide has acquired reproductive functions in insects, or that a substitution of a completely different nature has emerged.

Oxytocin receptors in invertebrates

As in vertebrates, the oxytocin-related peptides in invertebrates activate target cells through G-protein coupled receptors (GPCRs) (Garrison et al., 2012; Kanda et al., 2003;

Stafflinger et al., 2008). GPCRs usually modulate the activity of the target neurons through second messenger signaling cascades on biochemical timescales of seconds or minutes rather than directly depolarizing or hyperpolarizing the neurons (Hille, 1994). Consequently, oxytocin and other neuromodulatory systems follow a logic orthogonal to that of fast electrical and synaptic circuits: they reversibly modify the flow of information through fast circuits by transiently strengthening or weakening synaptic strength or excitability.

The ligand-receptor relationships between oxytocin-related peptides and their receptors are often inferred from homology, but have been validated by biochemical assays in heterologous systems for a few invertebrate species. Inotocin from the red flour beetle *T. castaneum* (**Table 1**) activates a predicted receptor at nanomolar effective concentrations (Stafflinger et al., 2008). *O. vulgaris* cephalotocin activates the cephalocotin receptor (CTR2) while octopressin activates the octopressin receptor (OPR) when heterologously expressed in *Xenopus* oocytes (Kanda et al., 2003). These heterologous expression experiments help elucidate ligand-receptor relationships, but they are less useful for understanding the biochemical consequences of receptor action, because the foreign expression systems may not have the G proteins and signaling pathways that the receptor would encounter in its host organism and cell type.

The significance of knowing the native signaling pathway is illustrated by the pond snail *Lymnaea stagnalis* (**Table 1**), which has a single oxytocin-related peptide receptor called Lys-conopressin receptor (LSCR) (van Kesteren et al., 1995b). Evidence suggests that the peptide signals through two pathways in its native context in the right cerebral ganglion (**Figure 1.2:** A): conopressin induces both a high-voltage activated (I-HVA)

pacemaker current via Protein Kinase C (PKC) and a low-voltage activated (I-LVA) pacemaker current by a mechanism that may involve cAMP (Van Soest et al., 2000).

The *Caenorhabditis elegans* oxytocin-related peptide nematocin (**Table 1**) activates two G protein-coupled receptors, NTR-1 and NTR-2. Genetic knockouts of these receptors yield partial defects in mating behavior, less severe than those of nematocin peptide-deficient animals (see below). Knocking out both receptors recapitulates the full mating defect of the peptide loss. Because *C. elegans* has a complete anatomical wiring diagram for its nervous system (Jarrell et al., 2012; White et al., 1986), the sites of peptide and receptor expression patterns inferred from reporter genes and immunocytochemistry can be compared to the anatomical circuits. This comparison shows that the vast majority of nematocin receptor-expressing cells do not have direct synaptic connections to a peptide-expressing cell (Beets et al., 2012; Garrison et al., 2012) (**Figure 1.2:** B), and therefore that nematocin must communicate extrasynaptically with its target cells.

Lymnaea stagnalis: peptide partnership in male behavior

Oxytocin's functional role in reproduction has been deeply investigated in the pond snail *L. stagnalis*. Conopressin, the oxytocin–related peptide in gastropods, either directly or indirectly modulates every aspect of mating behavior in this species. *L. stagnalis* is a simultaneous hermaphrodite with genital positioning that makes self-insemination possible but cumbersome. *L. stagnalis* usually mates with a conspecific, where one partner assumes the role of "male," or inseminator, and the other assumes the role of "female," receiving the sperm for her eggs (**Figure 1.3:** A). Like the mating behavior of more complex animals, male mating behavior in *L. stagnalis* consists of a series of distinct sub-behaviors that are

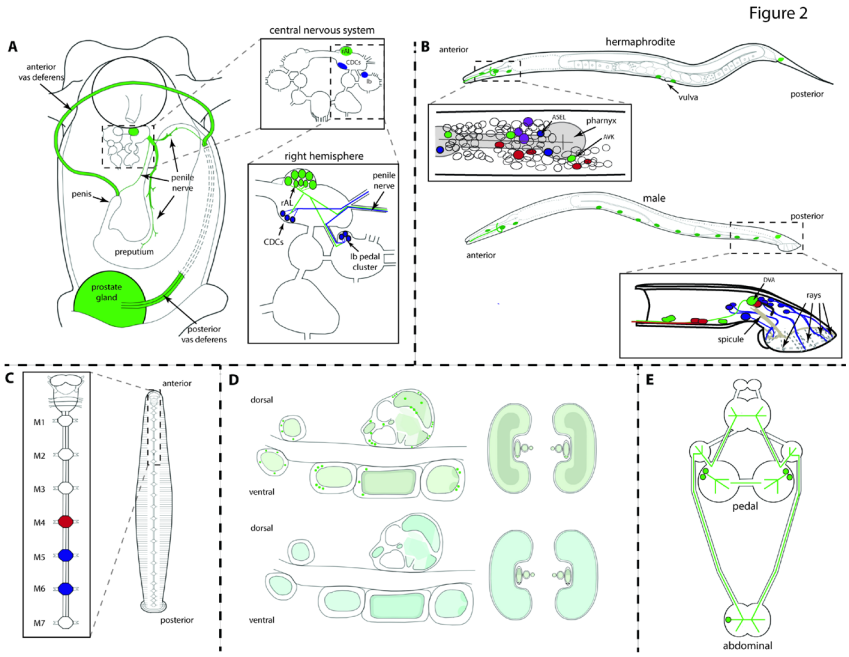

Figure 1.2: Neuroanatomical sites of oxytocin production and action in selected invertebrates. **A:** Conopressin in the reproductive system of *L. stagnalis*. *Left:* Illustration of a dissected male gonopore. *Right Top:* The CNS of *L. stagnalis.* *Right Bottom*: Right hemisphere of the CNS. Structures where conopressin is present are labeled in *green.* Ganglia targets of conopressin are labeled in *blue*. Adapted from Figure 1 in De Lange, *et al.* (1998). **B:** The nematocin neuromodulatory system in *C. elegans*. *Top:* Hermaphrodite with a detail of the head neurons. *Bottom*: Male with a detail of the tail neurons. Nematocin-expressing neurons are labeled in *green*. NTR-1-expressing neurons are labeled in *blue*; NTR-2-expressing neurons in *red*; and neurons expressing both receptors in *purple*. Expression data combined from Garrison, *et al.* (2012) and Beets, *et al.* (2012) **C**: Body and anterior motor ganglia of the medicinal leeches. Ganglia responsible for the oxytocin-driven CPG are labeled in *blue* and *red*. **D:** Dual peptide immunostaining of the *S. officinalis* CNS. *Left:* sub-esophogeal and supra-esophogeal ganglion. *Right*: Optic lobes. *Top row:* Immunostaining pattern using a mammalian oxytocin antibody in *hunter green*. *Bottom row:* Immunostaining pattern using a mammalian vasopressin antibody in *teal green*. Shade intensity is representative of the immunostaining density. Adapted from Figure 3 of Bardou, *et al.* (2009) **E:** Conopressin immunostaining of the CNS of *A. californica*. Peptide presence is labeled in *green*. Adapted from Figure 2 of Martinez-Padron, *et al.* (1992)

coordinated in a specific temporal pattern, with the sub-behaviors varying in duration depending on the animal's motivational state (Koene, 2010). First, the penile complex is everted and probes for the female gonopore. Once positioned correctly, intromission takes place and sperm is transferred from the seminal vesicles down the vas deferens and penis into the vagina. After sperm transfer, the retractor muscles revert the penile complex back into the snail (De Lange et al., 1998)(**Figure 1.3:** A).

Conopressin is released from a cluster of neurons in the right anterior lobe (rAL) of the cerebral ganglia (Van Golen et al., 1995; Van Kesteren et al., 1995a) (**Figure 1.2:** A). Conopressin-positive fibers run throughout the male gonopore, including the penile nerve, the only nerve that innervates the penile complex (Van Kesteren et al., 1995a), the vas deferens (Van Golen et al., 1995), the prostate gland, and the region of the penis tip containing sensory neurons that detect successful vaginal penetration (De Lange et al., 1998). Conopressin induces a subset of male mating responses such as spontaneous contractions in the vas deferens (Van Golen et al., 1995; Van Kesteren et al., 1995a), but it does not elicit full male mating behavior (De Boer et al., 1997). This is likely due to the fact that conopressin co-modulates the mating behavior of *L. stagnalis* with nine other peptides and the neurotransmitter serotonin (5HT) (De Lange et al., 1998). The most notable of these co-regulators is the APGW-amide peptide, which can induce eversion of penile structures and colocalizes with conopressin in the rAL neurons that show increased activity during penile eversion (De Boer et al., 1997; Van Golen et al., 1995) (**Figure 1.2:** A) (**Figure 1.3:** A). Co-release of APGW-amide and conopressin has the potential to

organize subsequent mating behaviors, with APGW-amide acting to evert the penile complex and conopressin acting to sensitize the penile tip for vaginal probing.

Conopressin and APGW-amide may be co-released, but they have antagonistic effects on the vas deferens (Van Golen et al., 1995). Application of conopressin increased the number and

frequency of spontaneous contractions in the vas deferens in a dose-dependent manner, whereas application of APGW-amide had a dose-dependent inhibitory effect on the posterior vas deferens (Van Golen et al., 1995). In this context, conopressin and APGW-amide appear to balance each other's activity, not to synergize.

Finally, conopressin inhibits female behavior. Immuno-positive axonal fibers run proximate to the caudodorsal cells (CDCs), neuroendocrine cells that release peptides association with egg-laying, egg mass production, and associated "female" reproductive behaviors. Bath application of conopressin resulted in the hyperpolarization of the CDCs and inhibition of their electrical activity, thereby preventing egg laying and its associated behaviors (Van Kesteren et al., 1995a).

Caenorhabditis elegans: classical genetics and cell-level resolution of mating

C. elegans is a free-living nematode that has been cultured in the laboratory as a genetic model organism since the 1960s (Brenner, 2009; Fitch, 2005). Most animals in the population are androdioecious hermaphrodites: "females" that transiently produce sperm, and therefore are capable of internally self-fertilizing. A small fraction of the population are males, which have dedicated structures in the tail for inseminating a hermaphrodite (**Figure 1.2:** B, **Figure 1.3:** B) (Ellis and Schedl, 2007; Haag, 2005). *C. elegans* males

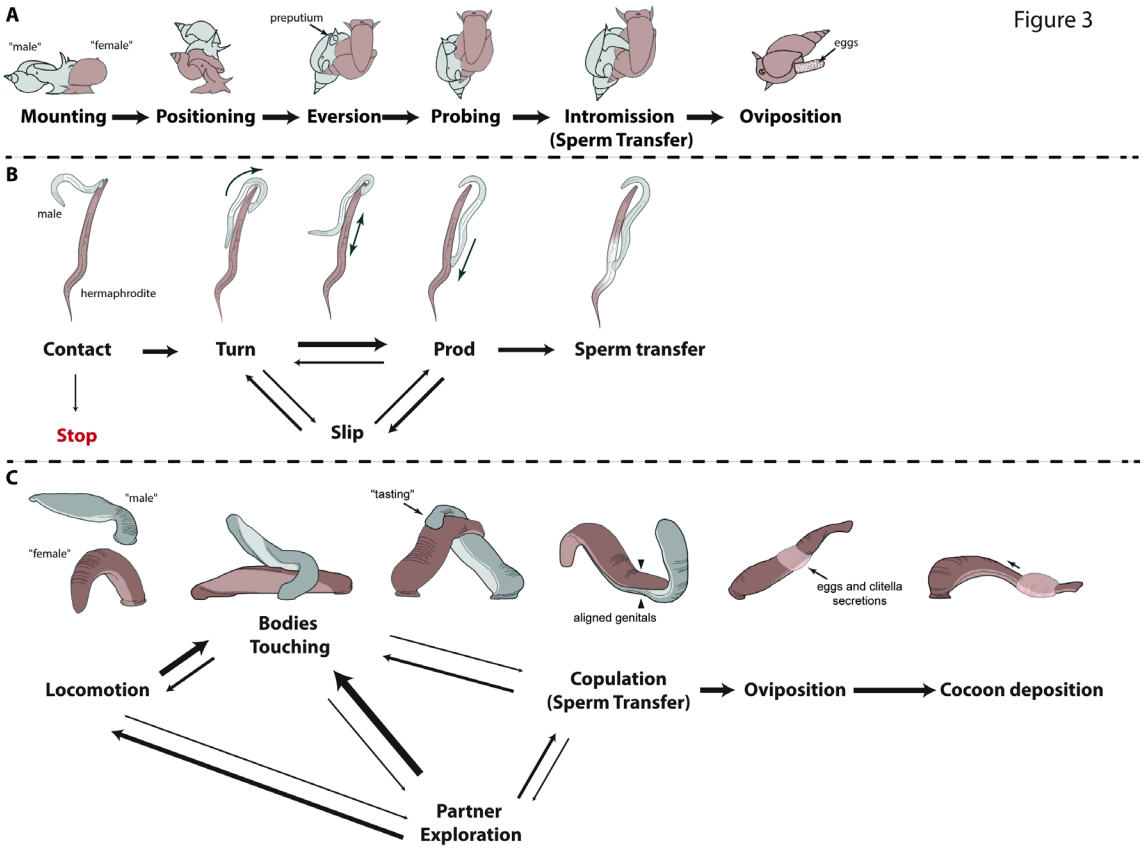

Figure 1.3. Ethograms for oxytocin-mediated reproductive behaviors. A: Reproductive behavior in *L. stagnalis* (two hermaphrodites). Adapted from Jarne, P. *et al.* (2010). **B:** Mating behavior in *C. elegans* (male and hermaphrodite). In **A** and **B,** inseminating partners are labeled in *gray*, and egg-laying partners are labeled in *brown*. **C:** Reproductive behavior in medicinal leeches. Adapted from Figure 1 in Wagenaar, *et al.* (2010). Two hermaphrodites are shown in different colors, but either or both partners might inseminate or subsequently lay eggs; it is unclear whether they take different roles in a single mating event. In **B** and **C**, arrow weight represents frequency of transition between the sub-behaviors during copulation. In **A,** data on transitions is not available, and, all arrow weights are the same by default. In **C,** the time frames of oviposition and cocoon deposition post-copulation are long, and the transition frequencies unknown.

mate by progressing through a series of stereotyped sub-behaviors of variable duration, depending on the animal's motivational state. Mating is initiated when the male makes contact with a hermaphrodite with the copulatory apparatus in his tail. (**Figure 1.2:** B,

Figure 1.3: B) Once contact is made, the male begins backing along the hermaphrodite, executing turns when he reaches the hermaphrodite's head or tail, until he locates the vulva. Males sometime repeatedly slip back and forth along the hermaphrodite in the course of mating. The male then prods at the vulva while attempting to insert his needle-like spicules. Once the spicules are successfully inserted, sperm is released and flows into the hermaphrodite's uterus (Barr and Garcia, 2006) (**Figure 1.3:** B).

C. elegans mutants lacking nematocin or its receptors have striking defects in male mating behavior. Males deficient in the nematocin or nematocin receptor genes were capable of mating, but did so with decreased efficiency and sired fewer progeny. These animals spent more time in and cycling through the sub-behaviors leading up to successful sperm transfer; engaged in more non-productive behaviors, e.g. slipping along the hermaphrodite or prodding at stimuli other than the vulva; and more frequently abandoned the hermaphrodite before completion of mating (Garrison et al., 2012) (**Figure 1.3:** B). This evidence suggests that nematocin orchestrates the sub-behaviors of male mating to give the process coherence and momentum.

The expression patterns for nematocin and its receptors in *C. elegans* are sexually dimorphic. The peptide is expressed in one head neuron, one tail neuron, the vulva motor neurons, and some male-specific motor neurons. The nematocin receptors are expressed in many male-specific neurons in the tail and many sensory neurons in the head that are common to both sexes (**Figure 1.2:** B). Thus nematocin receptors function both in anatomical circuits that are present only in the sexually mature male, and as components of circuitry that is shared by all developmental stages and both sexes. A single neuron, DVA, is the source of nematocin in the tail for both sexes. Males deficient in nematocin in

DVA recapitulated the majority of the mating defects in the knockout (Garrison et al., 2012). As mentioned earlier, none of the receptor-expressing cells are reported to be post-synaptic to DVA in the male *C. elegans* neural wiring diagram (Jarrell et al., 2012). Rather, DVA acts as a source for diffusible nematocin that may act on multiple target neurons in the region of the male tail.

Annelids: both female and male behavior, and the underlying circuits

The oxytocin-induced activity of parturition is remarkably conserved. In the hermaphrodite earthworm *E. foetida*, injection of the oxytocin-related peptide annetocin induces canonical behaviors associated with egg-laying (Oumi et al., 1996) (**Table 1**). These include mucus secretion, contraction of the clitellum (uterus), and body shape changes that accompany oviposition (elongation of anterior and posterior segments, and transverse expansion of the segments near the clitellum). Some animals even secreted a cocoon membrane and laid eggs. Notably, animals are susceptible to annetocin only during the breeding season (Oumi et al., 1996). Very similar effects on oviposition are induced by annetocin injection in the medicinal leech *Whitmania pigra*, another simultaneous hermaphrodite (Fujino et al., 1999; Oumi et al., 1996) (**Table 1, Figure 1.3:** C).

In another species of medicinal leech, the simultaneous hermaphrodite *Hirudo verbana*, oxytocin stimulates both the male and female components of reproductive behavior (Wagenaar et al., 2010) (**Table 1**, **Figure 1.3:** C). *H. verbana* mating is initiated by the animal flaring its mouth and twisting its body around its partner's longitudinal axis. The leech scans its mate, confirming by taste that its partner is a conspecific, and precisely aligns the male and female gonopores (genitals) for insemination. After successful

copulation, one or both leeches deposit fertilized eggs in cocoons secreted by glands in the clitellum (**Figure 1.3:** C). Conopressin injection is a potent inducer of these mating behaviors even in the absence of a partner (Wagenaar et al., 2010). The time course of peptide action is slow: body twisting and mouth flaring began 10 minutes after injection; thrusting, resembling cocoon deposition, after 50 minutes (**Figure 1.3:** C). Twisting continued for up to 48 hours, suggesting very long-lasting peptide effects (Wagenaar et al., 2010).

Electrophysiological characterization in *H. verbana* has identified a conopressin-controlled central pattern generator (CPG) circuit for the twisting motion that allows gonapore alignment. Oxytocin caused strong, bilaterally synchronized oscillations in motor neuronal activity with a period of 5-20 seconds. These bursts varied in amplitude (stronger on the left, then stronger on the right) with a period of about 5 minutes (Wagenaar et al., 2010) (**Figure 1.2:** C). In the isolated ganglia, oxytocin induced the strongest oscillations from the segments specialized for male (M5) and female (M6) genital functions. Although it does not control the motor pattern directly, the motor ganglion M4 showed weak but autonomous oscillations, suggesting that it may have a reproductive role as well (**Figure 1.2:** C). The mechanistic basis of the slow five-minute oscillation is unknown, and an interesting topic for future study (Wagenaar et al., 2010).

Gustatory associative learning in Caenorhabditis elegans

The physiological role of vasopressin in fluid homeostasis in mammals is well established (Christ-Crain and Fenske, 2016). Invertebrates often use behavioral strategies in addition to internal regulatory systems to maintain physiological homeostasis. In *C.*

elegans, nematocin regulates salt homeostasis by modulating sensory neurons during gustatory associative learning (Beets et al., 2012), a behavior at the intersection of salt homeostasis and behavioral preference (**Table 1**). Nematocin receptors are expressed in several chemosensory neurons in the animal's head that sense salt and other gustatory cues. *C. elegans* loses its attraction to low concentrations of sodium chloride after salt is associated with food deprivation (Appleby, 2012); animals deficient in nematocin or its receptor are defective in this form of learning. With the cell-level resolution possible in *C. elegans*, transgenic rescue implicated the otherwise uncharacterized interneuron AVK as the peptide source and the sensory neuron ASEL as its essential target for gustatory associative learning (Beets et al., 2012) (**Figure 1.2:** B).

Long-term memory formation in Sepia officinalis

At the opposite end of invertebrate complexity, the cuttlefish *S. officinalis* has a large brain size consistent with the notable cognitive abilities of cephalopods. In most animals, oxytocin-expressing neurons are localized to a few central areas, but in the decentralized nervous system of *S. officinalis*, oxytocin-producing neurons are scattered throughout the body (Henry et al., 2013) (**Figure 1.2:** D). The two oxytocin-related peptides of cuttlefish show overlapping but distinct expression patterns, and are present in the neural centers that are involved in learning, the vertical lobe complex and the optic lobes (Bardou et al., 2009) (**Figure 1.2:** D).

S. officinalis demonstrates cognitive learning abilities that modify innate behaviors. Hatchlings feed on the same kind of prey and use similar capture strategies as adults (von Boletzky, 2003). Gradual increases in prey capture behavioral plasticity and

learning occur simultaneously with the maturation of specific brain structures including the vertical lobe complex (Dickel et al., 2001). Notably, the number of cells that express oxytocin-related peptides increases dramatically in the vertical lobe complex and optic lobes in the timeframe that these behaviors mature (Bardou et al., 2010b).

Direct functional evidence supports a role for oxytocin-related peptides in learning and memory. Intravenous injection of cephalotocin in to *S. officinalis* enhanced memory retention 24 hours after training in a passive avoidance task (learning not to strike its tentacles at inaccessible prey held in a glass tube). Octopressin enhanced memory retention at a low dose, but attenuated it at a high dose (Bardou et al., 2010a).

Food arousal states in Aplysia californica

In the gastropod sea slug *Aplysia californica*, an oxytocin-related peptide is present in the abdominal ganglion and in two neurons in the pedal ganglia, with axonal fibers running throughout the CNS (Martinez-Padron et al., 1992) (**Figure 1.2:** E). Application of conopressin to the abdominal ganglion suppressed the siphon-evoked gill withdrawal reflex, and increased the frequency of spontaneous gill movements. These two behavioral effects resemble the food-aroused state in *A. californica* (Martinez-Padron et al., 1992), but their full significance is unknown.

Oxytocin as poison: proto-venom in Conus tulipa

Evolution is opportunistic, making use of available tools to solve biological problems, and this principle applies to oxytocin-related peptides. The venomous marine conesnails *Conus tulipa*, *Conus geographus*, and *Conus striatus* all secrete variants of

conopressin in their venom, which suggests that these peptides act not on the snail but on its prey, *e.g.* teleost fish. Conopressin-T is a strong, selective antagonist to the human vasopressin receptor V1a and a weak agonist for both the vasopressin receptor V1b and the oxytocin receptor (Dutertre, *et al.* 2008). It is not yet known how conopressin-T affects the envenomed fish, but exogenously applied vasotocin causes reduced physical activity in a cichlid fish (Huffman et al., 2015).

Summation

Reproductive behavior is a common thread in the evolution of oxytocin from roundworms to humans. In some of the more extensively studied invertebrate species, such as *L. stagnalis*, *C. elegans*, and *H. verbana*, oxytocin seems to play a role in providing organization and coherence to a complex mating behavior (De Boer et al., 1997; Garrison et al., 2012; Wagenaar et al., 2010). This role is likely achieved through modulation of multiple circuits and through coordination with other neuromodulators, such as APGW-amide in *L. stagnalis*. Oxytocin-like peptides can regulate mating behaviors in a sexually dimorphic manner, affecting one or both sexes, or helping a hermaphrodite switch between male and female behaviors. They can influence a particular behavior in opposite directions depending on the species: conopressin in *L. stagnalis* inhibits egg-laying, while annetocin in *E. foetida, W. pigra,* and *H. verbana* induces egg-laying.

Oxytocin-related peptides show both conservation and plasticity in their functions among the invertebrates. The peptide and its receptors are found throughout *Bilateria*, undergoing secondary loss in some lineages (**Figure 1.1**). In *Platyhelminthes* and *Rotifera*, the loss seems to be accompanied by a global reduction in the complexity of the animal,

including the de-emphasis on sex as a reproductive strategy. On the other hand, in arthropods, the loss occurs in lineages that have some of the most complex courtship behavior among invertebrates. We speculate that oxytocin-related peptides help individual animals to choose between *alternative* reproductive pathways. The choice between alternatives (and therefore the requirement for oxytocin-related peptides) would be particularly important in animals with highly flexible mating strategies, like hermaphrodite invertebrates that show both male and female behaviors, as well as mammals with complex, context-dependent reproductive behaviors; it might be less important in animals with fixed mating strategies.

Oxytocin-related peptides participate in learning and memory in cephalopods, and they drive both reproductive and learning behaviors in *C. elegans*. In mammals, the reproductive and learning roles of oxytocin are directly linked: pairing oxytocin with pup calls enhances neuronal responses to those calls in auditory cortex, thereby driving learning in maternal behavior (Marlin, *et al.* 2015). This example of coupled reproductive and learning roles shows how a single molecule, oxytocin, can drive increasingly more complex behaviors in complex brains.

The receptors for oxytocin-related peptides are critical for understanding the mechanisms of the peptide's function in behavior, and should be investigated more intensively in their natural settings *in vivo*. The well-defined invertebrate nervous systems can be exploited to ask which G protein signaling pathways and target molecules are regulated by the peptides, whether these signaling pathways are different in different neuronal circuits, and how receptor activation alters circuit function as a whole.

Although oxytocin can be a systemic signal – as it is in mammalian birth – most oxytocin signaling is likely to be regional, involving extrasynaptic diffusion to targets across various distances. Because extrasynaptic signaling does not require precise point-to-point connectivity, it is intrinsically evolvable. Small genetic changes in cis-regulatory elements, such as promoters and enhancers, could lead to alteration in expression patterns of oxytocin-related peptides and their receptors, thereby creating, destroying, or changing circuits without altering anatomical connectivity. These types of gene expression changes could underlie rapid adaptations in behavior (Young, *et al.* 1997). Better tools for measuring receptor expression patterns and receptor signaling activities are required to address this question in closely related species that have differences in oxytocin-mediated behaviors.

Oxytocin-related peptides have been studied extensively using pharmacological tools in invertebrates, but only in *C. elegans* has this study extended to genetics. Genetics has a remarkable ability to surprise, by uncovering biological functions that had never been suspected, as well as power to dissect known functions. In the past, however, it has not been an option for most invertebrate species. New genome editing technologies such as CRISPR should make it possible to generate both global and cell-type specific oxytocin-deficient mutants in a wide array of non-model organisms. As a complement to the addition of exogenous peptide, it will be possible to disrupt the endogenous peptide or receptors and assay natural behavior in intact animals. Genome editing could also provide a way to deliver transgenic tools for optical sensors of neural activity such as GCaMP, as well as chemo- and opto- genetic molecular tools to precisely manipulate the cells and circuits used by oxytocin and other neuromodulators.

In this review we have focused primarily on behaviors performed by adult animals. There is much left to discover about the ontogeny of oxytocin-mediated behaviors. In addition to the studies in *S. officinalis* (Bardou, *et al.* 2010), oxytocin-related peptides and receptors are expressed in the larval stages of several invertebrates including *C. elegans* (Garrison et al., 2012) and *T. castaneum* (Stafflinger et al., 2008), sometimes at much higher levels than in adults. It would be interesting to investigate the developmental and/or physiological roles of oxytocin-like peptides during the maturation of these animals.

Invertebrate models have much to offer our understanding of how oxytocin influences circuit function to generate behavior, and how behaviors rapidly evolve despite the strong genetic and functional conservation of oxytocin and its receptors. Future studies should take a comparative approach to integrate genes, cells, circuits, and behavior in diverse animals, to define what is fundamental and what is accidental in the relationship between oxytocin-related peptides and behavior.

CHAPTER II: THE ETHOLOGY OF *CAENORHABDITIS* MATING

Introduction

The nematode roundworm *Caenorhabditis elegans* provides an ideal model for deep, ethological inquiry into reproductive behavior. More than merely a composite of sensory inputs and responses, male mating behavior in *C. elegans* recapitulates all of the qualities described in ethologically relevant behavior. Male mating is innate, not learned. The first attempt at mating is often the most successful. Male mating is spontaneous, elicited by an internal drive, not merely by the presence of the stimuli. Males participate in what ethologists describe as *vacuum activity* (Tinbergen, 1951), sexually scanning themselves or each other in the absence of mates. Finally, male *C. elegans* reproductive behavior can be broken down into its components with *supernatural stimuli*. In one study, paraformaldehyde-fixed hermaphrodites were sufficient to suppress male exploratory behavior (Barrios et al., 2008). Taken together, this suggests that mating behavior is governed largely by what the ethologists described as *innate releasers*, which correspond in part to what scientists now know to be neuromodulators like non-canonical neurotransmitters (serotonin, dopamine, etc.) and neuropeptides (flps, nlps, neurophysins, etc.). Indeed, neuromodulatory *releasers* have been implicated in the regulation of male mating behavior for 35 years, and continue to be in current research.

The classical ethologist Niko Tinbergen provided a philosophical framework for asking biological questions about behavior based on Aristotle's four αιτια, or "causal explanations" (Aristotle, 1970; Tinbergen, 1951). A summary of them and their organization as Tinbergen conceived of it are presented in **Table 2**. According to Tinbergen, explanations can be broken down into two perspectives, the static and dynamic,

and two viewpoints, the proximate and the ultimate. These then interact with each other to provide four distinct forms of inquiry of explanation: mechanistic, developmental/ontological, functional/adaptive, and phylogenetic/evolutionary.

Table 2: Table of Categories for Questions and Explanations. Based on the chart in Nikolaas Tinbergen's *Study of Instinct*, this presents the 4 modalities of inquiry for the ethologist.

		diachronic vs. synchronic perspective	
		Static View: *Explanation of the current form of species*	**Dynamic view** *Explanation of current form in terms of a historical sequence*
How vs. Why Questions	**Proximate view** ***How*** an individual organism's structures function	**Mechanism (causation)** Mechanistic explanations for how an organism's structures work	**Ontogeny (development)** Developmental explanations for changes in ***individuals***, from DNA to their current form
	Ultimate (evolutionary) view ***Why*** a species evolved the structures (adaptations) it has	**Function (adaptation)** A species trait that solves a reproductive or survival problem in the **current** environment	**Phylogeny (evolution)** The history of the evolution of sequential changes in a ***species*** over many generations

The research literature on *Caenorhabditis* mating behavior already provides a framework for pursuing studies that touch all four of these modalities of inquiry. In this chapter, I intend to highlight the work previously conducted within an ethological narrative, focusing specifically on chemical and neuromodulatory signaling in the male that governs this complex reproductive behavior. I will begin by discussing the behavior,

then briefly touch on what is known about male physiology. From there, I will take time to discuss the contributions that the chemical signals serotonin, acetylcholine, dopamine, and the neuropeptides make to male mating behavior. Finally, I close with a brief discussion of the mating behavior of other species, including female behavior in closely related, purely sexual species.

The behavior

The mating behavior of the male *C. elegans* can be broken down into distinct steps, or sub-behaviors (Liu and Sternberg, 1995). These steps are referred to as sub-behaviors, and not behaviors, because they are not independent of one another, but rather they build upon one another: one leads to the next. They are also, however, not a rigidly fixed motor program. The redundancy in sensory feedback at each step allows the male to respond to his dynamic environment with plasticity (Liu and Sternberg, 1995). In their 1995 paper, Liu *et al.* describe the steps of male mating behavior that largely still frame experimental studies in mating behavior today.

Contact

All male mating in *C. elegans* begins when the male's tail, his sexual organ, makes contact with the hermaphrodite mate. This can occur either dorsally or ventrally, and there are ray sensilla oriented in either direction for each scenario (Liu and Sternberg, 1995). Ventral facing rays are redundant with the hook, post-cloaca sensilla (p.c.s.), and spicules in initiating a sexual response to contact (Liu and Sternberg, 1995). Response to contact is defined as the occurrence of three events: the halting of forward motion, the placement of the ventral side of the male tail against the body of the hermaphrodite, and the initiation

of backwards scanning (Liu and Sternberg, 1995). I define this as a categorical behavioral trait, either happening or not, with no time component.

Backing

Once *contact* has been made, male animals scan the body of the hermaphrodite through backward locomotion. This is done at varying speeds, and for varying durations (Garrison et al., 2012; Liu and Sternberg, 1995), Thus, *backing* is a quantitative behavioral trait. Males in which the hook sensilla have been ablated protract their spicules and engage in a slower *backing* behavior, for example (Liu and Sternberg, 1995). For the purposes of my study, I combine *backing* and *turning* under the category of *vulva search*.

Turning

When the male approaches the head or tail of the hermaphrodite, he must execute a turning motion requiring the coordination of his entire body. The *turn* can be broken into two components: the sharp ventral arch, and the proper timing of that arch behavior (Liu and Sternberg, 1995). *Turning* can be broken into its components genetically and through neuronal manipulation (Liu and Sternberg, 1995; Liu et al., 2007). Males with rays 7-9 ablated are unable to regulate *turning* timing, and swim off the end of the hermaphrodite (Liu and Sternberg, 1995). Dopamine-deficient animals, affecting rays 5, 7, and 9, have defects in executing the "arch," and make sloppy, wide turns (Liu and Sternberg, 1995).

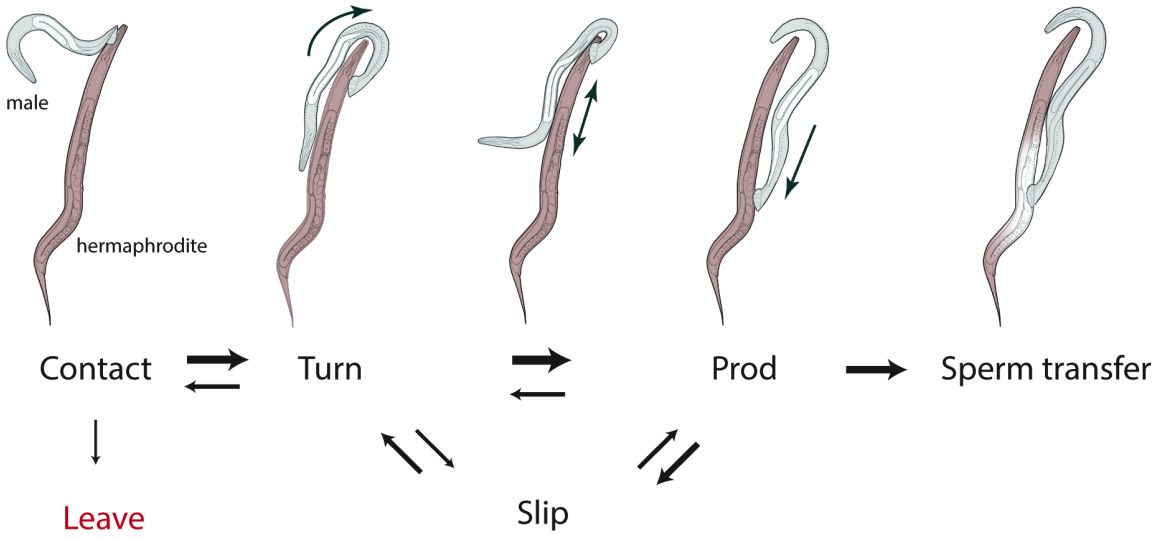

Figure 2.1: A step-by-step schemata for male *C. elegans* mating. Hermaphrodite is depicted in brown, male is depicted in gray, and sperm is depicted in white. Sub-behaviors are labeled below the illustrations that represent them. Arrows represent transitions between the sub-behaviors. The sub-behavior *Leave* is represented in red.

Prodding

In the wild-type, un-manipulated male *C. elegans*, vulva location and spicule insertion are inseparable, and so are given the collective name *prodding* (Garrison et al., 2012). *Prodding* begins with the cessation of backward motion at the location of the hermaphrodite's vulva, followed by thrusting as the male attempts to insert its spicules. This tends to be the most difficult step of mating behavior for wild-type males to accomplish, and the step at which males fail if they are unable to mate in the 5 minutes provided by the assay.

Slipping

Liu, *et al.* conceived of *slipping* behavior as part of vulva location/spicule insertion, but Garrison *et al.* reported it as its own, "non-productive" behavior in a 2012 *Science* article. *Slipping* is defined as the repetitive back and forth rubbing of the male with his tail

along the body of the hermaphrodite. This occurs sometimes along a part of the body directly proximate to the vulva, but also can occur along the body at other locations. It differs from *backing* because it is not a scanning, backward only locomotion. The male often will arch his body away from the mate when *slipping*, as opposed to keeping it close and straight as he does in *backing*. While I am uncomfortable making judgments about the productivity or unproductivity of mating sub-behaviors, I believe *slipping* is of a different character than *vulva search* or *prodding*, and that it is a deviation from the canonical motor program of mating behavior, perhaps a process that allows the male to respond to changing environmental cues.

Sperm transfer

Once the spicules are inserted, the anal sphincter contracts, allowing the cloaca to open and sperm to travel from the seminal vesicle to the vas deferens and into the hermaphrodite's uterus (Liu and Sternberg, 1995). Males transfer between 30 and 180 sperm in each ejaculation, and each transfer takes on average 4 seconds (Liu and Sternberg, 1995). Despite occurring quickly, males leave their spicules inserted into the hermaphrodite for an average of 27 seconds (Liu and Sternberg, 1995). This is thought to be a vestigial feature of a common nematode mating behavior that has been lost in the Bristol strain of *C. elegans'*: the deposition of a copulatory plug on the mated hermaphrodite.

Leaving

Leaving occurs when the male animal aborts mating prior to *sperm transfer* by disengaging contact with the hermaphrodite and swimming away. This was first described

as a sub-behavior in the Garrison *et al.* Like *contact*, *leaving* is not a quantitative sub-behavior, but rather a categorically scored sub-behavior.

Anatomy and physiology of male mating

Non-tail, male specific anatomy and physiology

Compared to the adult hermaphrodite nervous system, with 302 neurons, 8 of which are sex-specific (2 HSN and 6 VC neurons), the adult male nervous system has 383 neurons, 89 of which are sex-specific (Sulston et al., 1980). All but 22 of these neurons are located in the male tail, the sexual organ of the animal. Among the neurons that are not in the tail are the four CEM neurons, which are cholinergic, ciliated sensory neurons in the head that project dendrites into the male's nose (Knobel et al., 2008; Pereira et al., 2015). These neurons are responsible for the male's response to hermaphrodite-derived hormone via the TRPP2-like channel *pkd-2*/*lov-1* (Bae and Barr, 2008). The other 18 non-tail, male specific neurons are the nine CPs, of which CP1-CP6 are serotonergic (Serrano-Saiz et al., 2017b), and the nine cholinergic CA neurons, that run along the ventral chord of the male (Pereira et al., 2015). CA1- CA4 may also be serotonergic (Serrano-Saiz et al., 2017b). The CP7 and CP8 neurons also express the neuropeptide pigment dispersing factor (*pdf-1*), and all CPs express nematocin (*ntc-1*) (Barrios et al., 2012; Garrison et al., 2012). CP neurons have been implicated in the coordination of turning behavior (Loer, 1993).

The male tail

The male tail has a distinctive, fan-like anatomy that surrounds a cloaca from which protract the spicules, two needle-like tubes that are inserted into the hermaphrodite's vulva during copulation. The "fan" is made up of nine bilateral sensilla called the rays. Each ray

is innervated by two neurons: an A and a B neuron (Sulston et al., 1980). Rays 1, 5, and 7 have exposed ciliated

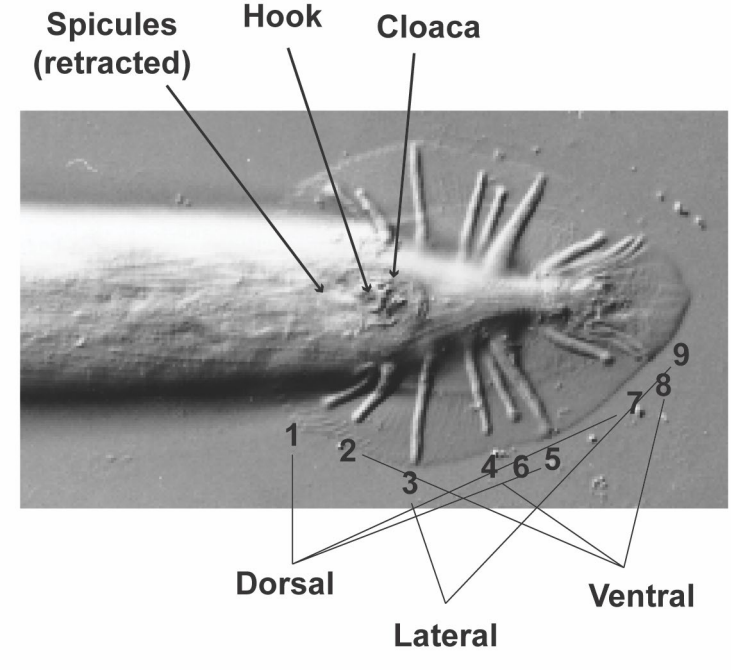

Figure 2.2: Anatomy of the *C. elegans* male tail. Ventral side up of the posterior portion of an adult male under DIC microscopy. Ray sensilla are labeled 1 through 9. Ventral facing, dorsal facing, and lateral facing rays are also indicated. Hook sensilla and cloaca are indicated with arrows, as is the approximate location of the retracted spicules inside the male's body. Photo adapted from (Nguyen et al., 1999).

endings that open dorsally and respond to dorsal contact (Liu and Sternberg, 1995). Rays 2, 4, and 8 open ventrally, and assist in ventral contact (Liu and Sternberg, 1995). Rays 3 and 9 open laterally, and Ray 6 does not have exposed ciliated endings (Liu and Sternberg, 1995). The "hook," located just anterior to the cloaca is also innervated by two sensory neurons, HOA and HOB, with two support cells (Sulston et al., 1980). Anatomy suggests that the HOA neuron, which terminates its ciliated, dendritic ending before reaching the hook opening, is mechanosensory, while HOB, which has a ciliated ending exposed externally through a socket in the hook, may be chemosensory (Barr and Garcia, 2006).

The post-cloaca sensilla (p.c.s) is innervated by three neurons: PCA, PCB, and PCC, and three support cells. It is responsible for communicating vulva location (Sulston et al., 1980). The spicule functions with SPC, a proprioceptive neuron associated with the spicule protractor muscles (Sulston et al., 1980). SPC works with SPV to successfully drive insertion of the male's spicules into the hermaphrodite's vulva (Liu and Sternberg, 1995). SPC also heavily innervates the male gonad, along with PCB and PCC, and likely plays a role signaling sperm transfer under the conditions of vulva contact and spicule protraction (Barr and Garcia, 2006).

61 of the male sex specific neurons are found in the male's tail (Sulston et al., 1980), but its sexual dimorphism runs deeper, both at the level of connectivity (Garcia and Portman, 2016) and in neurotransmitter/neuromodulator synthesis (Serrano-Saiz et al., 2017b). Neurons common between hermaphrodites and males show different connectivity in the different sexes (Garcia and Portman, 2016), as well as different neurotransmitter and neuromodulator expression (Serrano-Saiz et al., 2017b). For example, the embryonic M cell lineage is the progenitor for both the egg laying muscles and the spicule protractor muscles (White et al., 1986). Each of these muscles is innervated by cholinergic neurons (VC neurons in the hermaphrodite, PCC and SPC in the male). In addition, the hermaphrodite uses the neurotransmitter serotonin from the sex-specific neuron HSN to control the frequency and timing of egg-laying, while the male uses glutaminergic neurons, such as PCA, to control the frequency and timing of spicule protraction (Garcia and Portman, 2016).

Sometimes a neuron takes on an additional role in one sex compared to the other. The neuron DVA is used for locomotive control in both sexes, but also plays a large

neuromodulatory role in male mating by releasing nematocin (Garrison et al., 2012; Hums et al., 2016; Oranth et al., 2018).

Yet another example of sexually dipmorphic circuitry can be found in the varying responses of the two sexes to the same pheromone. Wild-type hermaphrodites are repulsed by the ascaroside C9, sensed by the neuron ADL, while males are attracted to it. Jang, *et al.*'s model suggests that sexual dimorphism in ADL's response to C9 balances the antagonistic circuit with RMG and ASK, thereby decreasing avoidance and promoting attraction (Jang et al., 2012).

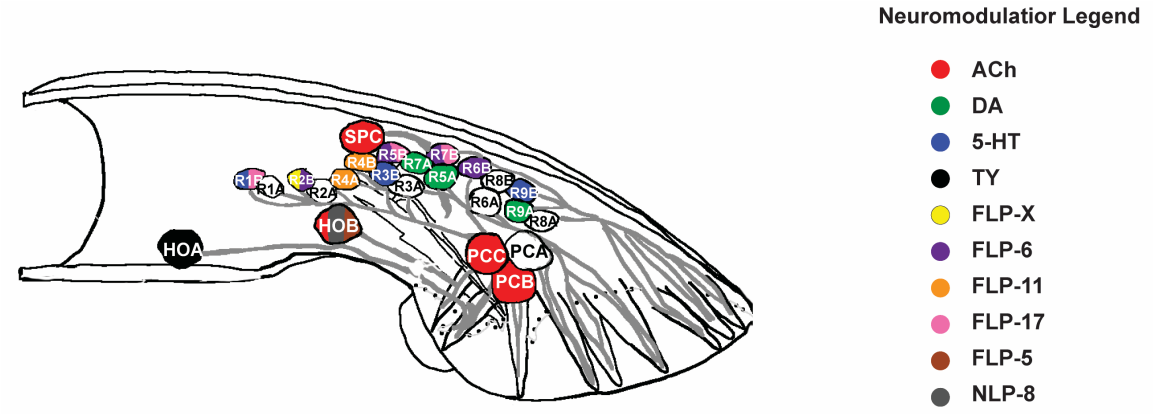

Figure 2.3 Expression of neuromodulators in male sensory neurons. *Left*, schemata of the *C. elegans* male tail with labeled sensory neurons. Dendritic projections are in *light gray*. *Right* color legend for neuromodulator identity. Neuron color represents the presence of the corresponding neuromodulator. Neurons with two or more neuromodulators are striped with corresponding color. While acetylcholine is a classical neurotransmitter (signaling to excitatory and inhibitory channels, not G-coupled protein receptors), I include it in this diagram for two reasons. One, it is the most broadly expressed neurotransmitter in the male nervous system. Secondly, it has an antagonistic role with dopamine, so knowing its sites of expression is important to understanding the many ways in which dopamine neuromodulates male mating.

Figure 2.3 shows neuromodulator expression in sensory neurons of the male tail. Many of these neurons also express the classical neurotransmitters glutamate and GABA, but those is not depicted (Serrano-Saiz et al., 2017b). The two main points to take away from this figure are 1.) there is a tremendous amount of neuromodulatory signaling in the male tail; and 2.) many of the neurons release more than one modulator, and therefore likely participate in different circuits involved in carrying out male reproductive behavior. A few neurons shared between hermaphrodites and males also show sexually dimorphic neurotransmitter expression. AIM in the animal's head is glutaminergic in hermaphrodites, and cholinergic in males (Serrano-Saiz et al., 2017b). PHC, a sensory neuron in hermaphrodites and a hub neuron in males, scales its glutamate levels in a sexually dimorphic manner (Serrano-Saiz et al., 2017a), and the sex-shared neuron AVG dimorphically scales its acetylcholine levels (Serrano-Saiz et al., 2017b). Finally, PVN, upon maturation in males, begins to express glutamate in addition to the cotransmitter acetylcholine (Serrano-Saiz et al., 2017b). These neurotransmitter expression patterns provide an inviting starting point to investigate the mechanistic, functional, developmental, and evolutionary features of *C. elegans* reproductive behavior.

In the next section, I will briefly discuss what is known about the male reproductive behaviors governed by these neuromodulatory circuits.

Serotonin in mate search and tail curling

The connection between serotonin and the modulation of mating behavior is seductive, especially in light of the well-established fact that loss of libido is a common side effect to SSRI antidepressants (Montejo et al., 2001). A loss-of-function mutation in

the serotonin reuptake transporter of *C. elegans*, *mod-5*, abolishes mate search behavior (Emmons and Lipton, 2003), and *tph-1* mutant males, deficient in serotonin, leave patches of food where mates are present less than wild-type males (Lipton et al., 2004), suggesting that excess serotonin decreases the drive for males to mate, while lower levels increases it. Serotonin is also known to play a role in the turning behavior of male mating. Loer and Kenyon discovered that the addition of serotonin causes male *C. elegans* and not hermaphrodites to curl their tails ventrally (Loer, 1993). Ablation of the male-specific, serotinergic CP neurons led to males making sloppy turns during mating and the inability to make the tight, ventral turns seen in wild-type male behavior (Loer, 1993). Thus, serotonin regulates reproductive behavior of male *C. elegans* at least two levels: the level of motivation in mate search, and in full body coordination when conducting the complex locomotive task of executing a turning during vulva search.

Dopamine and acetylcholine in copulation and intromission

Acetylcholine is the most broadly used neurotransmitter in the male *C. elegans* sexually dimorphic circuitry (Pereira et al., 2015). Male-specific neurons can be divided into 24 classes, and of those, 16 are cholinergic (Pereira et al., 2015), including the CEMs, the CAs, and many of the tail sensory-motor neurons that synapse directly onto muscles (Liu et al., 2011; Pereira et al., 2015).

Dopamine antagonizes the cholinergic mating circuits of male vulva location, spicule protraction, intromission, and sexual satiation/recovery (Correa et al., 2012; Correa et al., 2015; LeBoeuf et al., 2014). Dopamine-deficient males have precocious spicule protraction. The same phenotype can be recapitulated pharmacologically with an

acetylcholine agonist, and reversed by the exogenous application of dopamine (Correa et al., 2012). Mutant males lacking D2-like dopamine receptors *dop-2* and *dop-3* were unaffected by the addition of dopamine (Correa et al., 2012). These inhibiting, dopamine receptors are expressed both in cholinergic neurons involved in copulation (such as PCB) and copulation musculature. The *dop-2;dop-3* double mutant displays less rhythmic mating behavior that results in more random, sustained prods of rapid, shallow thrusting (Correa et al., 2012). Dopaminergic ray neurons (R5A, R7A, and R9A) display calcium transients upon vulva location during mating, and R7A shows transients when cholinergic p.c.s. neurons PCB and PCC are stimulated (Correa et al., 2012). Dopamine also modulates communication between the cholinergic neurons of the p.c.s (PCB and PCC) and the glutaminergic neurons of the p.c.s. and hook sensilla (PCA and HOA) via a D2-like receptor (Correa et al., 2015). Finally, dopamine release from the socket support cells of the spicule, not the neurons, promote ejaculation and extend refractory periods post-coitus, presumably by modulating the cholinergic spicule neurons SPV and SPD, which innervate the gonad (LeBoeuf et al., 2014). Thus, at many levels of the mating circuit, dopamine antagonizes the sensory/motor cholinergic neurons to direct the movement and repetitions of mating behavior in a goal-oriented fashion.

Neuropeptides in C. elegans mating

Neuropeptides regulate *C. elegans* mating behavior on the level of motivation/drive (Barrios et al., 2012), global organization (Garrison et al., 2012), execution of complex steps in mating (Liu et al., 2007), and behavior in response to the presence or absence of larvae (Scott et al., 2017). The FMRF-like neuropeptides *flp-8, flp-10, flp-12,* and *flp-20*

regulate wild-type turning during male mating (Liu et al., 2007). By rescuing the ubiquitous neuropeptide processing enzyme *egl-3* in specific neurons, Liu and researchers determined that the touch receptor neurons, shared by males and hermaphrodites, are the sources of these neuropeptides relevant to the turning phenotype. *flp-8* expression specifically in PVM rescued turning behavior, a neuron previously thought not to have a function (Liu et al., 2007). This regulation is directly mediated by the touch neuron's response to touch, and independent of serotonergic signaling (Liu et al., 2007).

With the neuropeptide *pdf-1*, Barrios *et al.* was able to: 1.) dissect appetitive and consummatory reproductive behavior of the *C. elegans* male; and 2.) demonstrate how a circuit and peptide common between the sexes can be coopted for two sexually dimorphic purposes (Barrios et al., 2012). *pdf-1* and *pdfr-1* mutant males were defective in mate exploratory search behavior and responded less "avidly" to hermaphrodite contact (appetitive behaviors), but were able to mate with the competency of wild-type males (consummatory behavior) (Barrios et al., 2012). PDF-1 promotes sexual exploratory behavior in male *C. elegans* (Barrios et al., 2012), and foraging exploratory behavior in hermaphrodites (Flavell et al., 2013). Overexpression of PDF-1 in males led to a two-fold increase in male exploratory behavior dependent on the PDFR-1 receptor, whereas overexpression in hermaphrodites did not lead to increased exploratory behavior (Barrios et al., 2012). Laser ablation and genetic rescue experiments indicate that the common interneuron AIM is the relevant source of PDF-1 for male exploratory behavior (Barrios et al., 2012). Interestingly, AIM is the neuron that Pereira *et al.* report switching neurotransmitter expression, from glutamate to acetylcholine, between hermaphrodites and males (Pereira et al., 2015).

The oxytocin homolog nematocin has been shown to regulate both appetitive and consummatory behaviors of male *C. elegans* mating, from hermaphrodite contact, to turning, to vulva prodding efficiency (Garrison et al., 2012). Like, *pdf-1*, nematocin is released from the two neurons shared between males and hermaphrodites: AFD in the head and DVA in the tail (Garrison et al., 2012). Unlike *pdfr-1*, however, nematocin's receptors NTR-1 and NTR-2 express predominately in male-specific neurons, especially in the tail (Garrison et al., 2012). Garrison, *et al.* demonstrate that DVA is the primary source of nematocin for male mating behavior by knocking the gene out in DVA specifically, and showing these males recapitulate the majority of the mating defects. Thus, it would seem that DVA has been coopted for a new function in the male *C. elegans* mating circuitry. It has also been suggested that nematocin is responsible for suppressing adult exploratory behavior in the presence of conspecific larva (Scott et al., 2017).

The girls: mating ethology of other Caenorhabditis species

Up until this point, I have only discussed the mating behavior of male *C. elegans.* Furthermore, the majority of these experiments were performed on hermaphrodite mating partners with either genetically, pharmacologically, or physically compromised locomotion, to effectively observe and quantitatively score the male behavior. But males are only half of the story in *Caenorhabditis* mating ethology. In this section, I turn my attention to what is known about hermaphrodite and female mating behavior.

Looking at the *Caenorhabditis elegans* species alone, one might conclude that hermaphrodites do not have any mating behavior at all. Young adult hermaphrodite *C. elegans* actively "buck" and run away from a male attempting to mate (Garcia et al., 2007).

They also "pinch" off their vulva to avoid spicule insertion (Garcia et al., 2007). This avoidance dissipates as the hermaphrodite ages, however, and hermaphrodites that have been adults for 72 hours move less and are much more effectively inseminated than their 24 hour counterparts (Garcia et al., 2007). *fog-2* mutants, lacking hermaphroditic sperm, showed less escape behavior than their wild-type counterparts, but were not permissive to spicule insertion, suggesting that the behavior of the 72 hour adults is a combination of age and sperm depletion (Garcia et al., 2007).

Garcia *et al.* examined mating in three *Caenorhabditis* species closely related to *C. elegans*: *C. briggsae* (hermaphroditic with males), *C. remanei* (pure sexual), and *C. brenneri* (pure sexual). Neither the 24 nor the 72 hour *C. briggsae* hermaphrodites mated efficiently, but females in both

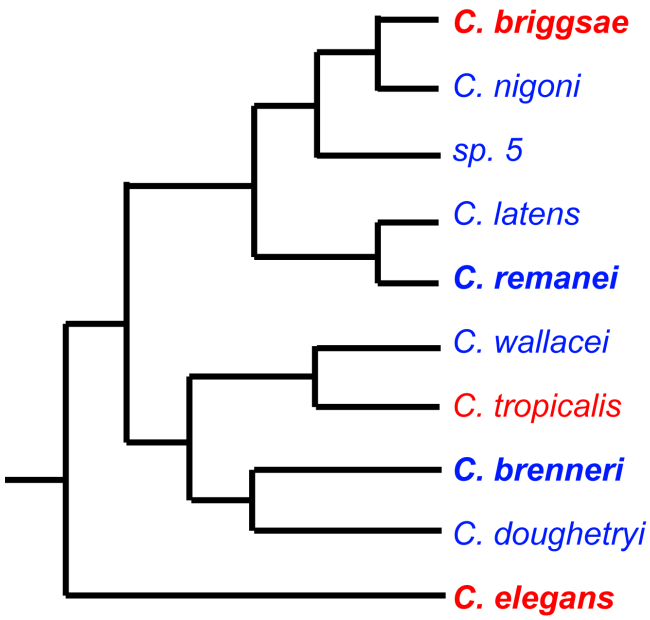

Figure 2.4: Phylogeny of the *Caenorhabditis* clade. Hermaphrodite-male species are indicated in *red*, male-female species are indicated in *blue*. Species discussed in this section are indicated in **bold.**

sexual species mated almost instantaneously due to an induced quiescence in the female partner (Garcia et al., 2007). *C. briggsae* males could induce the quiescence in the *C. remanei* female, but male *C. elegans* could not, perhaps because *C. briggsae* are more closely related to *C. remanei* (**Figure 2.4**; Garcia et al., 2007). Ablating the vulva precursor cells in *C. remanei* females destroyed the quiescent behavior (Garcia et al., 2007). Ablating the p.c.s. neurons in males partially reduced female quiescence, but when p.c.s. neurons were ablated in combination SPC in males, female escape behavior resembled that of the hermaphroditic species (Garcia et al., 2007). Interestingly, ablating the gonad of the male, as well as the Linker Cell, which connects the gonad to the spicule via the vas deferens in male development, also destroyed female quiescence, suggesting the male signal has its source in the gonad (Garcia et al., 2007).

The females of sexual *Caenorhabditis* species also exhibit an additional, social sexual behavior. When a mating pair initiates mating, females will swarm to the pair to form a mating ball around the male (Markert and Garcia, 2013). The cue is given through a volatile pheromone also delivered through the male's gonad when he comes in contact with a mate (Markert and Garcia, 2013). Ablating the gonad of the male destroys the attractive behavior (Markert and Garcia, 2013). Recently inseminated females lose the ability to be attracted to the mating couple, but regain it as time passes, suggesting that females also have something analogous to a "refractory period" (Markert and Garcia, 2013). The pheromone cue is species dependent. A *C. brenneri* mating couple cannot elicit the attraction of *C. remanei* females, nor can a *C. brenneri* male mating with a *C. remanei* female attract other *C. remanei* females (Markert and Garcia, 2013). The behavior is not seen in either *C. briggsae* or *C. elegans* hermaphroditic species.

Summation

The richness of behavior, current knowledge, and experimental tools available for *Caenorhabditis* mating behavior makes it an ideal model to pursue behavioral neuroscience in the ethological tradition. Foundations in neural connectivity (Jarrell et al., 2012), neurotransmitter expression (Serrano-Saiz et al., 2017b) and a well-characterized, replicable behavior (Liu and Sternberg, 1995) have elucidated mechanistic (Correa et al., 2015; Liu et al., 2011), functional (Barrios et al., 2012; Liu et al., 2007), ontological (Lints et al., 2004; Serrano-Saiz et al., 2017b), and evolutionary (Garcia et al., 2007; Markert and Garcia, 2013) insights into the nature of this complex and essential activity that nematodes must perform robustly, precisely, carefully, and flexibly all at the same time. With the advent of emerging molecular (Xu, 2015), imaging (Hudson, 2018), circuit manipulation (Husson et al., 2013), and computational (Anderson and Perona, 2014) tools and methodologies, I believe the field can expect to enjoy an even more synthetic picture of reproductive behavior and other behaviors of its kind.

CHAPTER III: PHARMACOGENETIC SILENCING OF DVA DURING MATING

Rationale for the experimental approach

An important feature to establish when studying the relationship between neuromodulators and behavior is the appropriate time scale in which the neuromodulator acts. Neuromodulators such as biogenic amines, neuropeptides, and steroids can act over seconds, minutes, or hours to exert their effects. In addition, a modulator can act at one time in development to affect circuit function and behavior at a much later time. The nematode *C. elegans* has a single, oxytocin-related peptide, nematocin, which has been implicated in male mating efficiency (Garrison, et al., 2012). Males lacking nematocin show quantitatively poor performance in a time-restricted, five-minute mating assay. The essential source of nematocin in the male is a single neuron DVA (Garrison, et al. 2012). However, nematocin function has only been studied in knockout mutants that lack nematocin function for the lifetime of the male, and DVA function only after laser ablation early in life (Garrison, et al. 2012).

Two techniques offer acute and reversible neuronal silencing: optogenetics and pharmaco-genetics. Although optogenetics allows for much finer temporal resolution (Yizhar et al., 2011), *C. elegans* has a natural sensitivity to light (Liu et al., 2010), that could compromise its mating behavior. For this reason, I chose a pharmacogenetic approach to acutely silence DVA.

To silence DVA, I used the heterologous, histamine-gated chloride channel (HisCl) as described in Pokala *et al.* (2014). Males expressing HisCl can be placed in the presence of histamine just prior to mating, allowing them to develop without perturbation. In the presence of histamine, HisCl hyperpolarizes the neuron(s) in which it is expressed, thereby

silencing them. This process is reversible, and neurons will return to normal activity levels after an incubation period off histamine. Finally, histamine levels are titratable, allowing for the possibility of more refined follow up studies on DVA neuronal dynamics (Pokala et al., 2014).

DVA activity is required for efficient mating

HisCl (**Figure 3.1**) was expressed under the DVA-selective *nlp-12* promoter fragment previously described (Garrison et al., 2012) and expression was confirmed with mCherry tagged with the 2A peptide (Ahier and Jarriault, 2014). Epifluorescence and DIC microscopy confirmed expression in DVA (**Figure 3.1**) in both males and hermaphrodites.

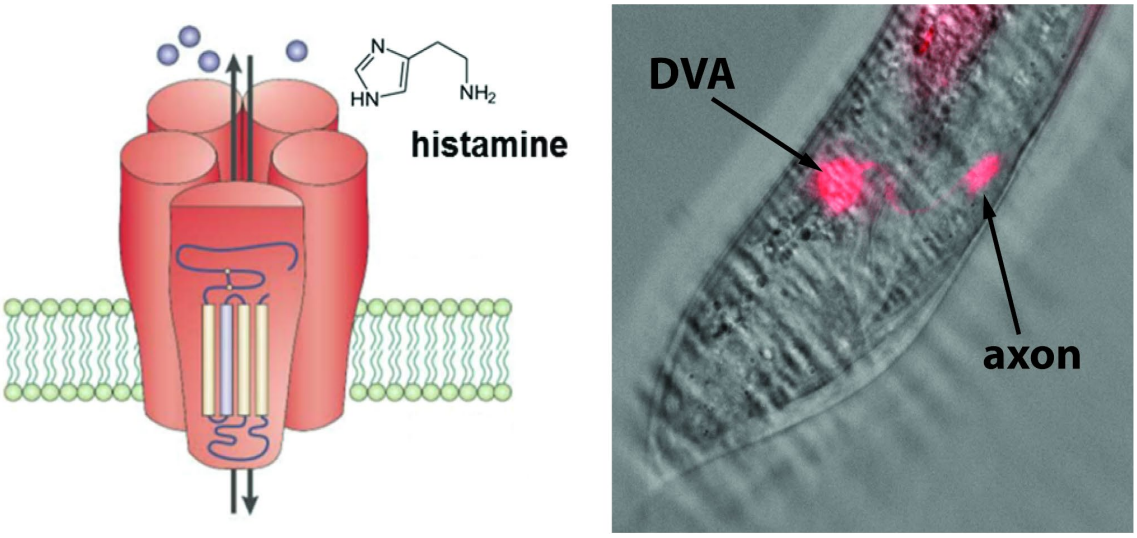

Figure 3.1 Diagram and expression of the histamine-gated chloride channel. *Left*: Pentameric schemata of the chloride channel in a lipid bilayer with the molecular structure of its ligand, histamine. *Right*: Overlay of epiflorescence and DIC microscopy images of an L4 male tail to show expression of HisCl under the *nlp-12* reporter fragment with an mCherry reporter. The DVA cell body and axon are labeled.

Mating of virgin males with nontransgenic *unc-64* hermaphrodites was videotaped for five minutes in the following conditions: males with no transgene and off histamine

(wild-type control); males with the HisCl transgene and off histamine; males with no transgene and on 10 mM histamine; and males with the HisCl transgene and on 10 mM histamine. Transgene-free males off histamine were controls for day-to-day variation in mating conditions. These controls were required to mate with at least 60% success rate (3/5) in order to keep the data from the day. Males with the HisCl transgene alone and in the presence of histamine alone were also tested to measure contributing effects of these reagents, if any. The experimental males with the HisCl transgene were incubated in the presence of histamine two hours prior to mating in order to silence DVA. A sample set of 20 was determined to the effective sample size to detect significant defects by a power calculation (*see* EXPERIMENTAL PROCEDURES *for details*). Mating results are shown below (**Figure 3.2**).

Wild-type and transgene positive animals in the absence of histamine mated at the same rate (**Figure 3.2**). In each, 17 out of 20 animals, or 85%, mated within five minutes. Wild-type animals exposed to histamine prior to the mating assay mated at a slightly lower rate that was not significantly different from the controls: 14 out of 20 or 70% mated within five minutes (**Figure 3.2**). This may suggest some effect of histamine itself on male mating. In animals both possessing the HisCl transgene and incubated in the presence of histamine, mating was significantly compromised (**Figure 3.2**). Only 8 out of 20 animals successfully mated in five minutes, or 40%. The Fisher's Exact Test with a False Discovery Rate multiple comparison correction yielded a p value of 0.016, statistically significant according to the ≤ 0.05 standard. This mating efficiency is comparable to that of males with *ntc-1* knocked out specifically in DVA (Garrison et al., 2012).

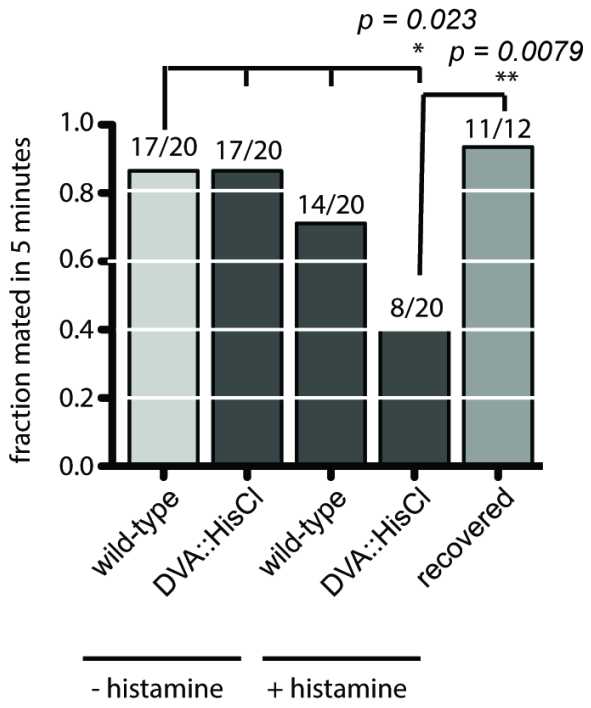

Figure 3.2: Mating efficiency of animals with pharmacogenetically silenced DVA. *x-axis:* the conditions and genotypes tested. DVA::HisCl indicates the presence of an integrated HisCl transgene expressed in DVA. "- histamine" indicates the absence of histamine, "+ histamine" the presence of 10 mM histamine. *y-axis*: the fraction of males that mated for each genotype/condition. Raw fractions are indicated above each bar. First bar (*light* gray) are the wild-type control animals. Bars 2-4 (*dark gray*) have the transgene (#2), histamine (#3) and both (#4). Last bar (*medium gray*) represents DVA-silenced males that did not mate in the first trial (4th bar) and were subsequently incubated off histamine for 2 hours before retesting (last bar). p-values for statistical significance were calculated with a Fisher's Exact Test with a False Discovery Rate multiple comparison correction.

The 12 animals that did not successfully mate in the presence of histamine were then moved to a histamine free incubation plate and allowed to recover for two hours. They were then retested for mating efficiency (**Figure 3.2**). 11 out of 12, or 92% of the animals mated during the second, histamine-free attempt. The result also yields a statistically significant p-value of 0.016 with the Fisher's Exact Test and a False Discovery Rate to

correct for multiple comparisons. This internally controlled experiment, combined with the externally controlled experiment of comparing two different sets of animals, indicate that DVA activity is necessary during mating.

The ethomics of male mating behavior

To examine the effects of DVA silencing on behavior in more detail, I tracked their behavior throughout the five-minute mating video, and constructed a model for dynamic mating behavior. I assigned each movie frame to the sub-behavior that the male was engaged in during that frame. Mating behavior was broken down into 6 sub-behaviors based on these categories (Garrison et al., 2012): *contact, vulva search, prodding, slipping, sperm transfer,* and *leaving.* For descriptions of how these behaviors are defined, please see **Chapter II: *The behavior***. *Contact, sperm transfer,* and *leaving* were deemed to be categorical sub-behaviors, meaning they either occurred or not, and time spent engaged in the given sub-behavior was not meaningful or relevant to the overall structure of mating behavior. *Vulva search, prodding,* and *slipping* were considered quantitative. Duration spent engaged in the sub-behavior was essential and meaningful to understanding the overall structure of mating behavior. **Figure 3.3** depicts a version of the mating ethogram in **Chapter II**, where the sub-behaviors have been condensed to the ones used for this study. It shows sub-behaviors, frequency of transitions between them (arrow weights), and schematic cartoons of the sub-behavior directly above them. Colors for each sub-behavior will be kept consistent in ethograms throughout this thesis: *blue* for *vulva search*, *green* for *prodding*, and *maroon* for *slipping*. **Figure 3.10**, at the end of this chapter, presents the raw mating traces for the DVA silencing experiment in wild-type animals.

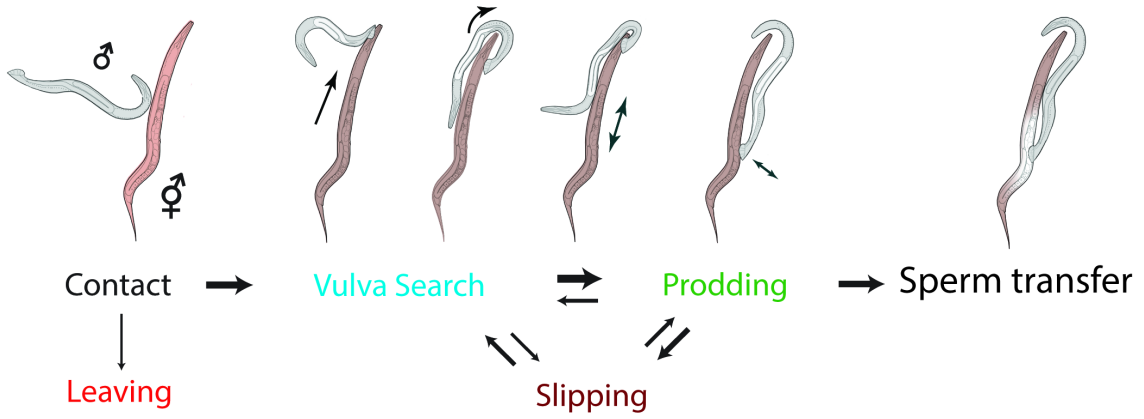

Figure 3.3: Condensed mating ethogram for wild-type male *C. elegans*. Males are depicted in gray and hermaphrodites are depicted in brown. Sub-behaviors are labeled below the cartoons that schematize them. Arrow weights depict transition frequencies as calculated in Garrison, *et al.*

Markov modeling of mating behavior

After tracking, the dynamics of mating behavior was modeled for all of the genotypes and conditions of the HisCl experiment tested. A Markov model was selected for a first attempt at modeling mating behavior for its simplicity. Transition probabilities were calculated for the frequencies that males moved between sub-behaviors. I used this model to determine how likely a male engaged in a given mating sub-behavior is to transition to another within an assigned time vector. One second was chosen as the time step, given its physiological relevance to mating behavior, which occurs on a time frame of seconds to minutes (*see* EXPERIMENTAL PROCEDURES). The means and standard deviations presented (full data in **Table 5** at the end of the chapter) were calculated by bootstrapping the empirical data of 20 animals over 1000 iterations (*see* EXPERIMENTAL PROCEDURES for a thorough treatment of this calculation). **Figure 3.8** presents the histograms of this bootstrapping. These bootstrapped distributions were then statistically compared to the experiment-to-experiment distribution of wild-type control data (*see* EXPERIMENTAL

PROCEDURES, **Table 15**). p values were calculated with an unpaired, two tailed student's t test, and statistical significance was determined with a False Discovery Rate multiple comparison correction. A summary of all statistically significant results are found in **Table 3**. Red font indicates a significant drop in transition probability compared to wild-type animals without histamine, and bold font indicates a significant rise in transition probability.

Figure 3.4 illustrates the results of silencing DVA on male mating behavior with quantitative ethograms. State durations for *vulva search*, *prodding*, and *slipping* were calculated as the percentage of mating behavior time spent engaged in the sub-behavior, represented as circle size (**Figure 3.4)** and associated numbers (*white*). Circle colors correspond to the color key in **Figure 3.4**. Arrow weights are representative of the transition probabilities between sub-behaviors, as calculated in the Markov model.

Table 3: Summary of significant results from Table 5. Mean transition probabilities for wild-type males(*w.t.*), males expressing the transgene (*+t.g.*), males on histamine with no transgene (*+his*), males both expressing transgene and on histamine (*+both*), and males after recovery (*rec.*) are shown. Mean values significantly higher than wild-type controls are in **bold**. Mean values significantly lower than wild-type controls are in *red*. Transition probabilities that present a pattern consistent with DVA silencing are indicated with an asterisk (*).

transition probability	w.t.	+ t.g.	+ his.	+ both	rec.
prod to vulva search*	0.20	**0.40**	0.13	**1.02**	**0.96**
prod to sperm transfer*	0.69	1.12	0.78	0.39	1.22
slip to vulva search*	1.70	**2.73**	1.23	1.12	**2.18**
slip to prod*	17.29	16.52	12.47	9.73	12.36

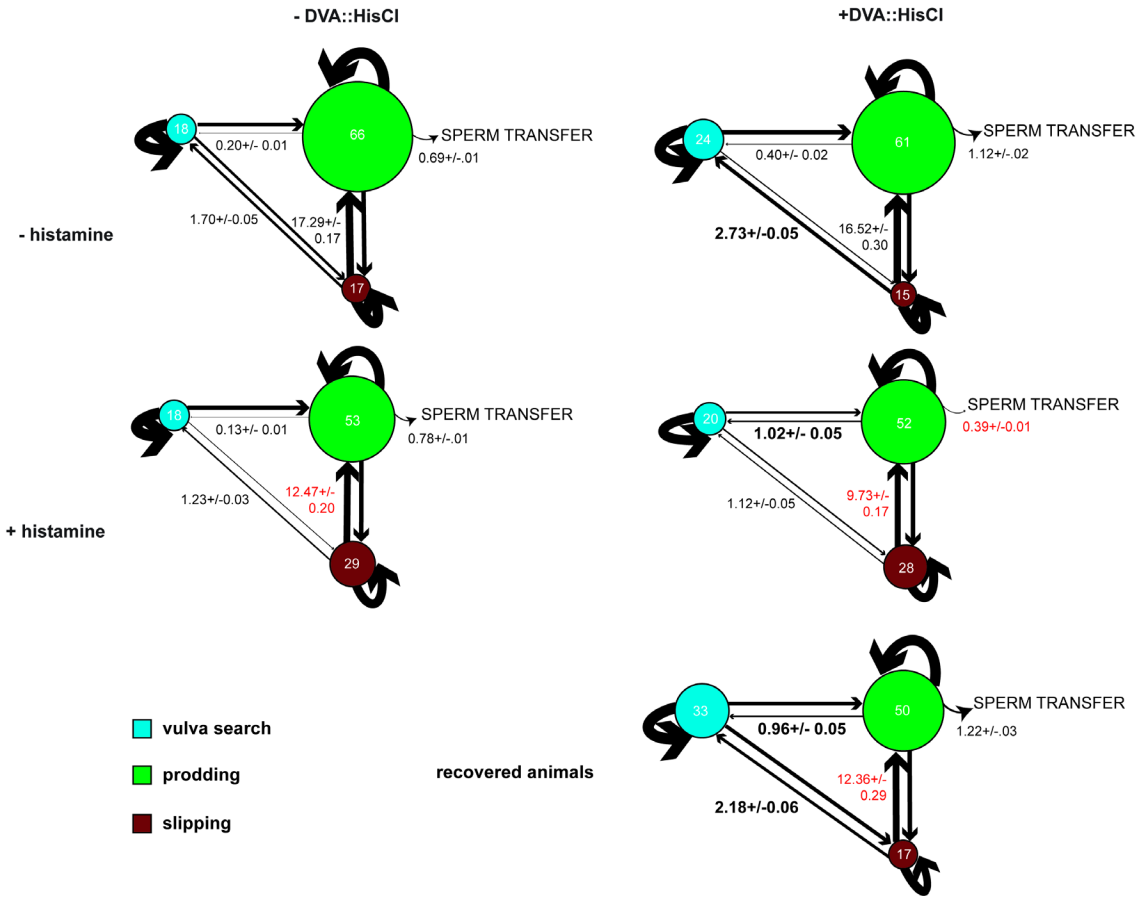

Figure 3.4 DVA silencing changes the dynamics of mating behavior. Numbers within a circle are the percentage of time in which the males engage in that sub-behavior when mating. Arrow weights represent the probability in a given second that the male will transition between the behaviors. Curved arrows pointing back toward the circle indicate the probability per second that the male will persist in the sub-behavior. *Left column* are ethograms of males without the DVA::HisCl transgene. *Right column* are males with the DVA::HisCl transgene. *Top row* are males tested in the absence of histamine. *Bottom row* are males tested in the presence of histamine. *Red* values illustrate statistically significant decreases, while **bold** values indicate statistically significant increases. Only transitions that were significantly affected by histamine silencing are presented (full data in **Table 5**).

Silencing DVA directionally affects transitions out of prodding state, and all transitions out of the slipping state.

When visualizing the ethograms, one is struck by how subtle and iterative the changes in transition frequency are that culminate in a significantly reduced overall mating efficiency. My statistical analysis of the DVA silencing experiment, however, reduced the problem from ten different transition probabilities to four transitions significantly perturbed by silencing DVA to an effect greater in size than the experiment-to-experiment variation in the control males. While the transgene slightly raises the *vulva search to prod* transition probability, from 0.20+/- 0.01% to 0.40+/- 0.02%, *vulva search to prod* transition probability more than doubles upon addition histamine, to 1.02+/- 0.05%, and remains elevated even after two hours of recovery off histamine. Because this value remains elevated even while mating efficiency is restored to wild-type levels (**Figure 3.2**), it is unlikely to be central for mating. *prod to sperm transfer* transition probabilities are less than half their value in the control data sets (**Table 3, Figure 3.4**), from 1.12+/- 0.02% to 0.39+/- 0.01%. *slip to vulva search* transition probabilities are elevated by the presence of the transgene alone, 2.73+/-0.05%, but drop with the addition of histamine, to 1.12+/- 0.05%, and recover to their elevated levels post recovery, 2.18+/-0.06%. Finally, *slip to prod* transition frequencies are slightly lower with the addition of histamine alone, from 17.29+/- 0.17% to 12.47+/-0.20%, still lower in the presence of both the transgene and histamine, 9.73+/-0.17%, and partially rebound after recovery off histamine to 12.36+/- 0.29%. Silencing DVA increases "backward" transitions out of *prodding* into *vulva search*, and decreases "forward" *prodding* transitions into *sperm transfer*. Both forward and

backward transitions out of *slipping*, into *vulva search* and *prodding* are affected by DVA silencing.

Acute silencing of DVA does not change mating efficiency in nematocin-deficient animals

The experiments to this point have identified acute effects of DVA on mating. Nematocin, however, is not the only neuromodulator produced by DVA, which also expresses the neuropeptide NLP-12 (Hu et al., 2011) and the neurotransmitter acetylcholine (Pereira et al., 2015). Consequently, there may be mating behavioral effects from silencing DVA that are not mediated by nematocin.

To parse the DVA-silenced behavioral phenotypes that are mediated by nematocin release from those that are not, I pharmacogenetically silenced DVA in nematocin-deficient males. Behavioral phenotypes that were mediated by nematocin release would not be further enhanced by DVA silencing and *vice versa,* whereas independent effects of nematocin deficiency and DVA-silencing would result in enhanced defects when the two manipulations were combined, compared to both alone. The raw traces of these ethograms can be found at the end of the chapter in **Figure 3.11**.

I first examined overall mating efficiency (**Figure 3.5**). 6/20 nematocin-deficient males mated successfully, or 30%, a fraction consistent with numbers previously reported (Garrison et al., 2012). Mating efficiency did not significantly change with the addition of the transgene or histamine alone (7/20 males, or 35% efficiency), nor did it change when DVA was effectively silenced in the males by the addition of both, 6/20 males or 30% efficiency. Animals that did not mate in the first instance were once again allowed to

recover off histamine for two hours before being retested. Those animals also had a similar mating efficiency of 4/14 or 29% efficiency. Thus, overall mating efficiency changed very little when DVA was silenced in nematocin-deficient males.

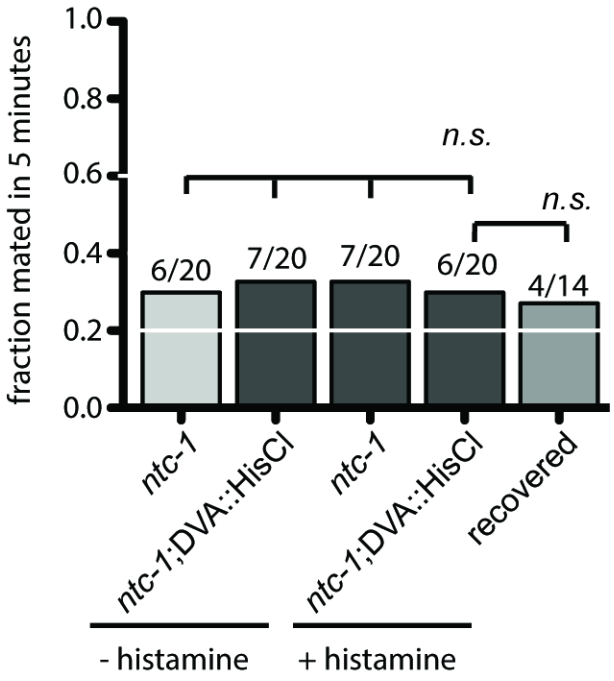

Figure 3.5 Mating efficiency of *ntc-1* males is not affected by DVA silencing. *x-axis:* the conditions/ genotypes tested. DVA::HisCl indicates the presence of an integrated HisCl transgene expressed in DVA. "- histamine" indicates the absence of histamine, "+ histamine" the presence of histamine. *y-axis*: the fraction mated of each genotype/condition. Raw fractions are indicated above each bar graph. First bar (*light* gray) is the nematocin-deficient control males. Bars 2-4 (*dark gray*) have the transgene (#2), histamine (#3) or both (#4). Last bar (*medium gray*) represents DVA-silenced, nematocin deficient males that did not mate in the first trial (4th bar graph) and were subsequently incubated off histamine for two hours before retesting (last bar graph). p-values for statistical significance were calculated with a Fisher Exact Test. Because there were no statistically significant results, no multiple comparison correction was performed.

DVA silencing in nematocin-deficient animals alters two of the four transition probabilities affected by DVA silencing in wild-type animals.

I then analyzed the mating behavior dynamics of silencing DVA in nematocin-deficient males with the Markov model (*see* EXPERIMENTAL PROCEDURES) in the same manner as before. Transition probability means and standard deviations are reported in **Table 6** at the end of the chapter**,** and the histograms from the data bootstrapping are presented in **Figure 3.9**. These distributions were then statistically compared to the experiment-to-experiment variability of nematocin-deficient males using a two-tailed, unpaired Student's t test to identify changes with meaningfully large effect sizes (**Table 16**). **Table 4** summarizes the statistically significant findings.

Table 4: Summary of statistically significant results from Table 5. Mean transition probabilities for wild-type (*w.t.*), expressing the transgene (*+t.g.*), on histamine with no transgene (*+his*), both expressing transgene and on histamine (*+both*), and after recovery (*rec.*) are shown. Mean values significantly higher than wild-type controls are in **bold**. Mean values significantly lower than wild-type controls are in *red*. Transition probabilities that follow a pattern consistent with HisCl neuronal silencing are indicated with an asterisk (*).

transition probability	w.t.	+ t.g.	+ his.	+ both	rec.
vulva search to vulva search	93.36	94.96	94.44	93.51	91.14
prod to vulva search*	0.73	0.77	0.74	**2.37**	**1.19**
prod to prod	96.95	93.00	94.52	93.00	93.82
prod to slip	2.04	**6.00**	**4.46**	**4.31**	3.81
slip to vulva search*	0.59	0.63	0.62	**2.26**	**1.43**
slip to prod	11.33	6.99	10.94	8.56	8.01

In this experiment, some of the statistically significant results followed a pattern consistent with DVA silencing, and some did not. *Vulva search to Vulva search*, that is, the tendency for the males to persist in *vulva search* was only significantly lower after two hours recovery (**Table 4**), from 94.96+/- 0.08% to 91.14+/- 0.04% (**Figure 3.6, Table 4**).

prod to prod transition probabilities, the tendnecy to persist in *prodding* were lower with the addition of the transgene and the addition of histamine alone, but did not lower any further upon the additon of both (transgene alone: 93.00+/- 0.11% v.s. transgene and histamine: 93.00+/-0.13%, **Figure 3.6, Table 4**). A similar pattern is seen with *slip to prod* transitions, lowered by the transgene alone (6.99+/-0.11%, **Figure 3.6, Table 6**) and remaining lowered with the addition of both (8.56+/-0.35%, **Figure 3.6, Table 4**). *prod to slip* transitions also showed a reciprical pattern, elevating with the addition of either the transgene or the histamine, but remaining elevated to comparable levels with the addition of both (6.00+/- 0.10% v.s. 4.31+/- 0.10%, **Figure 3.6**, **Table 4).**

Prod to vulva search and *slip to vulva search* both showed changes in transition probability consistent with DVA silencing. Transition probabilities rose only upon the addition of both the transgene and the histamine, from 0.77+/-0.03% to 2.37+/-0.05% in the instance of *prod to vulva search*, and 0.53+/- 0.01% to 2.26+/- 0.09% (**Figure 3.6, Table 4**) in the instance of *slip to vulva search*. Both these transition probabilities remained elevated even after 2 hours of recovery off histamine: 1.19+/-0.05% and 1.43+/-0.09%, respectively (**Figure 3.6, Table 4**). DVA silencing affected these two transition probabilities in a similar way when conducted in a wild-type genetic background (**Figure 3.4, Table 3**). The result suggests that the effects of silencing DVA on these two transitions are independent of nematocin. Further, because they do not return to their wild-type values after recovery, when wild-type mating effeciency recovery, the data strongly indicate that they are also independent of DVA's acute effects on mating efficiency.

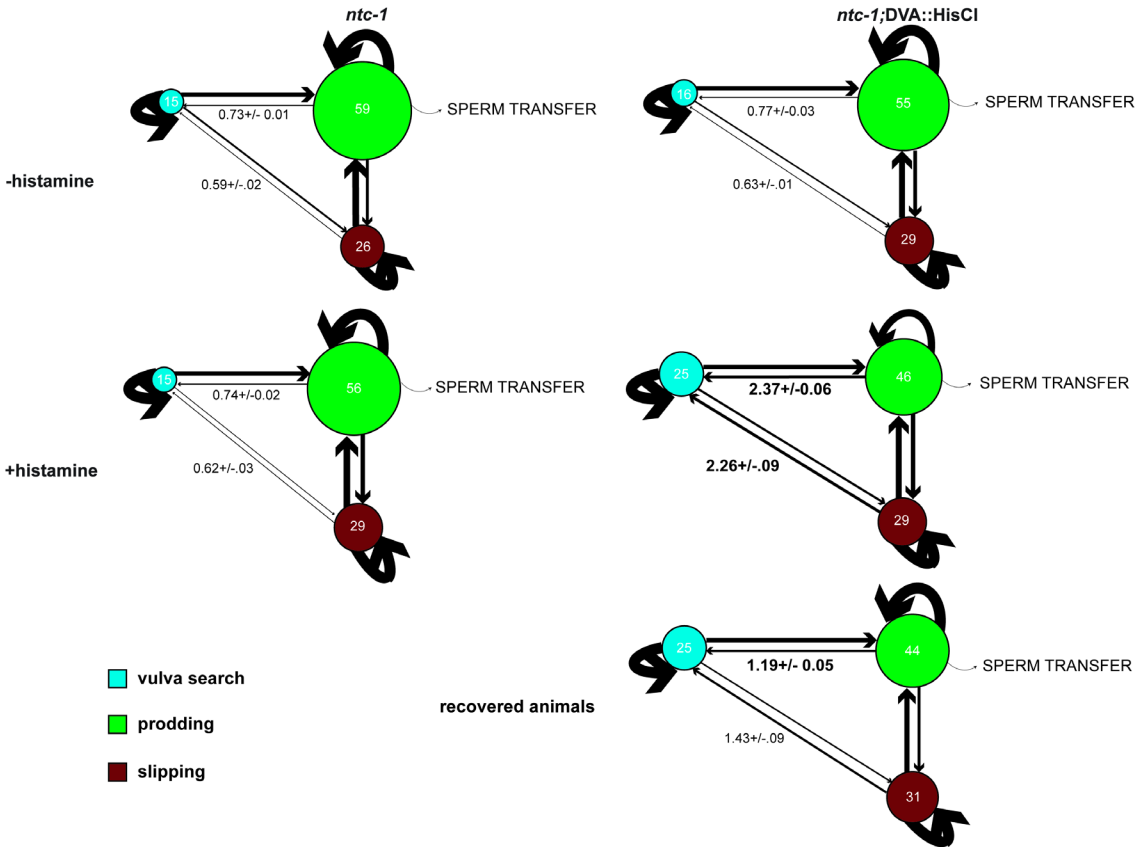

Figure 3.6 Mating dynamics of DVA-silenced, nematocin-deficient males Numbers within a circle are the percent time in which the males engage in that sub-behavior when mating. Arrow weights represent the probability in a given second that the animal will transition between the behaviors. Curved arrows pointing back toward the circle indicate the probability per second that the male will persist in the sub-behavior. *Left column* are ethograms of males without the DVA::HisCl transgene. *Right column* are males with the DVA::HisCl transgene. *Top row* are males tested in the absence of histamine. *Bottom row* are males tested in the presence of histamine. *Red* values illustrate statistically significant decreases, while **bold** values indicate statistically significant increases.

Silencing DVA does not affect locomotive of behavior hermaphrodites on food

DVA is strongly implicated in governing normal body posture, proprioception (Li et al., 2006), and coordination between the anterior and posterior parts of the hermaphrodite

during locomotion. Severe kinking and postural defects were reported in *Garrison et al.* when DVA was ablated from L1 males by laser (Garrison et al., 2012).

How then do we know that the mating defects observed from pharmacogenetically silencing DVA are not the result of perturbing normal locomotion? I characterized the effects of DVA silencing on locomotion in hermaphrodites (**Figure 3.7**). Two hour movies were made of 20 adult hermaphrodites on and off food. Using code developed in the lab (Pokala et al., 2014), I characterized locomotive behavior with respect to forward speed, angular speed, body posture eccentricity, reversal frequency, reversal length, reversal type, and other parameters. No changes in locomotion were detectable other than a change in forward speed off food. Wild-type hermaphrodites showed an increase in forward locomotion over time off food both in the presence and absence of histamine (**Figure 3.7**: *column 2*). Hermaphrodites expressing the DVA::HisCl transgene alone showed the same (**Figure 3.7**: *column 4, top*) but slowed locomotion when DVA was silenced (**Figure 3.7**: *column 4, bottom*) compared to intact animals off food. Tracking software was not able to robustly segment the males, so this experiment could not be conducted on male locomotion. Because I conduct the mating assays on food, locomotion changes off food are unlikely to adversely affect the locomotion of the mating animals that I assay. However, locomotion tracking and analysis of males is necessary to confirm this result.

Discussion

Only in *C. elegans* are there experimental tools available to study the action of oxytocin neurons in real time. Difficult to access, oxytocin-releasing neurons in mammals are located in the peri-ventricular and supra-optic nuclei of the hypothalamus, deep within

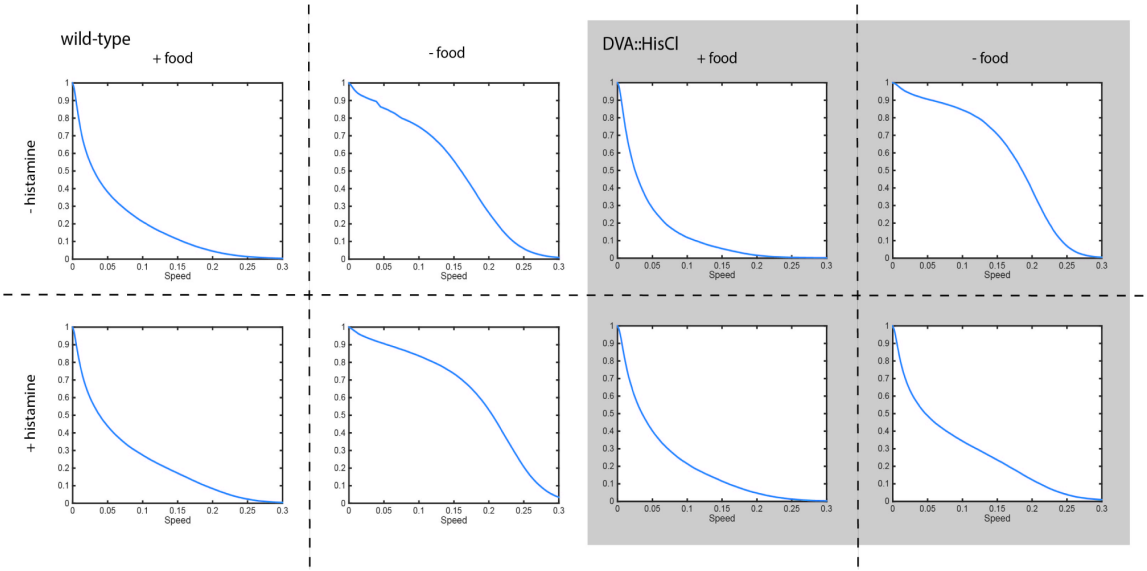

Figure 3.7 DVA silencing affects hermaphrodite locomotion speed off food. Cumulative distributions of forward velocity of hermaphrodites of the following genotypes/conditions: *left* (*white)* wild-type hermaphrodites, *right (gray*) hermaphrodites expressing the DVA::HisCl transgene; *top row*, hermaphrodites off histamine; *bottom row*, hermaphrodites on histamine; *first, third columns*, hermaphrodites on food; *second, fourth columns*, hermaphrodites off food. DVA-silenced hermaphrodites do not increase their speed over time when off food (*2nd row, fourth column*) unlike their wild-type counterparts (*2nd row, 2nd column*).

the brain (Sofroniew, 1983). Constitutive genetic knockouts of the mammalian oxytocin (OXT) and its receptor OXTR yield different phenotypes, likely due to cross-activation of its homolog arginine-vasopressin (AVP) (Ragnauth et al., 2004). Constitutive AVP knockouts are embryonically lethal, due to it its role in fluid homeostasis of the circulatory system (Young and Gainer, 2003). Many common invertebrate models, such as *Drosophila melanogaster,* have lost the oxytocin gene over the course of evolution (Stafflinger et al., 2008). *C. elegans* males, on the other hand, have only one oxytocin-related peptide.

Animals lacking nematocin show a quantitative phenotype of poorer performance in a five-minute mating assay (Garrison et al., 2012). Its main source for this circuit in the male tail is a single neuron, DVA, with a well-established, cell-specific promoter fragment (Hu et al., 2011). All of these features can be exploited in an inquiry into the mechanism of acute nematocin action during mating.

My results suggest that nematocin is acutely released from DVA to mediate the mating behavior of male *C. elegans*. Neuropeptides have been shown to have acute effects on behavior, on the order of minutes to several hours, as observed for the Agouti-related peptide's (AgRP) role in appetite stimulation (Aponte et al., 2011) or the peptide ATRP's central role in regulating the ingestion cycle of *Aplysia* (Jing et al., 2010). Other neuropeptides have been shown to trigger effects over much longer timescales, from several hours to days to even years, affecting the developmental trajectory of the animal, such as the eclosion hormone (EH) or the ecdysis-triggering hormone (ETH) in *Drosophila* (Zitnan et al., 1996).

To decipher whether nematocin was acutely required from DVA with mating, or whether it played a developmental role in the male mating circuit before sexual maturation, I needed to be able to silence DVA just prior to mating and observe the behavior effects. Because genetic knockouts lack the peptide for their entire lifespan, genetic studies alone are not sufficient to tackle such a question alone. Neither are neural ablations, genetically (by caspase expression) (Chelur and Chalfie, 2007) or physically (by laser microsurgery) (Bargmann and Avery, 1995), because they also prohibit neural function over most or all of the animal's lifespan. Pharmacogenetic silencing of DVA afforded me a number of advantages over previous methods. By using the heterologous histamine-gated chloride

channel, I was able to distinguish acute effects of nematocin release from longer occurring effects by allowing the animals to mature unperturbed, manipulating the neuron only in the adult hours prior to mating. This generated a measureable mating defect that could then be restored by restoring neuronal activity to DVA in a two-hour incubation off histamine. In a way that I did not anticipate, this acute silencing may have also circumvented the locomotive defects observed in other neuronal manipulations (**Figure 3.7**), such as laser ablation (Garrison, et al. 2012), allowing me to parse the authentic mating phenotypes from the general locomotion and body posture phenotypes.

The assay allowed me to look at the phenomena with both an endpoint analysis (**Figures 3.2** and **3.5**) and a dynamic mating model (**Figures 3.4** and **3.6**). From the end point analysis, I was able to establish that mating efficiency was compromised by silencing DVA (**Figure 3.2**) in a way comparable to genetically knocking out the gene for nematocin (**Figure 3.5**). By modeling mating dynamics with behavioral ethograms, I was able to identify a set of transition probabilities between the mating sub-behavioral states that changed significantly and meaningfully when DVA was silenced (**Figure 3.4**).

By performing the same ethomic analysis on DVA silenced, nematocin-deficient males, I identified two transition probabilities that changed (**Figure 3.6**) even though all of the experimental sets had equivalent mating efficiencies. Interestingly, these were also the transition probabilities that did not return to wild-type levels upon recovery, suggesting that they are peripheral to the behavior of interest to me.

Thus, I have identified 2 transition probabilities mediated by the acute release of nematocin from DVA during mating: *prod to sperm transfer* and *slip to prod*. One is a progressive transition out of *prodding*, and one is a progressive transition into *prodding*.

Interestingly, *slip to prod* seems to be mediated by nematocin release from DVA, but *prod to slip* does not. These observations will inform our experimental interpretation going forward as I genetically probe the mechanism for acute nematocin release from DVA during mating.

Because DVA has functions outside of mating, such as locomotion, proprioception, and posture, it is possible that silencing DVA could adversely affect mating behavior indirectly and not directly. I performed a control experiment to characterize changes in locomotion resulting from acute DVA silencing. Due to the limitations of my tracking code, this unfortunately had to be performed in hermaphrodites and not males. Regardless, the only locomotive phenotype observed was a defect in forward locomotion speed off food (**Figure 3.7**). Because my mating assays are conducted on food, I am not concerned about this defect. Nematocin-deficient males have been previously characterized as having normal locomotive behavior (Garrison et al., 2012). Silencing DVA in nematocin-deficient animals did not have any measurable additive effects on mating efficiency. If the DVA-silenced phenotype observed in wild-type animals was due solely to compromising the locomotion of the animals, one would expect to see an additive effect in mating efficiency in the nematocin-deficient experiment. Additionally, there was no visibly perceptive postural defect in DVA-silenced males, wild-type or nematocin deficient, whereas the DVA ablated animals had visible "kinks" in their body. Taken together, this evidence suggests that I need be minimally concerned with the locomotive effects of acute DVA silencing, if any, on my results.

Table 5: Means and standard deviations for all transition probabilities in DVA silencing experiment. p values were determined by an unpaired, two-tailed Student's t test with the mean and s.d. from wild-type controls calculated in **Table 15** (*See EXPERIMENTAL PROCEDURES*). Statistical significance was determined by the p value and a False Discovery Rate multiple comparison correction.

index	genotype	condition	transition	mean	s.d.	p val	sig?
1	wt	-his	searchtosearch	95.07	0.10	0.0321	
2	wt	-his	searchtoprod	3.00	0.05	2.082	
3	wt	-his	searchtoslip	1.73	0.06	0.3470	
4	**wt**	**-his**	**prodtosearch**	**0.20**	**0.01**	**0.0042**	**
5	wt	-his	prodtoprod	95.07	0.05	0.0215	
6	wt	-his	prodtoslip	4.04	0.04	0.2041	
7	wt	-his	prodtosperm	0.69	0.01	0.0489	
8	wt	-his	sliptosearch	1.70	0.05	0.0240	
9	wt	-his	sliptoprod	17.29	0.17	0.0302	
10	wt	-his	sliptoslip	81.01	0.18	0.0152	
11	wt	+his	searchtosearch	93.68	0.14	0.3300	
12	wt	+his	searchtoprod	4.69	0.13	0.5425	
13	wt	+his	searchtoslip	0.62	0.02	0.3548	
14	wt	+his	prodtosearch	0.13	0.01	0.0570	
15	wt	+his	prodtoprod	93.49	0.08	0.7783	
16	wt	+his	prodtoslip	5.60	0.08	0.6893	
17	wt	+his	prodtosperm	0.78	0.01	0.1606	
18	wt	+his	sliptosearch	1.23	0.03	0.2763	
19	**wt**	**+his**	**sliptoprod**	**12.47**	**0.20**	**0.0086**	**
20	wt	+his	sliptoslip	86.30	0.22	0.7540	
21	DVA::HisCl	-his	searchtosearch	91.29	0.22	0.1433	
22	DVA::HisCl	-his	searchtoprod	5.32	0.07	0.7086	
23	DVA::HisCl	-his	searchtoslip	0.74	0.05	0.4649	
24	**DVA::HisCl**	**-his**	**prodtosearch**	**0.40**	**0.02**	**<0.0001**	***
25	DVA::HisCl	-his	prodtoprod	93.85	0.10	0.4083	
26	DVA::HisCl	-his	prodtoslip	4.62	0.06	0.4964	
27	DVA::HisCl	-his	prodtosperm	1.12	0.02	0.2023	
28	**DVA::HisCl**	**-his**	**sliptosearch**	**2.73**	**0.05**	**0.002**	**
29	DVA::HisCl	-his	sliptoprod	16.52	0.30	0.1395	
30	DVA::HisCl	-his	sliptoslip	80.74	0.33	0.0281	
31	DVA::HisCl	+his	searchtosearch	94.03	0.06	0.1905	
32	DVA::HisCl	+his	searchtoprod	4.99	0.04	0.8846	
33	DVA::HisCl	+his	searchtoslip	0.98	0.05	0.7433	
34	**DVA::HisCl**	**+his**	**prodtosearch**	**1.02**	**0.05**	**<0.0001**	***
35	DVA::HisCl	+his	prodtoprod	93.07	0.12	0.7085	
36	DVA::HisCl	+his	prodtoslip	5.53	0.14	0.7474	
37	**DVA::HisCl**	**+his**	**prodtosperm**	**0.39**	**0.01**	**0.0012**	**

38	DVA::HisCl	+his	sliptosearch	1.12	0.05	0.4529	
39	**DVA::HisCl**	**+his**	**sliptoprod**	**9.73**	**0.17**	**<0.0001**	***
40	DVA::HisCl	+his	sliptoslip	88.48	0.19	0.1711	
41	DVA::HisCl	recovery	searchtosearch	93.71	0.07	0.3147	
42	DVA::HisCl	recovery	searchtoprod	3.30	0.07	0.0199	
43	DVA::HisCl	recovery	searchtoslip	2.99	0.10	0.0119	
44	**DVA::HisCl**	**recovery**	**prodtosearch**	**0.96**	**0.05**	**<0.0001**	***
45	DVA::HisCl	recovery	prodtoprod	94.72	0.14	0.0526	
46	DVA::HisCl	recovery	prodtoslip	2.87	0.06	0.0258	
47	DVA::HisCl	recovery	prodtosperm	1.22	0.03	0.0571	
48	**DVA::HisCl**	**recovery**	**sliptosearch**	**2.18**	**0.06**	**0.0022**	**
49	**DVA::HisCl**	**recovery**	**sliptoprod**	**12.36**	**0.29**	**0.0073**	**
50	DVA::HisCl	recovery	sliptoslip	84.84	0.23	0.6544	

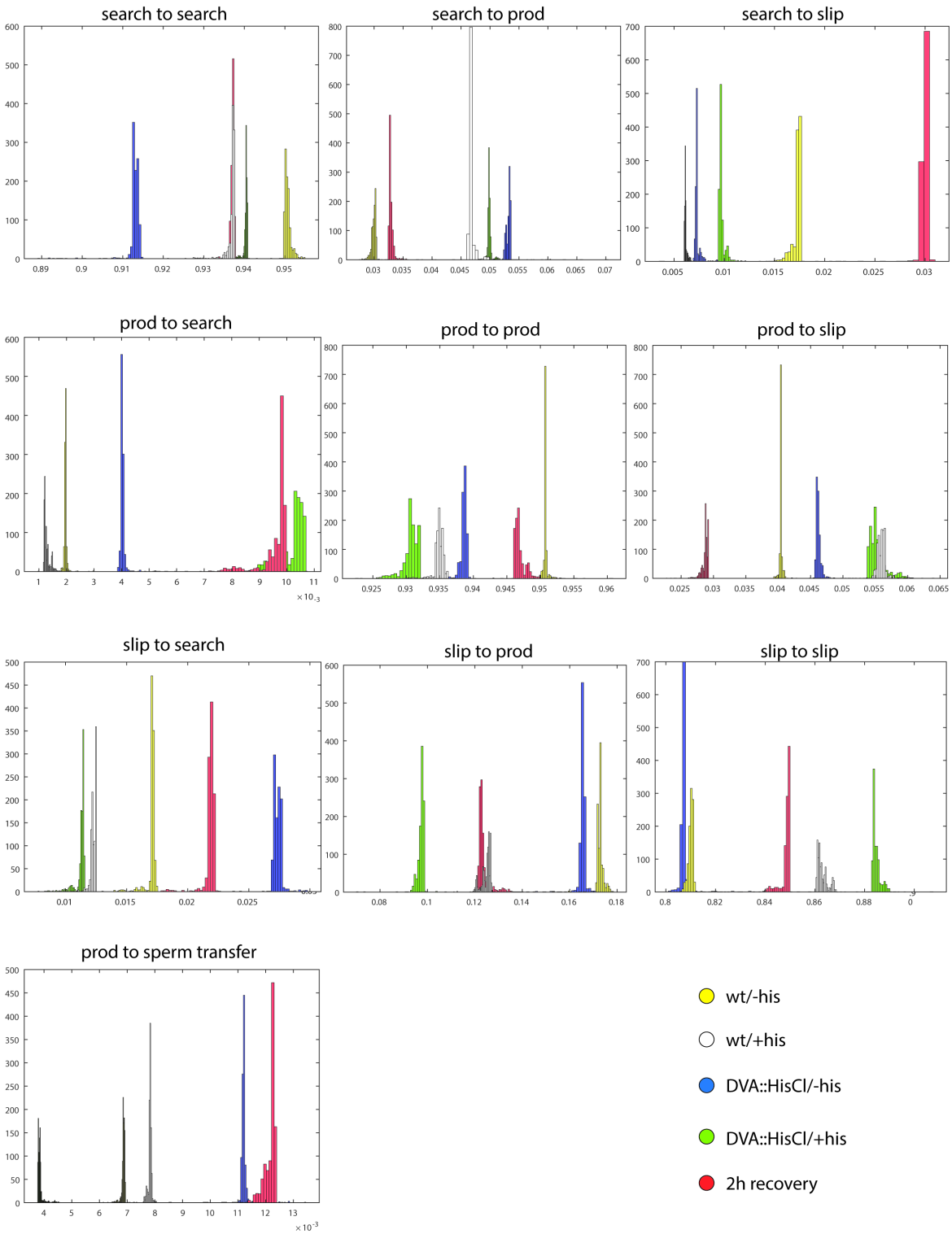

Figure 3.8: Bootstrap data distributions for all sub-behaviors of the wild-type, DVA silencing experiment.

Table 6: Mean and standard deviation for transition probabilities in nematocin-deficient, DVA-silencing experiment. p values were determined by an unpaired, two-tailed Student's t test with the mean and s.d. from nematocin-deficient controls calculated in **Table 16** (*See EXPERIMENTAL PROCEDURES*). Statistical significance was determined by the p value and a False Discovery Rate multiple comparison correction.

index	genotype	condition	transition	mean	s.d.	p val	sig?
1	*ntc-1*	-his	searchtosearch	93.36	0.23	0.9344	
2	*ntc-1*	-his	searchtoprod	4.07	0.06	0.5676	
3	*ntc-1*	-his	searchtoslip	1.29	0.05	0.4124	
4	*ntc-1*	-his	prodtosearch	0.73	0.01	0.3312	
5	*ntc-1*	-his	prodtoprod	96.95	0.04	0.1288	
6	*ntc-1*	-his	prodtoslip	2.04	0.03	0.1722	
7	*ntc-1*	-his	prodtosperm	0.27	0.05	0.2645	
8	*ntc-1*	-his	sliptosearch	0.59	0.02	0.3825	
9	*ntc-1*	-his	sliptoprod	11.33	0.25	0.0954	
10	*ntc-1*	-his	sliptoslip	87.99	0.27	0.0476	
11	*ntc-1*	+his	searchtosearch	94.44	0.10	0.2262	
12	*ntc-1*	+his	searchtoprod	4.92	0.08	0.0741	
13	*ntc-1*	+his	searchtoslip	0.64	0.02	0.1576	
14	*ntc-1*	+his	prodtosearch	0.74	0.02	0.2870	
15	***ntc-1***	**+his**	**prodtoprod**	**94.52**	**0.16**	**0.0040**	**
16	***ntc-1***	**+his**	**prodtoslip**	**4.46**	**0.14**	**0.0086**	**
17	*ntc-1*	+his	prodtosperm	0.28	0.01	0.2891	
18	*ntc-1*	+his	sliptosearch	0.62	0.03	0.5557	
19	*ntc-1*	+his	sliptoprod	10.94	0.18	0.2267	
20	*ntc-1*	+his	sliptoslip	88.45	0.2	0.2004	
21	*ntc-1*;DVA::HisCl	-his	searchtosearch	94.96	0.08	0.0289	
22	*ntc-1*;DVA::HisCl	-his	searchtoprod	3.74	0.09	1.000	
23	*ntc-1*;DVA::HisCl	-his	searchtoslip	1.31	0.02	0.3737	
24	*ntc-1*;DVA::HisCl	-his	prodtosearch	0.77	0.03	0.1827	
25	***ntc-1*;DVA::HisCl**	**-his**	**prodtoprod**	**93.00**	**0.11**	**<0.0001**	***
26	***ntc-1*;DVA::HisCl**	**-his**	**prodtoslip**	**6.00**	**0.10**	**0.0003**	***
27	*ntc-1*;DVA::HisCl	-his	prodtosperm	0.23	0.01	0.0933	
28	*ntc-1*;DVA::HisCl	-his	sliptosearch	0.63	0.01	0.6180	

29	***ntc-1*;DVA::HisCl**	**-his**	**sliptoprod**	**6.99**	**0.11**	**0.0005**	***
30	***ntc-1*;DVA::HisCl**	**-his**	**sliptoslip**	**92.22**	**0.11**	**0.0002**	***
31	*ntc-1*;DVA::HisCl	+his	searchtosearch	93.51	0.08	0.1989	
32	*ntc-1*;DVA::HisCl	+his	searchtoprod	3.91	0.05	0.7659	
33	*ntc-1*;DVA::HisCl	+his	searchtoslip	1.56	0.03	0.1033	
34	***ntc-1*;DVA::HisCl**	**+his**	**prodtosearch**	**2.37**	**0.06**	**<0.0001**	***
35	***ntc-1*;DVA::HisCl**	**+his**	**prodtoprod**	**93.00**	**0.13**	**<0.0001**	***
36	***ntc-1*;DVA::HisCl**	**+his**	**prodtoslip**	**4.31**	**0.10**	**0.0124**	*
37	*ntc-1*;DVA::HisCl	+his	prodtosperm	0.31	0.01	0.5311	
38	***ntc-1*;DVA::HisCl**	**+his**	**sliptosearch**	**2.26**	**0.09**	**<0.0001**	***
39	***ntc-1*;DVA::HisCl**	**+his**	**sliptoprod**	**8.56**	**0.35**	**0.0145**	*
40	*ntc-1*;DVA::HisCl	+his	sliptoslip	89.08	0.43	0.9500	
41	***ntc-1*;DVA::HisCl**	**recovery**	**searchtosearch**	**91.14**	**0.04**	**<0.0001**	***
42	*ntc-1*;DVA::HisCl	recovery	searchtoprod	3.88	0.05	0.8061	
43	*ntc-1*;DVA::HisCl	recovery	searchtoslip	1.16	0.03	0.7142	
44	***ntc-1*;DVA::HisCl**	**recovery**	**prodtosearch**	**1.19**	**0.05**	**0.0009**	***
45	***ntc-1*;DVA::HisCl**	**recovery**	**prodtoprod**	**93.82**	**0.28**	**0.0009**	***
46	*ntc-1*;DVA::HisCl	recovery	prodtoslip	3.81	0.14	0.0535	
47	*ntc-1*;DVA::HisCl	recovery	prodtosperm	0.53	0.05	0.0325	
48	***ntc-1*;DVA::HisCl**	**recovery**	**sliptosearch**	**1.43**	**0.09**	**0.0004**	***
49	***ntc-1*;DVA::HisCl**	**recovery**	**sliptoprod**	**8.01**	**0.24**	**0.0037**	**
50	*ntc-1*;DVA::HisCl	recovery	sliptoslip	88.53	0.19	0.2578	

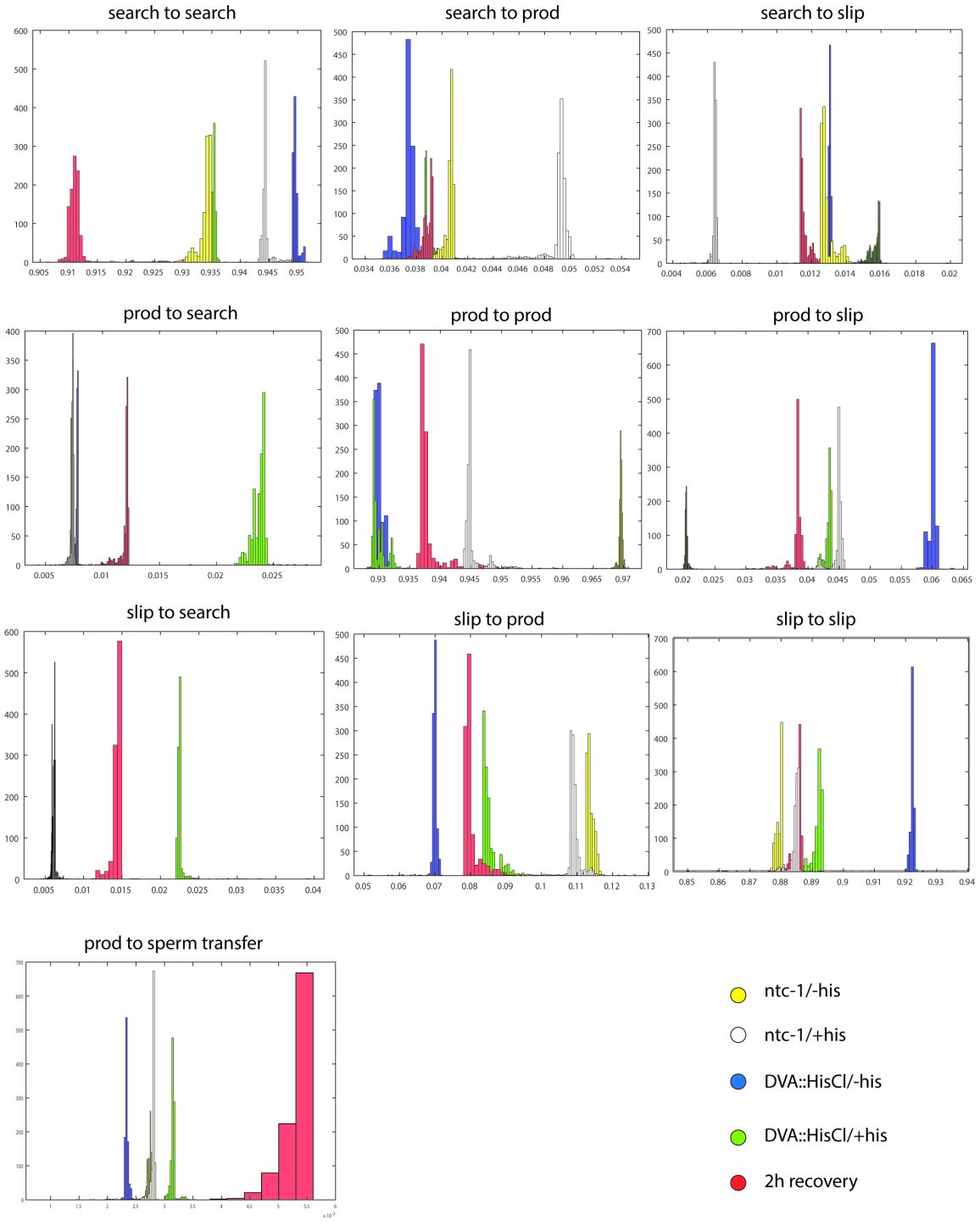

Figure 3.9: Bootstrap data distributions for all sub-behaviors of the nematocin-deficient, DVA silencing experiment.

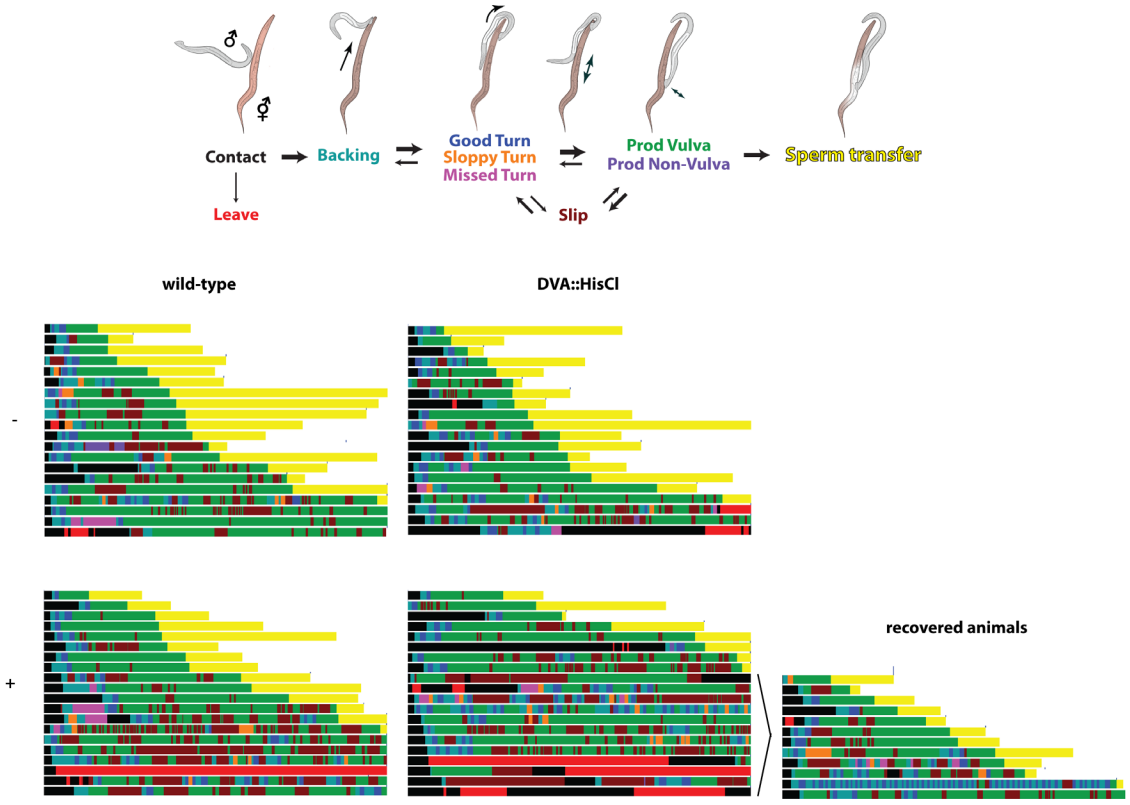

Figure 3.10: Raw mating traces from silencing DVA in wild-type males. *Top*, colorized mating schema indicating the color code for the behavioral traces. *Bottom*, raw mating traces for wild-type and transgenic positive males in both the presence and absence of histamine. *Right*, males that did not mate from the DVA-silenced test group retested after a two hour incubation off histamine. Each mating trace is five minutes. *White* space indicates the conclusion of mating after sperm has been transferred.

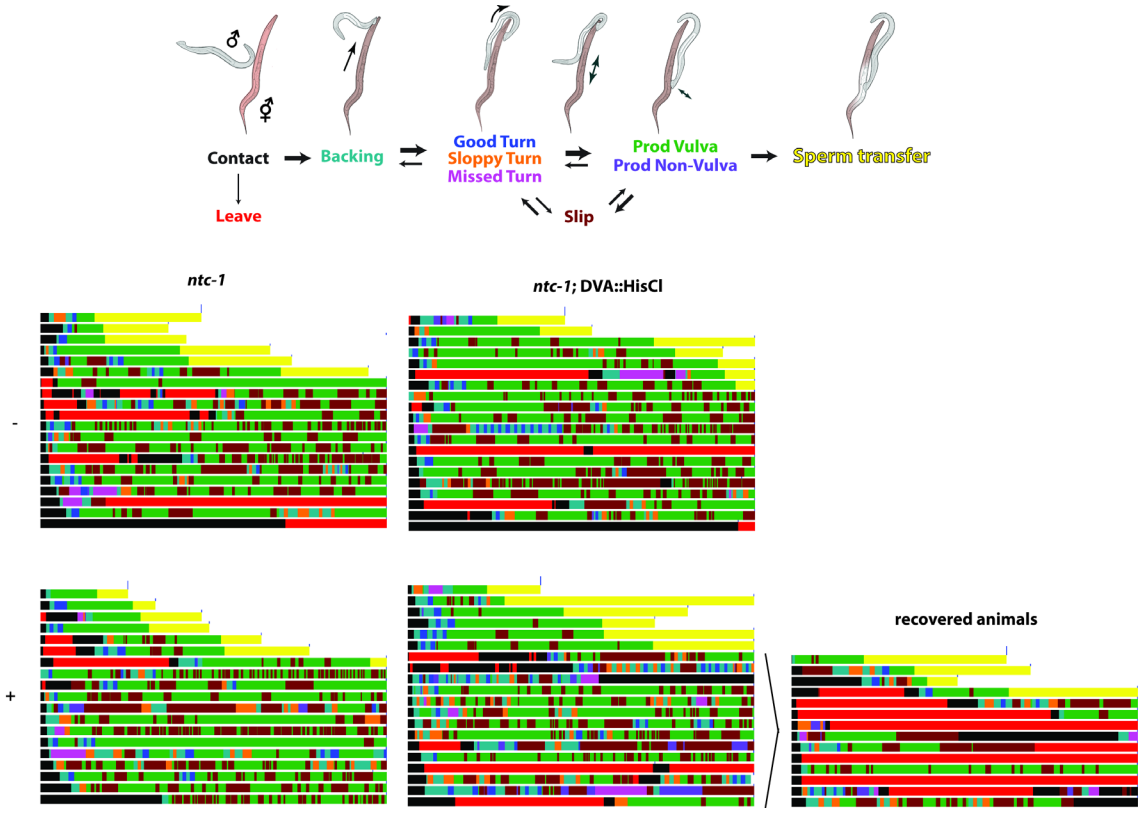

Figure 3.11: Raw mating traces from silencing DVA in nematocin-deficient males. *Top*, colorized mating schema indicating the color code for the behavioral traces. *Bottom*, raw mating traces for nematocin-deficient and transgene positive, nematocin-deficient males in both the presence and absence of histamine. *Right*, males that did not mate from the DVA-silenced test group retested after a two hour incubation off histamine. Each mating trace is five minutes. *White* space indicates the conclusion of mating after sperm has been transferred.

CHAPTER IV: DOPAMINE REGULATION OF OXYTOCIN DURING MATING

A genetic candidate screen to parse the circuitry of nematocin action

To begin investigating the mechanism for nematocin action, I made a list of genetic candidates that targeted the function of neurons upstream to DVA in the male wiring diagram (Jarrell et al., 2012, **Figure 4.1, Table 7**). I included genetic candidates to disrupt DVA sensory function, as DVA has been proposed to be a propriception neuron (Li et al., 2006) and thereby may auto-trigger nematocin release. *lov-1* animals are incapable of mating (Shawn Xu and Barr, 2007), and *mec-4* animals mate less efficiently due to their inability to complete turns during vulva scanning (Liu and Sternberg, 1995). I probed the function of *nlp-12, trp-4*, and *cat-2* in wild-type and nematocin-deficient genetic backgrounds, looking for genetic interaction with *ntc-1*. In doing so, I found all three canonical forms of genetic evidence: additive, overlapping, and epistasis. Here, I discuss

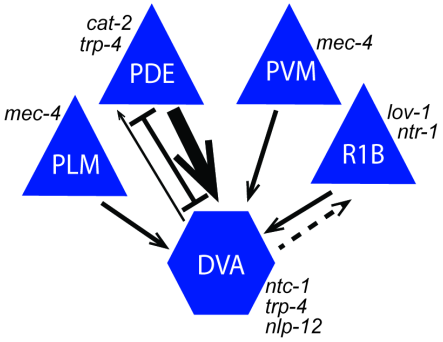

gene	associated neuron(s)	description
mec-4(e1339)	PVM, PLM	encodes an amiloride-sensitive Na+ channel protein (degenerin) required to sense gentle mechanical stimuli along the body wall
cat-2(e1112)	PDE, R5A, R7A, R9A	encodes a tyrosine hydroxylase, the rate limiting enzyme in the synthesis of catecholamines (e.g. dopamine)
trp-4(sy695)	DVA, PDE	encodes the pore-forming subunit of a mechanosensitive TRPN channel; required for a mechanosensitive conductance in a ciliated mechanosensory neuron and, specifically, for stretch-receptor-mediated proprioception
nlp-12(ok335)	DVA	encodes two predicted neuropeptide-like proteins part of a LQFamide neuropeptide family
lov-1(ok522)	RnBs, CEM, HOB	encodes a transmembrane protein required for response to hermaphrodite contact and vulva location; acts with PKD-2

Figure 4.1 and Table 7: Genetic candidate screen to manipulate the sensory inputs of DVA. *Left*: Wiring diagram for neurons upstream of DVA in male *C. elegans*. Sensory neurons are represented with triangles, and interneurons with hexagrams. Solid arrows represent synapses, bars represent gap junctions, and dotted arrows represent potential extra-synaptic communication. Arrow weights are representative of the number of connections between the neurons of each type. Neurons are labelled with the genetic candidates that they express. *Right*: A table of the genetic candidates, their associated neurons, and a description of their function.

the additive and overlapping evidence (*nlp-12* and *trp-4*, respectively) briefly by describing only endpoint mating efficiency results. The bulk of the chapter will be spent addressing nematocin's genetic epistasis with dopamine (*cat-2*), experimentally and computationally, and its implications.

Nematocin's copeptide NLP-12*: additive effects*

Because nematocin and the neuropeptide NLP-12 are both released from DVA, I hypothesized that acute co-release during mating may contribute to coherent mating behavior. To test this, I looked at the mating behavior of males with a loss-of-function mutation in *nlp-12,* comparing it to wild-type and nematocin-deficient animals tested in tandem, as well as the nematocin-NLP-12 double mutant. 8/20 nematocin-deficient males mated (40% efficiency, **Figure 4.**), and 11/20 NLP-12-deficient males mated (55% efficiency, **Figure 4.2**). 4/20 of the double mutant males mated, or 20% efficiency, approximately 50% of the nematocin- deficient males (**Figure 4.2**). Although not significantly different from the mating efficiency of nematocin-deficient males, the mating efficiency of the double mutant males appears to be the additive combination of the single mutants alone. Additionally, double mutants mate successfully at a rate lower than acutely silencing DVA just prior to mating (20% vs. 35%). Raw traces of the full ethomic tracking can be found at the end of the chapter in **Figure 4.13**. These results suggest that the effects of the NLP-12 and nematocin on mating are independent and additive, despite release from an overlapping neuron.

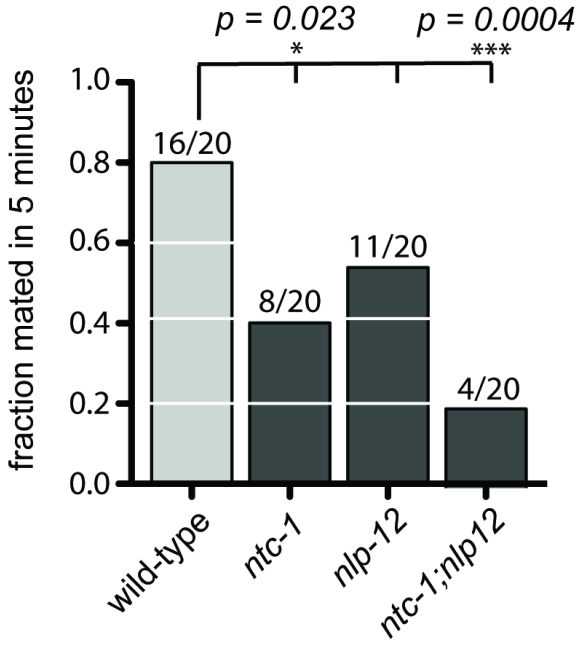

Figure 4.2: Additive genetic effect of nematocin and copeptide NLP-12. *Light gray*: wild-type control males. *Dark gray*, mutant test males. *Y-axis*: fraction of males mated in five-minute assay. Actual fraction mated is labelled above its respective bar. p values were calculated with a Fisher Exact Test and a False Discovery Rate to correct for multiple comparisons.

Genetic overlap of nematocin and TRP-4 *suggests related functions*

I next investigated the relationship between nematocin and TRP-4, a TRP-N channel expressed in DVA that could be a mechanism for DVA proprioception (Li et al., 2006). Mating for single and double mutants was analyzed in a mating efficiency endpoint assay as described above. Nematocin-deficient and TRP-4-deficient males mated at comparable efficiencies: 8/20 or 40% and 7/20 or 35%, respectively (**Figure 4.3**). 8/20 double mutants mated, also at an efficiency 40% (**Figure 4.3**). Thus, the two genes had no additive effect on the phenotype. Raw traces of the full ethomic tracking can be found at

the end of the chapter in **Figure 4.14**. This result suggests that TRP-4 and nematocin overlap in their functions in the mating circuit.

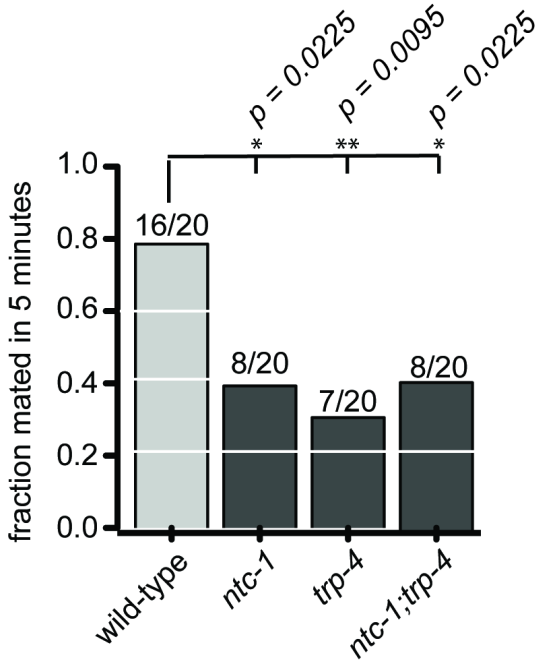

Figure 4.3: Overlapping genetic phenotype of nematocin and channel TRP-4. *Light gray*: wild-type control males. *Dark gray*, mutant test males. *Y-axis*: fraction of males mated in five-minute assay. Actual fraction mated is labelled above its respective bar. P values were calculated with a Fisher Exact Test and a False Discovery Rate to correct for multiple comparisons.

Classical epistasis between nematocin and dopamine

A major synaptic input into the nematocin-producing DVA neuron is the dopaminergic neuron PDE, both in male and hermaphrodite *C. elegans* (Han et al., 2017, **Figure 4.1**). Dopamine has been strongly implicated in the regulation of male mating behavior: in addition to PDE, the male-specific rays R5A, R7A, and R9A are also dopaminergic (Barr and Garcia, 2006). Consequently, I next investigated the genetic interaction between nematocin and dopamine.

6/20 *ntc-1* males mated (30%, **Figure 4.4**), compared to control males that mated at 16/20 or 80% efficiency (**Figure 4.4**). 2/20 *cat-2* males mated, (10% efficiency) consistent with previous reports (**Figure 4.4**, *3rd bar graph*) (Liu and Sternberg, 1995). When the mutations were combined, 12/20 males mated, restoring mating efficiency to 60% (**Figure 4.4**,), and resembling the nematocin-deficient mutant. Raw traces of the full ethomic tracking can be found at the end of the chapter in **Figure 4.15**. These results demonstrate classical genetic epistasis in which the nematocin mutant is epistatic to the dopamine mutant. To verify the authenticity of the result, I rescued the nematocin peptide with a transgene under its native promoter (*see* EXPERIMENTAL PROCEDURES). 3/20 transgenically rescued males mated--a rate of 15%--recapitulating the severe mating defect of the dopamine-deficient animals (**Figure 4.4**).

Dopamine-deficient males exhibited additional mating defects compared to those of nematocin-deficient males. Notably, dopamine-deficient males often abandoned their mates or aborted mating attempts prior to consummation. In both wild-type and nematocin-deficient animals, aborted mating occured at a rate of 1/20 males, or 5% (**Figure 4.5**, *1st and 2nd bar graphs*). Dopamine-deficient males aborted mating attempts at a rate of 9/20 males, or 45% (**Figure 4.5**). Aborted mating attempts were restored to wild-type or nematocin-deficient rates, 2/20 or 10%, in the nematocin and dopamine defective mutant (**Figure 4.5**). Confirming the result, transgenic rescue of nematocin in the double mutant resulted in an increase in aborted mating attempts, akin to the rate of males deficient in dopamine alone (9/20 males, **Figure 4.5**). Thus, the more severe mating defect in dopamine-deficient males is due at least in part to the action of nematocin.

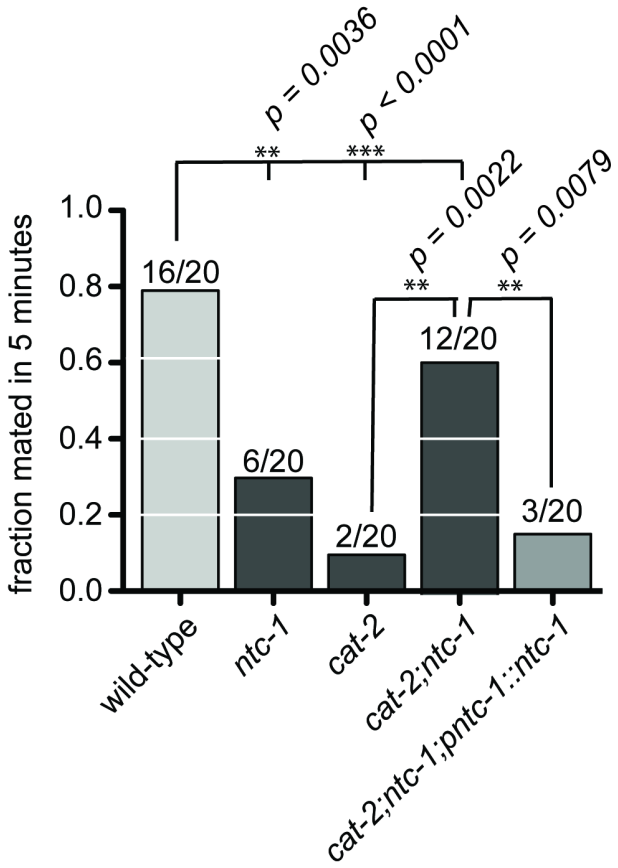

Figure 4.4: Nematocin and dopamine mutants show a classical epistasis. *Light gray*: wild-type control males. *Dark gray*, mutant test males. *Y-axis*: fraction of males mated in five-minute assay. Actual fraction mated is labelled above its respective bar. p values were calculated with a Fisher Exact Test and a False Discovery Rate to correct for multiple comparisons.

Dynamic behavioral modeling of nematocin-deficient and dopamine-deficient males

To explore further how dopamine's effect differed from nematocin's in kind or in degree, and to elucidate the interaction between the two modulators, I returned to the quantitative description of mating behavior described in **Chapter III** (*see also* EXPERIMENTAL PROCEDURES). I modeled the mating behavior of wild-type, nematocin-deficient, dopamine-deficient, double-deficient, and males with the nematocin transgenically rescue via the Markov method previously described (*see* EXPERIMENTAL PROCEDUES).

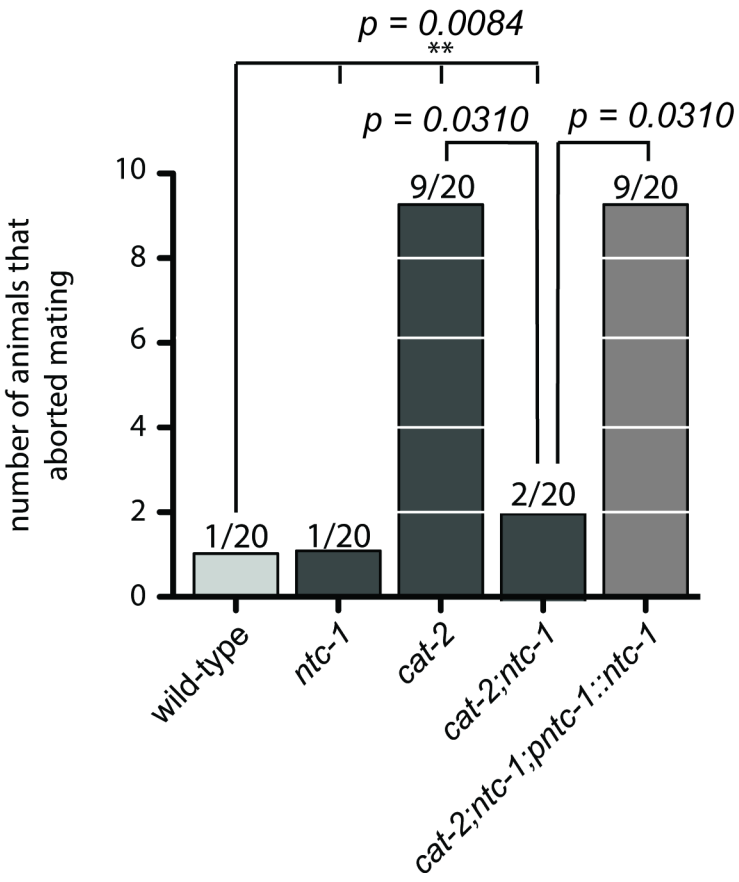

Figure 4.5: Genetic evidence for increased aborted mating attempts in dopamine-deficient animals. *Light gray*: wild-type control males. *Dark gray*, mutant test males. *Y-axis*: Number of males that abandoned their mates during the five-minute assay. Actual fraction is labelled above its respective bar. P values were calculated with a Fisher Exact Test and a False Discovery Rate to determine statistical significance.

Means and standard deviations from this analysis can be found at the end of this chapter in **Table 10,** and the histograms of the bootstrapped data can be found in **Figure 4.11.** In the same manner as before, I then identified meaningful changes in probability that fulfilled the criteria of being both statistically significant from the control sets conducted along with the experiment, and having an effect size larger than that of the experiment-to-experiment variability of the wild-type controls. A summary of the significant results from **Table 10**

can be found in **Table 8**. **Figure 4.6** illustrates the results of the modeling with graphical mating ethograms.

Table 8: Summary of significant results from Table 10. Mean transition probabilities for wild-type (*w.t.*), nematocin-deficient (*ntc-1*), dopamine-deficient (*cat-2*), the double mutant (*cat-2;ntc-1*), and the transgenic rescue of nematocin (*rescue*) males are shown. Mean values significantly higher than wild-type controls are in **bold**. Mean values significantly lower than wild-type controls are in *red*. Transition probabilities that follow a pattern consistent with epistasis are indicated with an asterisk (*). p values and statistical significance were determined by statistically comparing the distributions with the mean and standard deviations of **Table 15** (*see* **Table 10**).

transition probability	w.t.	*ntc-1*	*cat-2*	*cat-2;ntc-1*	rescue
prod to vulva search	0.00	**0.79**	0.05	0.00	**0.82**
prod to prod*	91.89	**96.01**	93.65	**96.67**	92.51
prod to sperm transfer*	1	0.26	0.09	0.58	0.30
slip to prod*	13.88	9.52	12.65	9.28	2.19
slip to slip	85.46	89.59	87.57	88.07	**97.08**

Five transition probabilities out of ten showed statistically significant changes, and three of these demonstrated a pattern consistent with genetic epistasis. Of the two that did not, *prod to vulva search* was slightly but significantly elevated in the nematocin-deficient males and in the transgenic rescue (0.79+/-0.04% and 0.82+/-0.03%, respectively, **Figure 4.6, Table 8**), but not in the dopamine-deficient or double mutant males (0.05+/-0.01% and 0.00+/-0.00%, respectively, **Figure 4.6, Table 8**). Males where nematocin was transgenically rescued also tended to persist in *slipping* more than any of the genotypes (97.08+/-0.07%, compared to wild-type's transition probability of 85.46+/-0.14%, **Figure 4.6, Table 8**). *prod to sperm transfer*, *prod to slip*, and persistence in *prodding* all had changes transition probability consistent with epistasis. *prod to sperm transfer* transition probabilities fell from 1.00+/-0.01% to 0.26+/-0.01% in nematocin-deficient males, and to

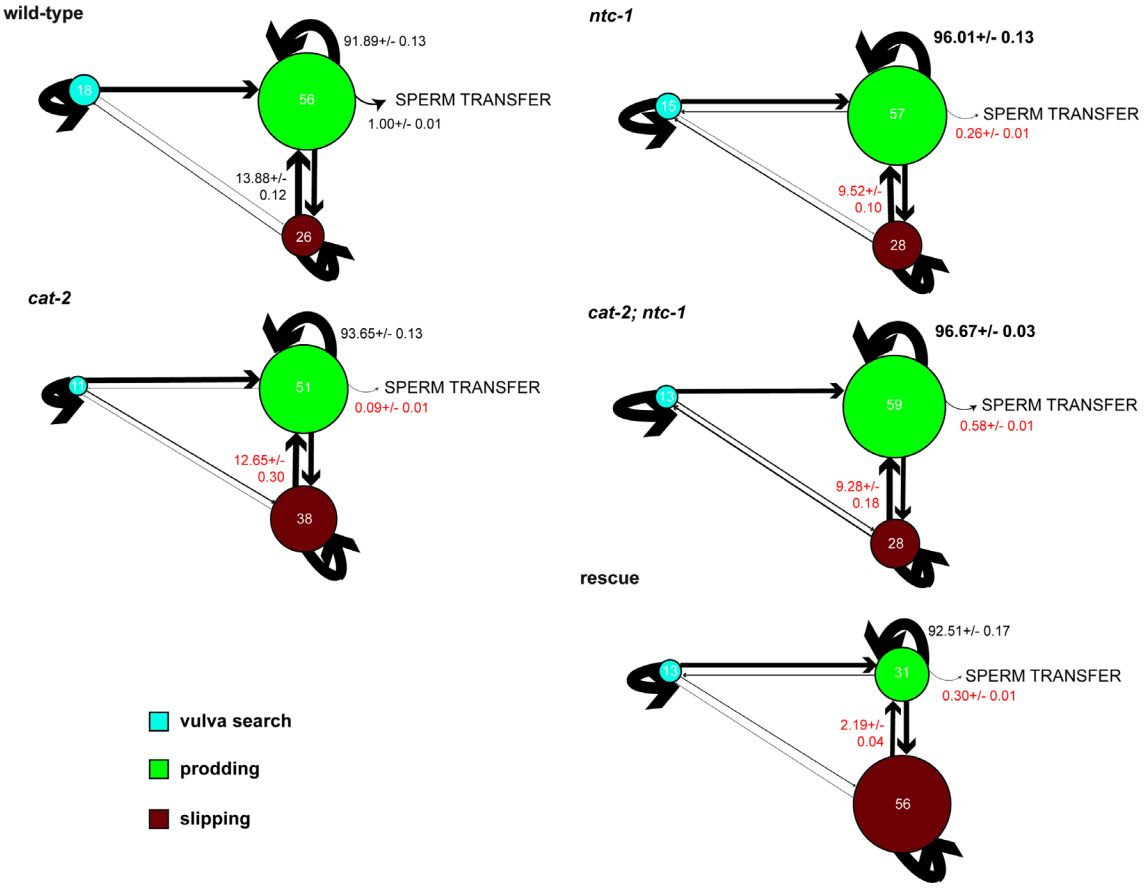

Figure 4.6: Mating dynamics of nematocin and dopamine mutant males. Numbers within a circle are the percent time in which the males engage in that sub-behavior when mating. Arrow weights represent the probability in a given second that the animal will transition between the behaviors. Curved arrows pointing back toward the circle indicate the probability per second that the male will persist in the sub-behavior. Genotypes are labeled above the ethograms. statistically significant decreases in transition probability are labeled in *red*. Statistically significant increases in transition probability are labeled in **bold**.

0.09+/-0.01% in dopamine-deficient males. In the double mutant, this transition probability rose to 0.58+/-0.01%, and once again lowered in value when nematocin was rescued transgenically in the double mutant (0.30+/-0.01%, **Figure 4.6, Table 8**). Persistence in *prodding* raised in nematocin-deficient animals by a significant amount, 91.89+/-0.13 % to 96.67+/-0.03 %, but not in dopamine-deficient males, 93.65+/-0.28%

(**Figure 4.6, Table 8**). Double mutants had an elevated transition probability (96.67+/-0.03) more similar to the nematocin-deficient males, which was restored to a wild-type equivalent level in double mutant males in which nematocin was transgenically rescued (92.51+/-0.17, **Figure 4.6, Table 8**).

Changes observed in the *slip to prod* transition frequency are more puzzling. In nematocin-deficient animals, I see *slip to prod* transition frequencies fall from 13.88+/-0.14% to 9.52+/-0.10% (**Figure 4.6, Table 8**). In dopamine-deficient animals, they fall only slightly, but significantly, to 12.65+/-0.30% (**Figure 4.6, Table 8**). Males defective in both dopamine and nematocin have a *slip to prod* transition frequency similar to nematocin-deficient males, 9.28+/-0.18% (**Figure 4.6, Table 8**). This probability is dramatically lower in double mutants in which nematocin is transgenically rescued, to 2.19+/-0.04% (**Figure 4.6, Table 8**). Whether this value is anomalously low, or whether the dopamine-deficient *slip to prod* transition probability is anomalously high, will become clearer with further experimentation.

Silencing DVA in dopamine deficient males rescues their mating defects

The classical interpretation of epistasis between dopamine and nematocin would indicate that dopamine is an upstream regulator of nematocin: that the severe mating defect in dopamine deficient animals is due to an excess of nematocin at the wrong time or place. To test the veracity of this hypothesis, I interrogated it with an orthogonal approach, by manipulating the release of nematocin with a circuit manipulation. To accomplish this, I returned to the pharmacogenetic manipulation of DVA with the histamine-gated ion

channel HisCl (Pokala et al., 2014). By silencing DVA just prior to mating, I hypothesized that I would be able to partially restore mating in dopamine-deficient animals.

Figure 4.7 depicts the mating endpoint results from this experiment. Raw traces of the full ethomic tracking can be found at the end of the chapter in **Figure 4.16**. Adding either the DVA::HisCl transgene (**Figure 4.7**) or histamine (**Figure 4.7)** alone did not change the overall mating efficiency of the dopamine-deficient animals, which mated at a rate of 2/20 males, or 10%, for all three conditions. When the reagents were combined to silence DVA, however, male mating efficiency was partially restored to a rate of 11/20, or 55% (**Figure 4.7**). Males that did not mate in this attempt were allowed to recover for two hours off histamine, just as before, and then were retested. 5/9 of these males successfully mated in the allotted five minutes, yielding a mating efficiency of 55% (**Figure 4.7**). Thus, the rescued mating defect persisted even after two hours of recovery off histamine.

I then investigated whether behaviors implicated in the dopamine and nematocin interactions were also affected by DVA silencing in dopamine-deficient males. First, I examined aborted mating attempts **(Figure 4.8**). Neither the transgene nor histamine alone appeared to significantly alter this phenotype (**Figure 4.8**). Aborted mating attempts fluctuated from 7/20 for dopamine-deficient animals, to 9/20 for dopamine-deficient animals with only the transgene, to 10/20 for the dopamine-deficient animals paired with histamine alone (35-50%). Silencing DVA in dopamine deficient animals restored aborted mating attempts to wild-type levels, 2/20 males or roughly 10% (**Figure 4.8**). Like mating efficiency, aborted mating attempts did not return to dopamine-deficient levels after two hours of histamine-free recovery.

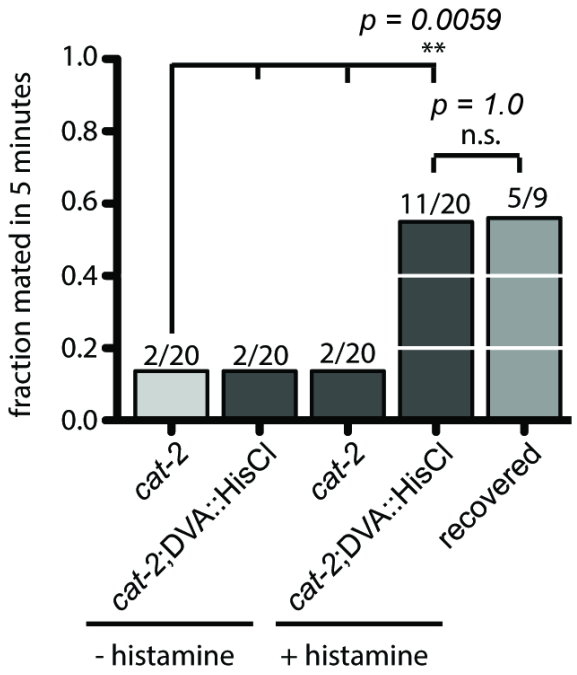

Figure 4.7: Mating efficiency of DVA-silenced, dopamine-deficient males. *x-axis:* the conditions/ genotypes tested. DVA::HisCl indicates the presence of an integrated HisCl transgene expressed in DVA. "- histamine" indicates the absence of histamine, "+ histamine" the presence of histamine. *y-axis*: the fraction mated of each genotype and condition. Raw fractions are indicated above each bar . First bar (*light* gray) are the nematocin-deficient control males. Bars 2-4 (*dark gray*) have the transgene (#2), histamine (#3) or both (#4). Last bar (*medium gray*) represents DVA-silenced, dopamine-deficient males that did not mate in the first trial (4th bar) and were subsequently incubated off histamine for two hours before retesting (last bar). p-values for statistical significance were calculated with a Fisher Exact Test and the False Discovery Rate to correct for multiple comparisons.

With the same Markov strategy as before, I modeled the mating behavior of DVA-silenced, dopamine-deficient animals (*see* EXPERIMENTAL PROCEDURES). The mating traces were bootstrapped to generate means and standard deviations for each of the transition probabilities (**Table 11, Figure 4.12**). In this experiment, the dopamine-deficient males are the control condition, and consequently experimental transition

probabilities need to be compared to dopamine-deficient transition probabilities to assess significant differences. Unlike wild-type and nematocin-deficient males, where I had four to five experimental sets to determine the experiment-to-experiment variability, I only have two experimental sets. To supplement this, I also included the "transgene only" and "histamine only" dopamine-deficient data sets (**Table 17**). I felt justified in doing so because, by definition, I am looking for effect sizes larger than the effect of either transgene alone. The adjusted mean and standard deviations for the transition probabilities in **Table 17** were then statistically compared to the experimental means and standard deviations in **Table 11** with an unpaired, two-tailed Student's t test and a False Discovery Rate threshold to correct for multiple comparisons. A summary of all significant results can be found in **Table 9.**

Four of the ten transition probabilities changed significantly. *prod to vulva search* rose from 0.10+/-0.00% in transgene only, dopamine-deficient males to 0.57+/-0.02%, as did *slip to vulva search*, from 0.97+/-0.01% to 1.26+/-0.03% (**Figure 4.9, Table 9**). *slip to vulva search* transition probabilities recovered when males were incubated off histamine, while *prod to vulva search* did not. Both of these transition probabilities increase in value when DVA is silenced in wild-type males and nematocin-deficient males. As in previous experiments, they appear to be independent of the mating phenotype in this case as well, and indicative of another function of DVA.

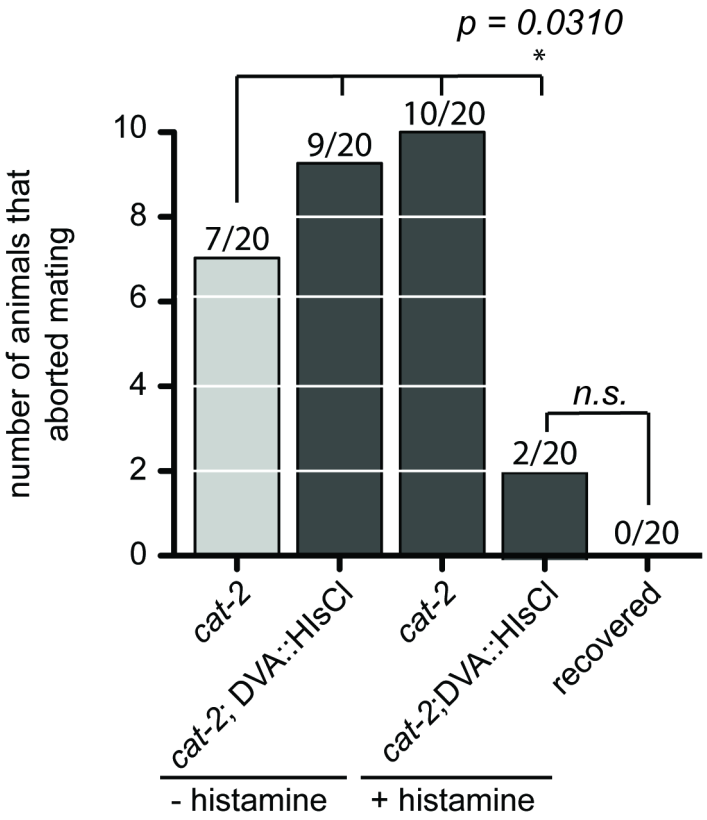

Figure 4.8: Aborted mating attempts of DVA-silenced, dopamine-deficient males. *x-axis:* the conditions/ genotypes tested. DVA::HisCl indicates the presence of an integrated HisCl transgene expressed in DVA. "- histamine" indicates the absence of histamine, "+ histamine" the presence of histamine. *y-axis*: the number of aborted mating attempts per 20 mating attempts. Raw fractions are indicated above each bar. First bar (*light* gray) represents the dopamine-deficient control males. Bar 2-4 (*dark gray*) have the transgene (#2), histamine (#3) and both (#4). Last bar (*medium gray*) represents DVA-silenced, dopamine-deficient males that did not mate in the first trial (4th bar) and were subsequently incubated off histamine for 2 hours before retesting (last bar). p-values for statistical significance were calculated with a Fisher Exact Test and a False Discovery Rate to correct for multiple comparisons.

Table 9: Summary of significant results from Table 11. Mean transition probabilities for dopamine-deficient (*cat-2*), transgene only (+*t.g.*) histamine only (+*his*), DVA-silenced (+*both*), and males allowed to recover off histamine (*rec.*) are shown. Mean values significantly higher than dopamine-deficient controls are in **bold**. Mean values significantly lower than dopamine-deficient controls are in *red*. Transition probabilities that follow a pattern consistent with DVA-silencing are indicated with an asterisk (*).

transition probability	*cat-2*	+ t.g.	+ his.	+ both	rec.
prod to vulva search*	0.00	0.10	0.08	**0.57**	**1.01**
prod to prod*	93.85	97.09	95.73	92.14	91.44
prod to sperm transfer*	0.13	**0.20**	0.15	**0.51**	**0.57**
slip to vulva search*	0.49	0.97	0.42	**1.26**	0.33

Persistence in *prodding* (*prod to prod*) and *prod to sperm transfer* also changed significantly when DVA was silenced in dopamine-deficient males. Transgene only, dopamine-deficient males persisted in *prodding* 97.09+/-0.19% of the time, whereas DVA-silenced, dopamine-deficient males did so 92.14+/-0.24% of the time (**Figure 4.9, Table 9**). *prod to sperm transfer* increased by silencing DVA, from 0.20+/-0.01% (transgene only males) to 0.51+/-0.01% (**Figure 4.9, Table 9**). These transition probabilities also changed in the DVA-silencing experiments performed in wild-type and nematocin-deficient males. Notably, here they change in the opposite direction of previous experiments. This is consistent with the experimental design. I am rescuing function in this instance, while I was disrupting function previously.

Slip to prod transitions did not change significantly as a result of DVA silencing in dopamine-deficient males. Transition probabilities rose from 4.23+/-0.19% (transgene only males, **Table 11**) to 9.31+/-0.13% (DVA-silenced males, **Table 11**). Due to the large experiment-to-experiment fluctuations in this transition probability among dopamine-

deficient males, this change did pass the Student's t test for statistical significance. Both conditions, DVA-silenced or not, had compromised, decreased *slip to prod* transition probabilities.

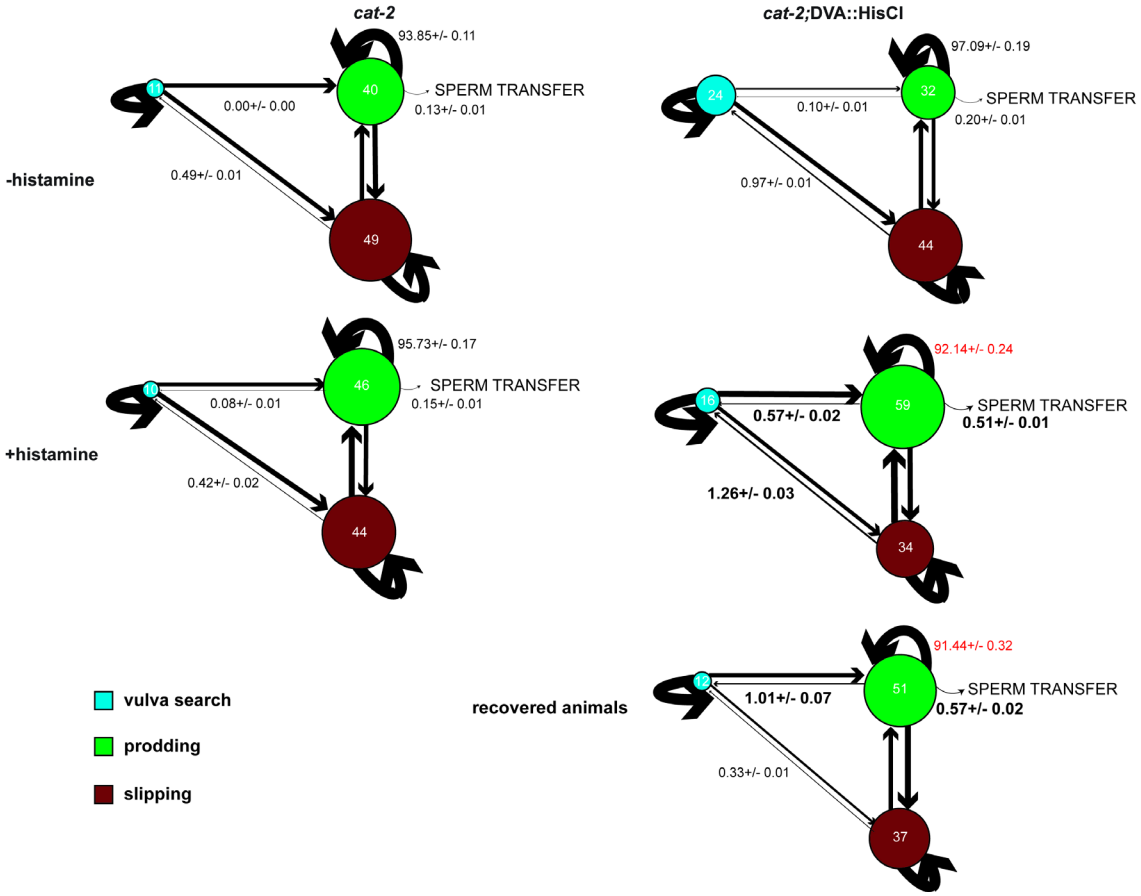

Figure 4.9: Mating dynamics of DVA-silenced, dopamine deficient animals. Numbers within a circle are the percent time in which the males engage in that sub-behavior when mating. Arrow weights represent the probability in a given second that the animal will transition between the behaviors. Curved arrows pointing back toward the circle indicate the probability per second that the animal will persist in the sub-behavior. *Left column* are ethograms of males without the DVA::HisCl transgene. *Right column* are males with the DVA::HisCl transgene. *Top row* are animals tested in the absence of histamine. *Bottom row* are animals tested in the presence of histamine.

A model for dopaminergic regulation of nematocin action

I began this chapter by exploring possible regulation of nematocin action in DVA by examining genes that targeted specific neurons. The overlapping genetic interaction between nematocin and *trp-4* led me to the dopaminergic neurons, which also express TRP-4. I found that nematocin mutants are epistatic to dopamine mutants, and confirmed the result with a transgenic rescue of nematocin. Ethomic investigation and modeling of the single and double mutants directed me to changes in transition probabilities common in both the nematocin-deficient males and the mating defects mediated by nematocin release from DVA (**Chapter III**), namely *prod to sperm transfer*, *slip to prod*, and persistence in *prodding*. Dopamine-deficient animals also exhibited additional mating defects, such as an increased rate in aborting mating attempts, that were also epistatic with nematocin deficiency. By silencing DVA in dopamine-deficient animals, I was able to recapitulate the epistasis result with an orthogonal, circuit manipulation. Here I saw increases in the *prod to vulva search* and *slip to vulva search* transition probabilities, as I have in every DVA silencing experiment regardless of genetic background. I also saw changes in *prod to sperm transfer* and persistence of the *prodding* state. These changes had the opposite sign of those observed by silencing DVA in wild-type males. This makes sense because the former experiment rescues mating, while the latter perturbs it. Significant defect in the *slip to prod* transition probability was observed in dopamine-deficient males, but the small changes observed from DVA silencing were not statistically significant.

Figure 4.10 diagrams the classical regulatory model for the genetic evidence that this chapter presents (Avery and Wasserman, 1992). As stated before, genetic epistasis suggests that dopamine is an upstream regulator of nematocin, and that the severe mating

deficiency observed in dopamine is due to either an excess of nematocin or a lack of nematocin regulation (nematocin at the wrong time or times). This hypothesis was validated by the acute silencing of DVA in dopamine-deficient animals, which altered the transition probabilities implicated in nematocin's action in DVA from prior experiments in order to rescue the mating defect. In the next chapter, we will explore DVA's activity at these critical transitions by characterizing the calcium dynamics of the neuron in freely moving males as they mate.

Figure 4.10: Classical genetic epistasis model for dopamine and nematocin. Bars are indicative of a regulatory function.

Table 10: Means and standard deviations for all transition probabilities for the investigation of nematocin and dopamine's genetic interaction. p values were determined by an unpaired, two-tailed Student's t test with the mean and s.d. from wild-type controls calculated in **Table 15** (*See EXPERIMENTAL PROCEDURES*). Statistical significance was determined by the p value and a False Discovery Rate multiple comparison correction. Statistically significant results are depicted in **bold**.

index	transition	genotype	mean	s.d.	p val	sig?
1	searchtosearch	wt	94.18	0.11	0.1491	
2	searchtoprod	wt	5.47	0.11	0.5435	
3	searchtoslip	wt	0.35	0.02	0.1806	
4	prodtosearch	wt	0.00	0.00	0.3494	
5	prodtoprod	wt	91.89	0.13	0.0512	
6	prodtoslip	wt	7.15	0.13	0.0593	
7	prodtosperm	wt	1.00	0.01	0.7399	
8	sliptosearch	wt	0.54	0.02	0.2632	
9	sliptoprod	wt	13.88	0.14	0.1306	
10	sliptoslip	wt	85.46	0.14	0.9125	
11	searchtosearch	*ntc-1*	93.92	0.03	0.2272	
12	searchtoprod	*ntc-1*	5.12	0.04	0.9496	
13	searchtoslip	*ntc-1*	0.33	0.01	0.1820	
14	**prodtosearch**	***ntc-1***	**0.79**	**0.04**	**<0.0001**	***
15	**prodtoprod**	***ntc-1***	**96.01**	**0.13**	**0.0024**	**
16	prodtoslip	*ntc-1*	2.94	0.10	0.0294	
17	**prodtosperm**	***ntc-1***	**0.26**	**0.01**	**0.0003**	***
18	sliptosearch	*ntc-1*	0.89	0.02	1.000	
19	**sliptoprod**	***ntc-1***	**9.52**	**0.10**	**<0.0001**	***
20	sliptoslip	*ntc-1*	89.59	0.11	0.1033	
21	searchtosearch	*cat-2*	92.09	0.10	0.4822	
22	searchtoprod	*cat-2*	6.04	0.13	0.1574	
23	searchtoslip	*cat-2*	0.86	0.03	0.5945	
24	prodtosearch	*cat-2*	0.05	0.01	0.8112	
25	prodtoprod	*cat-2*	93.65	0.28	0.6040	
26	prodtoslip	*cat-2*	6.20	0.28	0.3053	
27	**prodtosperm**	***cat-2***	**0.09**	**0.01**	**<0.0001**	***
28	sliptosearch	*cat-2*	0.33	0.02	0.0903	
29	**sliptoprod**	***cat-2***	**12.65**	**0.30**	**0.0125**	*
30	sliptoslip	*cat-2*	87.57	0.31	0.4034	
31	searchtosearch	*cat-2;ntc-1*	95.25	0.16	.0237	
32	searchtoprod	*cat-2;ntc-1*	4.04	0.14	0.1298	
33	searchtoslip	*cat-2;ntc-1*	0.70	0.03	0.4250	

34	prodtosearch	*cat-2;ntc-1*	0.00	0.00	0.3494	
35	**prodtoprod**	***cat-2;ntc-1***	**96.67**	**0.03**	**0.0006**	***
36	prodtoslip	*cat-2;ntc-1*	2.76	0.03	0.0212	
37	**prodtosperm**	***cat-2;ntc-1***	**0.58**	**0.01**	**0.0114**	*
38	sliptosearch	*cat-2;ntc-1*	1.34	0.04	0.1609	
39	**sliptoprod**	***cat-2;ntc-1***	**9.28**	**0.18**	**<0.0001**	***
40	sliptoslip	*cat-2;ntc-1*	88.07	0.17	0.2953	
41	searchtosearch	*cat-2;ntc-1; ntc-1* rescue	90.21	0.19	0.0223	
42	searchtoprod	*cat-2;ntc-1; ntc-1* rescue	3.90	0.07	0.0906	
43	searchtoslip	*cat-2;ntc-1; ntc-1* rescue	0.44	0.08	0.2288	
44	**prodtosearch**	***cat-2;ntc-1; ntc-1* rescue**	**0.82**	**0.03**	**<0.0001**	***
45	prodtoprod	*cat-2;ntc-1; ntc-1* rescue	92.51	0.17	0.2342	
46	prodtoslip	*cat-2;ntc-1; ntc-1* rescue	6.37	0.17	0.2306	
47	**prodtosperm**	***cat-2;ntc-1; ntc-1* rescue**	**0.30**	**0.01**	**0.0005**	***
48	sliptosearch	*cat-2;ntc-1; ntc-1* rescue	0.23	0.01	0.0532	
49	**sliptoprod**	***cat-2;ntc-1; ntc-1* rescue**	**2.19**	**0.04**	**<0.0001**	***
50	**sliptoslip**	***cat-2;ntc-1; ntc-1* rescue**	**97.08**	**0.07**	**0.0007**	***

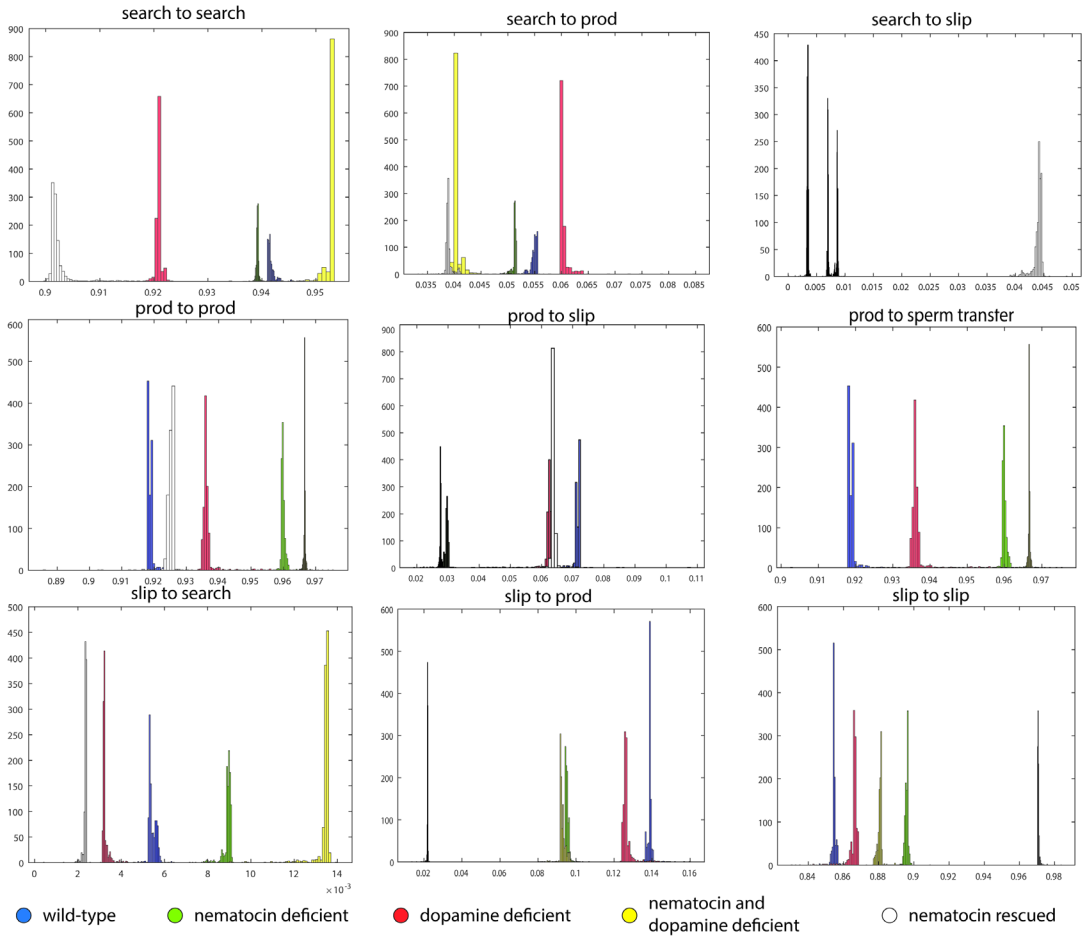

Figure 4.11: Bootstrap data distributions for all sub-behaviors of the *cat-2*, *ntc-1*, and double mutant genetic screen.

Table 11: Means and standard deviations for DVA-silenced, dopamine-deficient animals and controls. p values were determined by an unpaired, two-tailed Student's t test with the mean and s.d. from dopamine-deficient controls calculated in **Table 17** (*see* EXPERIMENTAL PROCEDURES). Statistical significance was determined by the p value and a False Discovery Rate multiple comparison correction. Statistically significant results are depicted in **bold.**

index	genotype	condition	transition	mean	sd	p val.	sig?
1	*cat-2*	-his	searchtosearch	90.33	0.11	0.5357	
2	*cat-2*	-his	searchtoprod	4.07	0.05	0.5903	
3	*cat-2*	-his	searchtoslip	3.93	0.05	0.7848	
4	*cat-2*	-his	prodtosearch	0.00	0.00	0.0240	
5	*cat-2*	-his	prodtoprod	93.85	0.11	0.1851	
6	*cat-2*	-his	prodtoslip	6.02	0.11	0.1800	
7	*cat-2*	-his	prodtosperm	0.13	0.01	0.5504	
8	*cat-2*	-his	sliptosearch	0.49	0.01	0.6936	
9	*cat-2*	-his	sliptoprod	2.12	0.08	0.0970	
10	*cat-2*	-his	sliptoslip	97.18	0.07	0.0555	
11	*cat-2*	+his	searchtosearch	90.84	0.13	0.7292	
12	*cat-2*	+his	searchtoprod	2.70	0.09	0.4934	
13	*cat-2*	+his	searchtoslip	5.41	0.13	0.1233	
14	*cat-2*	+his	prodtosearch	0.08	0.01	0.3694	
15	*cat-2*	+his	prodtoprod	95.73	0.17	0.4604	
16	*cat-2*	+his	prodtoslip	4.04	0.17	0.4588	
17	*cat-2*	+his	prodtosperm	0.15	0.01	0.5504	
18	*cat-2*	+his	sliptosearch	0.42	0.02	0.4055	
19	*cat-2*	+his	sliptoprod	7.50	0.17	0.7179	
20	*cat-2*	+his	sliptoslip	91.56	0.16	0.6756	
21	*cat-2*; DVA::HisCl	-his	searchtosearch	92.62	0.07	0.5321	
22	*cat-2*; DVA::HisCl	-his	searchtoprod	1.07	0.05	0.0633	
23	*cat-2*; DVA::HisCl	-his	searchtoslip	4.40	0.08	0.4735	
24	*cat-2*; DVA::HisCl	-his	prodtosearch	0.10	0.01	0.1004	
25	*cat-2*; DVA::HisCl	-his	prodtoprod	97.09	0.19	0.0508	
26	*cat-2*; DVA::HisCl	-his	prodtoslip	2.62	0.17	0.0502	
27	***cat-2*; DVA::HisCl**	**-his**	**prodtosperm**	**0.20**	**0.01**	**0.0090**	**

28	*cat-2*; DVA::HisCl	-his	sliptosearch	0.97	0.01	0.0275	
29	*cat-2*; DVA::HisCl	-his	sliptoprod	4.23	0.19	0.3363	
30	*cat-2*; DVA::HisCl	-his	sliptoslip	93.44	0.19	0.6353	
31	*cat-2*; DVA::HisCl	+his	searchtosearch	92.41	0.12	0.6077	
32	*cat-2*; DVA::HisCl	+his	searchtoprod	4.13	0.1	0.5546	
33	*cat-2*; DVA::HisCl	+his	searchtoslip	2.75	0.05	0.3940	
34	***cat-2*; DVA::HisCl**	**+his**	**prodtosearch**	**0.57**	**0.02**	**<0.0001**	***
35	***cat-2*; DVA::HisCl**	**+his**	**prodtoprod**	**92.14**	**0.24**	**0.0121**	*
36	*cat-2*; DVA::HisCl	+his	prodtoslip	6.78	0.24	0.0543	
37	***cat-2*; DVA::HisCl**	**+his**	**prodtosperm**	**0.51**	**0.01**	**<0.0001**	**
38	***cat-2*; DVA::HisCl**	**+his**	**sliptosearch**	**1.26**	**0.03**	**0.0028**	**
39	*cat-2*; DVA::HisCl	+his	sliptoprod	9.31	0.13	0.2874	
40	*cat-2*; DVA::HisCl	+his	sliptoslip	89.07	0.14	0.1432	
41	*cat-2*; DVA::HisCl	recovery	searchtosearch	95.03	0.08	0.0861	
42	*cat-2*; DVA::HisCl	recovery	searchtoprod	3.42	0.04	0.9637	
43	*cat-2*; DVA::HisCl	recovery	searchtoslip	1.55	0.07	0.0760	
44	***cat-2*; DVA::HisCl**	**recovery**	**prodtosearch**	**1.01**	**0.07**	**<0.0001**	***
45	***cat-2*; DVA::HisCl**	**recovery**	**prodtoprod**	**91.44**	**0.32**	**0.0048**	**
46	*cat-2*; DVA::HisCl	recovery	prodtoslip	6.98	0.27	0.0401	
47	***cat-2*; DVA::HisCl**	**recovery**	**prodtosperm**	**0.57**	**0.02**	**<0.0001**	**
48	*cat-2*; DVA::HisCl	recovery	sliptosearch	0.33	0.01	0.1802	
49	*cat-2*; DVA::HisCl	recovery	sliptoprod	4.09	0.19	0.2876	
50	*cat-2*; DVA::HisCl	recovery	sliptoslip	95.58	0.19	0.1924	

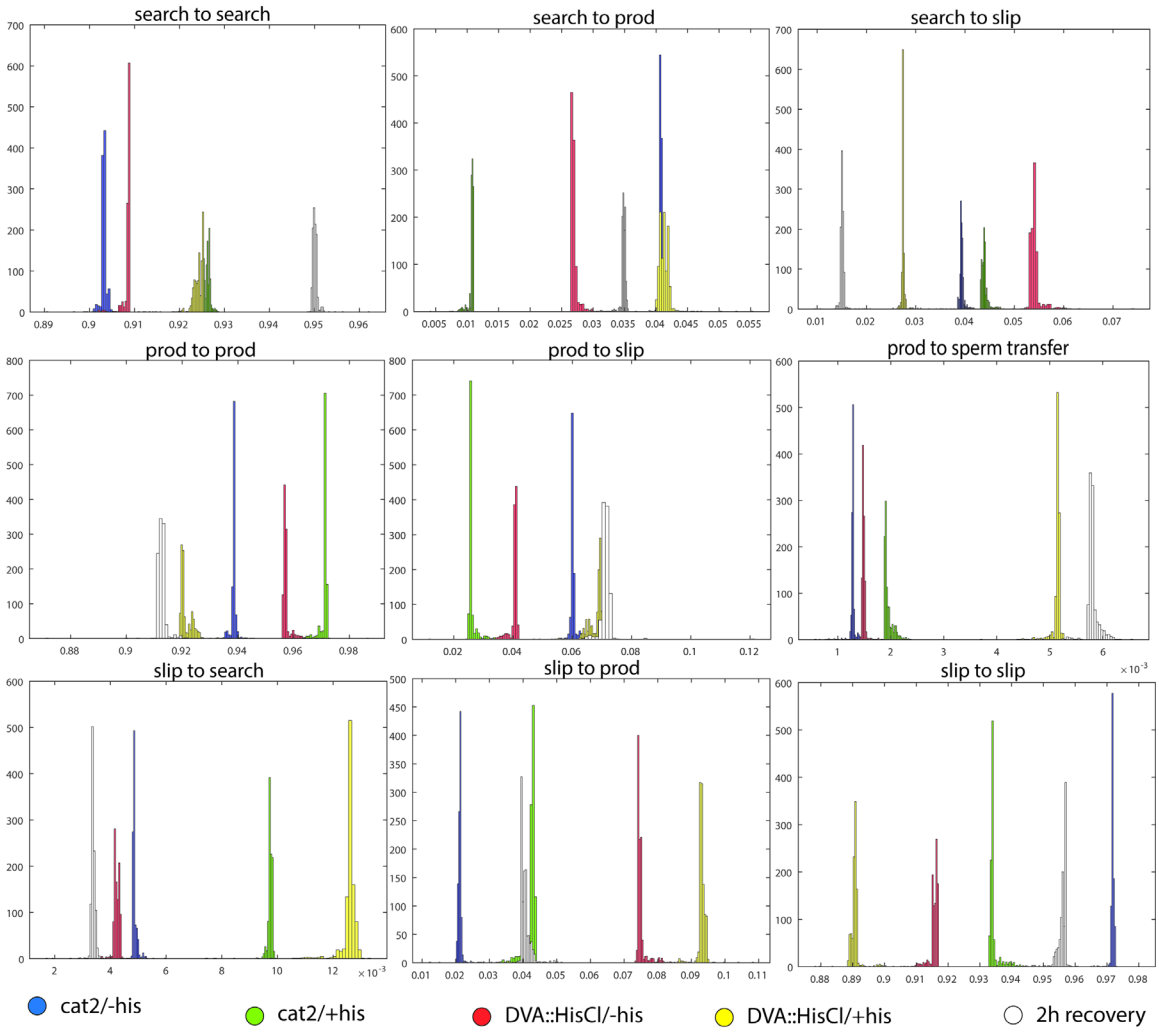

Figure 4.12: Bootstrap data distributions for all sub-behaviors of the *cat-2*, DVA-silencing experiment.

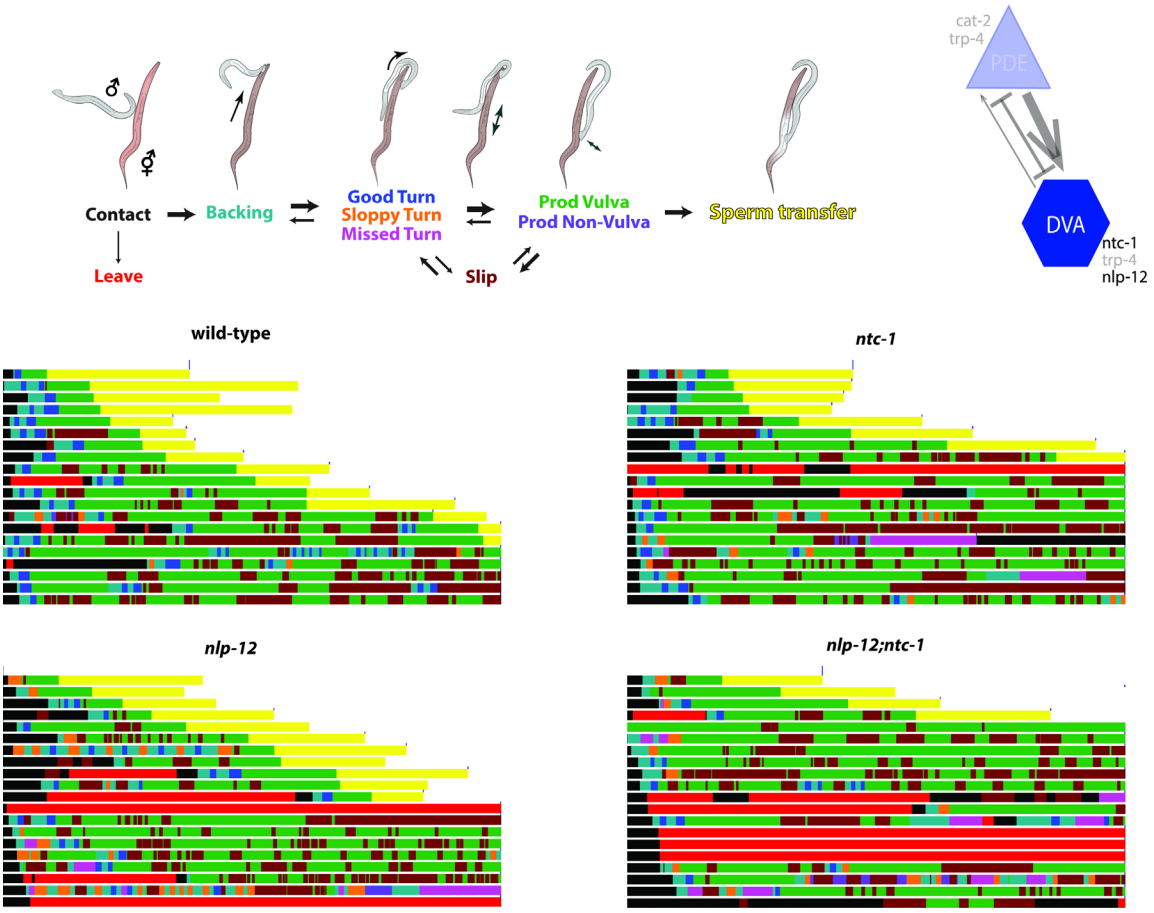

Figure 4.13: Raw mating traces from *nlp-12* mutant and epistatis with *ntc-1*. *Top*, colorized mating schema indicating the color code for the behavioral traces. *Bottom*, raw mating traces for wild-type, nematocin deficient (*ntc-1*), NLP-12 deficient (*nlp-12*), and the copeptide knockout (*ntc-1;nlp-12*). Wiring diagram (*top right*) indicates the neuron(s) affected by the gene.

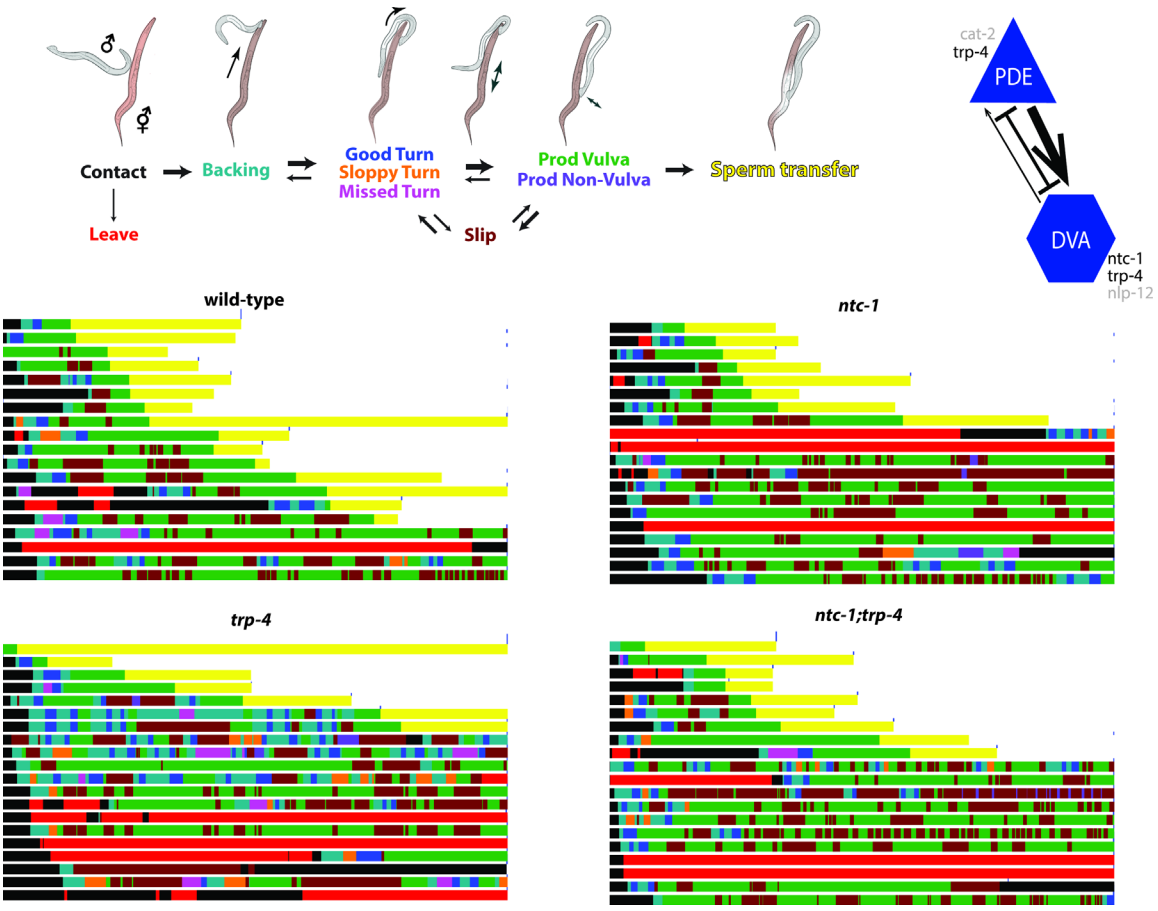

Figure 4.14: Raw mating traces from *trp-4 12* mutant and epistatis with *ntc-1*. *Top*, colorized mating schema indicating the color code for the behavioral traces. *Bottom*, raw mating traces for wild-type, nematocin deficient (*ntc-1*), TRP-4 channel deficient (*trp-4*), and the double knockout (*ntc-1;trp-4*). Wiring diagram (*top right*) indicates the neuron(s) affected by the gene.

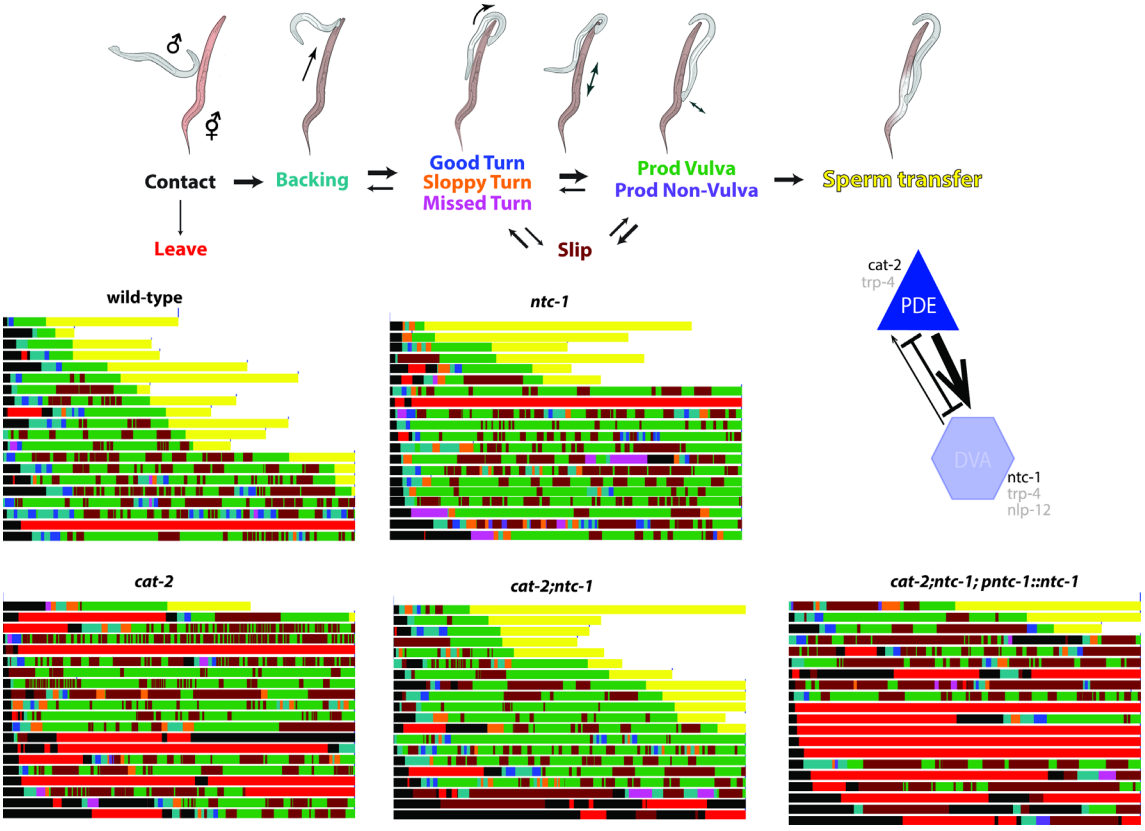

Figure 4.15: Raw mating traces from *cat-2 12* mutant and epistatis with *ntc-1*. *Top*, colorized mating schema indicating the color code for the behavioral traces. *Bottom*, raw mating traces for wild-type, nematocin deficient (*ntc-1*), Dopamine deficient (*cat-2*), and the double knockout (*cat-2;ntc-1*). Wiring diagram (*top right*) indicates the neuron(s) affected by the gene.

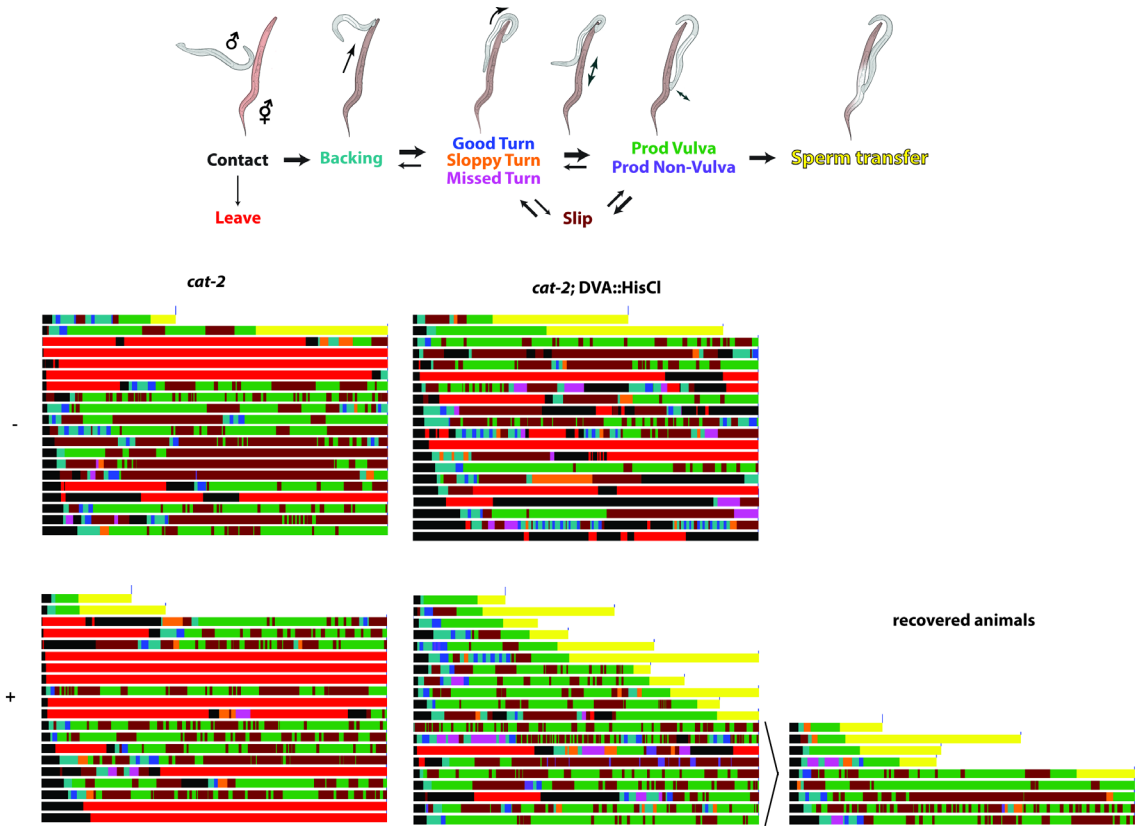

Figure 4.16:. Raw mating traces from silencing DVA in dopamine-deficient males. *Top*, colorized mating schema indicating the color code for the behavioral traces. *Bottom*, raw mating traces for nematocin-deficient and transgene positive, dopamine-deficient males in both the presence and absence of histamine. *Right*, males that did not mate from the DVA-silenced test group retested after a two hour incubation off histamine. Each mating trace is five minutes. *White* space indicates the conclusion of mating after sperm has been transferred.

CHAPTER V: DVA ACTIVITY DURING MATING

Introduction

In **Chapter III**, I established that DVA activity was important for coherent mating behavior, and that acutely silencing DVA just prior to mating disrupted mating at the *prod to sperm transfer* and *slip to prod* state transitions via the action of nematocin. In **Chapter IV**, I established that dopamine was responsible for the regulation of nematocin action. Dopamine deficiency leads to a disregulation of nematocin, either too much of the peptide, or release of the peptide at inappropriate times. From here, I wanted to understand DVA's activity in the context of mating, and how that activity changed in different genetic backgrounds, such as a dopamine-deficient background.

To do so, I expressed the fluorescent calcium indicator GCaMP5A (Akerboom et al., 2013) in DVA under the *nlp-12* cell-specific promoter fragment (Hu et al., 2011). These experiments were conducted in a *lite-1* background to reduce the effects of the fluorescent microscopy's excitatory light on the behavior of the mating males (Liu, J. et al. 2010). Males with the integrated GCaMP transgene were assayed for mating and imaged under GFP fluorescent microscopy settings as described in the EXPERIMENTAL PROCEDURES. Ten wild-type, dopamine-deficient, and nematocin-deficient males were tested, as well as five control males expressing GFP in DVA. 8/10 wild-type animals mated during the assay, 4/10 of the nematocin-deficient animals mated, and 0/10 of the dopamine-deficient animals mated, comparable to mating efficiencies under bright-field microscopy. **Figure 5.1** shows representative traces for wild-type, dopamine-deficient, and nematocin-deficient males of DVA calcium activity as they mate. **Figure 5.5, 5.6,** and **5.7** present all

raw traces of the data, and **Figure 5.8** presents the traces of animals expressing GFP in DVA in place of GCaMP.

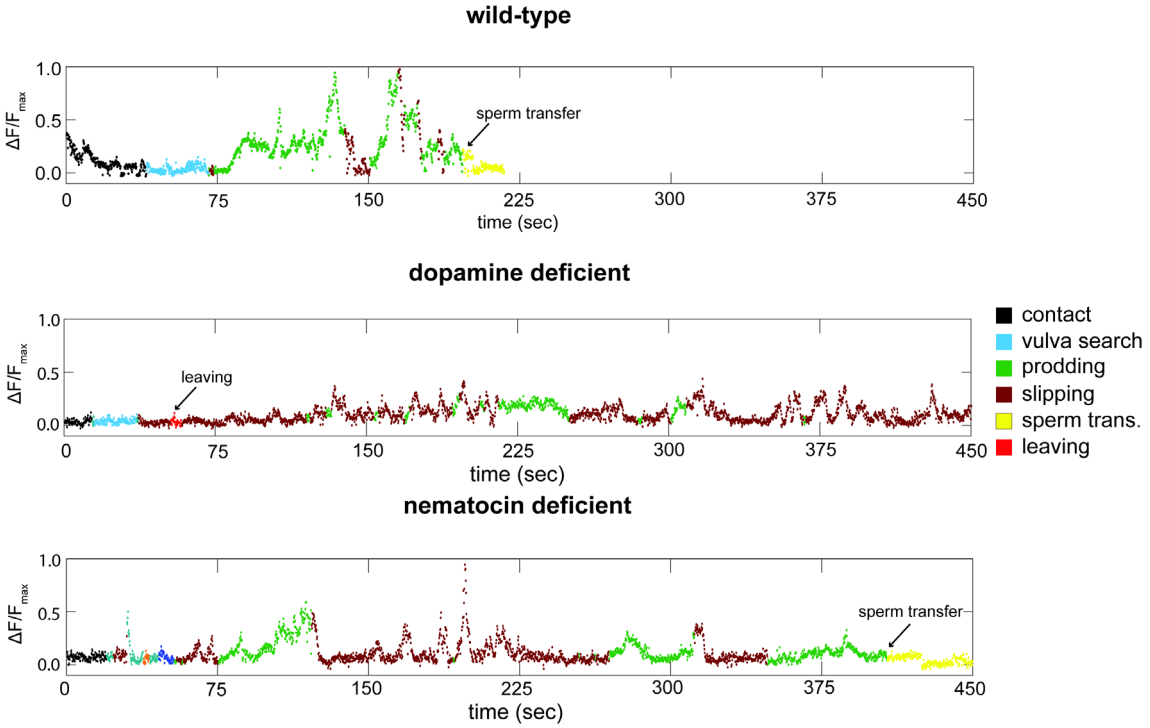

Figure 5.1: Examples of DVA activity in wild-type, dopamine-deficient, and nematocin-deficient males during mating. *Top*: Representative trace of DVA activity in a wild-type male while mating. *Middle:* Representative trace of DVA activity in a dopamine-deficient male while mating. *Bottom:* Representative trace of DVA activity in a nematocin-deficient male while mating. Colors correspond to the sub-behaviors being performed at the time (*x-axis*) according to the following key: *black-contact*; *light blue-vulva search*; *green-prodding*; *maroon-slipping*; *yellow-sperm transfer*; and *red-leaving*. *y-axis* is the $\Delta F/F_{max}$, background adjusted and then normalized on a 0 to 1 scale.

DVA activity correlates with mating behavior

From the raw calcium traces of the wild-type animals, I qualitatively established behavior patterns corresponding to patterns of DVA activity. Calcium signal in DVA reliably rose with the onset of *prodding* behavior (*green*) that followed *slipping* behavior (*maroon*) (**Figure 5.1, Figure 5.5**). *Slipping* behaviors were often accompanied or

preceded by a decrease in calcium signal. Furthermore, during a *prodding* event, calcium signals in DVA fell several second before *sperm transfer*.

In dopamine-deficient males, *prodding* events were not reliably accompanied by rises in DVA calcium levels, and DVA calcium signal both rose and fell in association with *slipping* (**Figure 5.1, Figure 5.6**). GCaMP signal appeared to have a higher resting state in these males, a smaller dynamic range, and were also less stable, "flickering" more during the course of the mating. In nematocin-deficient males, rises in calcium signal accompanied *prodding* events, but were less robust (**Figure 5.1, Figure 5.7**). As in dopamine-deficient males, rises and falls in signal were observed during *slipping* behavior. Calcium decreases preceding *sperm transfer* were also observed, but were less dramatic in nematocin-deficient males than in wild-type. The differences in the nematocin-deficient animals suggests that nematocin itself auto-regulates DVA activity through a feedback mechanism that remains to be elucidated.

DVA activity drops significantly prior to the onset of sperm transfer

To characterize these trends quantitatively, I performed "event-triggered analysis" on the data: aligning sections of traces based on the onset of a behavioral event, and taking the average of the signal during a time interval before and after the event. The onset of the event is defined as time = 0 and fluorescence at that point is by definition F_0. This allowed me to calculate changes in fluorescence with reference to the onset of this event. I first performed this analysis on the signal at the *prod to sperm transfer* transition in wild-type animals (**Figure 5.2**). Individual traces of these events can be seen in *green* during *prodding* and in *yellow* during *sperm transfer* (**Figure 5.2, A**). Signal was smoothed

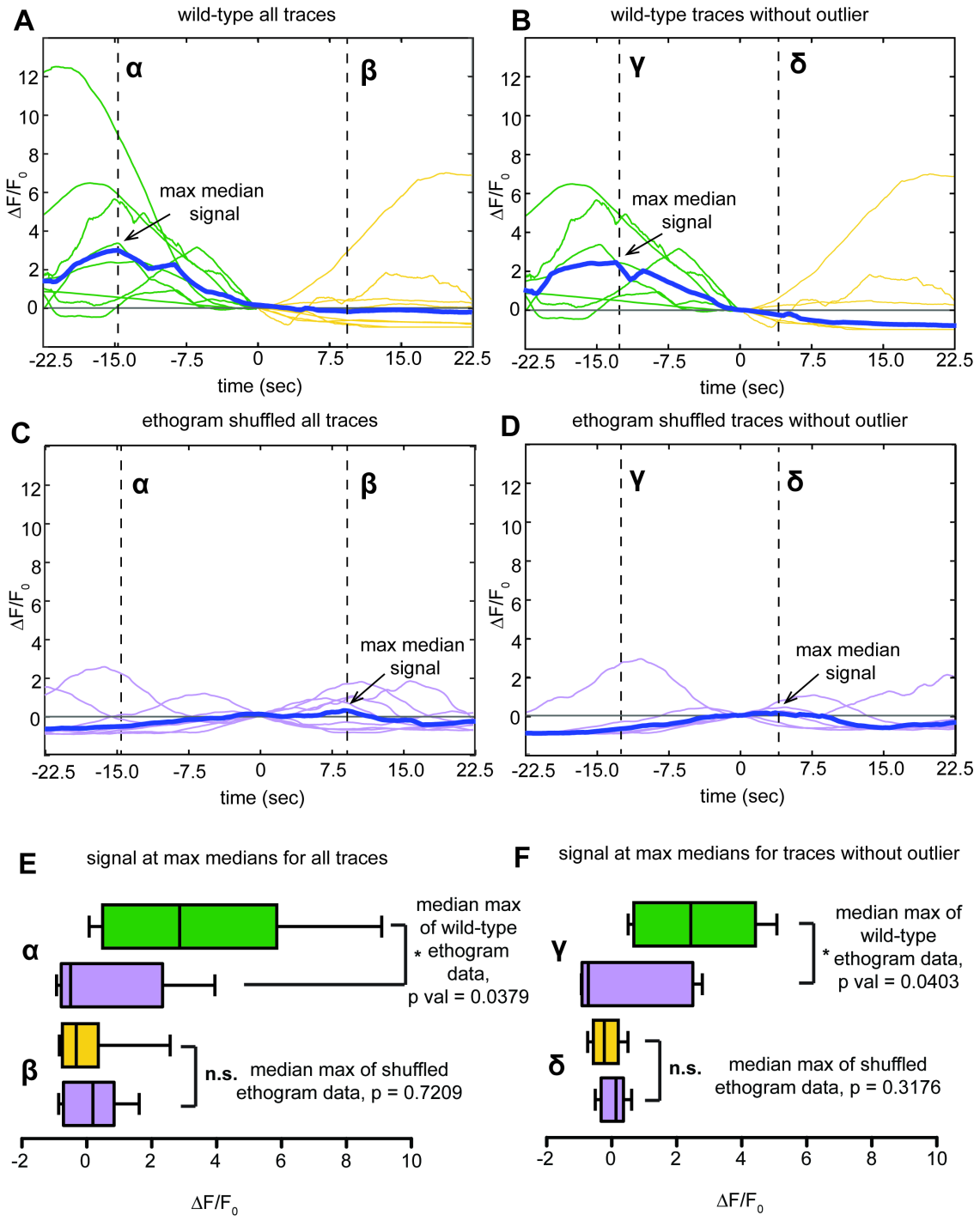

Figure 5.2: A significant drop in calcium signal precedes *sperm transfer* in mating males. A: individual calcium traces for wild-type males, aligned by the onset of *sperm transfer* (*yellow*). *Green/yellow* traces are the smoothed DVA::GCaMP signal from mating males. *Blue* line represents the median of all the trace values at the given time point. *x-axis* is time before and after the onset of the *sperm transfer* event (*0 sec*). *y-axis* is the

$\Delta F/F_0$, where F_0 is the fluorescence at the onset of *sperm transfer*. **B:** individual calcium traces for wild-type males without the "outlier trace." **C:** individual calcium traced for ethogram-shuffled DVA::GCaMP controls. **D**: individual calcium traced for ethogram-shuffled DVA::GCaMP controls without the "outlier trace." **E***:* Box and whisker plots of signal values at the maximum median values of the data. **α** compares the signal distribution of the wild-type and shuffled data at the timepoint of the wild-type's maxiumum median value. **β** compares the signal distribution at the timepoint of the shuffled data's maximum value. Whiskers show the minimum and maximum values of the distribution. P values were calculated with the Mann Whitney Test. **F**: Box and whisker plots of signal values at the maximum median values of the data without the outlier. **γ** compares the signal distribution of the wild-type and shuffled data at the timepoint of the wild-type's maxiumum median value. **δ** compares the signal distribution at the timepoint of the shuffled data's maximum value.

according to the "smoothdata" function in Matlab®, which averages the signal over an interval determined heuristically. The median of the traces is indicated with the *thick blue* line, and its maximum signal was calculated to be at time value **α**, approximately 15 seconds prior to the onset of *sperm transfer*. At this point, the median calcium signal for wild-type animals is 3-fold higher than at the moment of *sperm transfer*.

To determine if this decrease in signal was statistically significant, I created a control data set by shuffling the ethograms of the wild-type traces, selecting the same number of events as my wild-type data (in this instance, 8 traces), and re-running the analysis (*see* EXPERIMENTAL PROCEDURES). This triggered the "event" at random times in the GCaMP signal traces, which could then be sorted and analyzed in a similar fashion as the authentic traces (**Figure 5.2, C**). Constructing the control data in this fashion accounted for the internal noise of the samples being analyzed, as the data comes directly from those samples. I next graphed the median signal of these traces (*blue* line) and found

the maximum median value at timepoint **β,** approximately 8 seconds after the onset of *sperm transfer*, measuring <0.1 times F_0. All the trace values at timepoints **α** (~15 sec. before *sperm transfer*) and **β** (~8 sec. after *sperm transfer*) for the wild-type and ethogram shuffled data were then statistically compared with the Mann-Whitney Test. This data is presented both as a "box and whiskers" plot (**Figure 5.2, E**). Wild-type and ethogram shuffled traces varied significantly at timepoint **α**, with a p value of 0.0379, and were not significantly different at timepoint **β**, with a p value of 0.7209. Thus, the data suggests that there is a significant drop in activity in DVA approximately 15 seconds prior to the onset of *sperm transfer*. By performing the same analysis at the timepoint of the maximum median signal of my shuffled ethogram data, I do not "trigger" a false positive, as those distributions are not significant.

I then wondered if the trace containing the largest dynamic change (12-fold, approximately 2 times the fold change of the next dynamic trace) was skewing the distribution, and therefore my statistical results. To address this, I performed the same analysis on the data without this trace (**Figure 5.2**). Median signal is presented in *blue*, and the remaining 9 traces had their ethograms shuffled to create a control data set (**Figure 5.2, D**). The maximum median signal for the wild-type data was found to be at timepoint **γ** (~12 sec. before *sperm transfer*), and the maximum median signal for the shuffled ethogram was found to be at timepoint **δ** (~5 sec. after *sperm transfer***)**. All values for the traces of wild-type and ethogram-shuffled males at these corresponding timepoints were then compared using a Mann-Whitney test for statistical significance (**Figure 5.2**, **F**). The difference in distribution signal values at timpoint **γ** were for wild-type animals was statistically significant, with a p value of 0.0403, while the difference in signal at timepoint

δ was not statistically significant between the two data sets (p value of 0.3176). This result recapitulates the analysis including the outlying trace, and allows me to conclude that my result is not dependent on the existence of a single extreme data point.

Because none of the dopamine-deficient animals mated, a similar analysis on them could not be performed. By looking at the raw traces, I observe that none of the traces rise in levels comparable to wild-type animals during *prodding* events. I posit that if the signal never rises, it is never able to fall and trigger the *sperm transfer* event.

Wild-type animals show asymmetrical activity in DVA in slipping and prodding transitions

I next investigated DVA activity at the *prodding* and *slipping* transitions using the same "event-triggered" analysis. Individual traces that began in *slipping* (*maroon*), and transitioned into *prodding* (*green*) were aligned at the onset of *prodding* (**Figure 5.3**, **A**). The median of the signal traces is graphed with the same color convention in **Figure 5.3, C**. To characterize the observed increase in calcium signal after the onset of *prodding*, the maximum of the median signal was found at timepoint **ε**, approximately 6 seconds after the onset of *prodding*. A control data set was also constructed in the same manner as the *prod to sperm transfer* analysis: by randomly shuffling the ethogram to "trigger" the *prodding* even at random times in the calcium trace. The median of these signal traces is graphed in *purple* (**Figure 5.3**, **C**). The difference in the distribution of signals of the wild-type and ethogram-shuffled data sets was then statistically analyzed with a Mann-Whitney test (**Figure 5.3, E**), and determined to be statistically significant (p value of 0.0226). Thus, the increase in signal succeeding the onset of the prodding event is quantitatively verified.

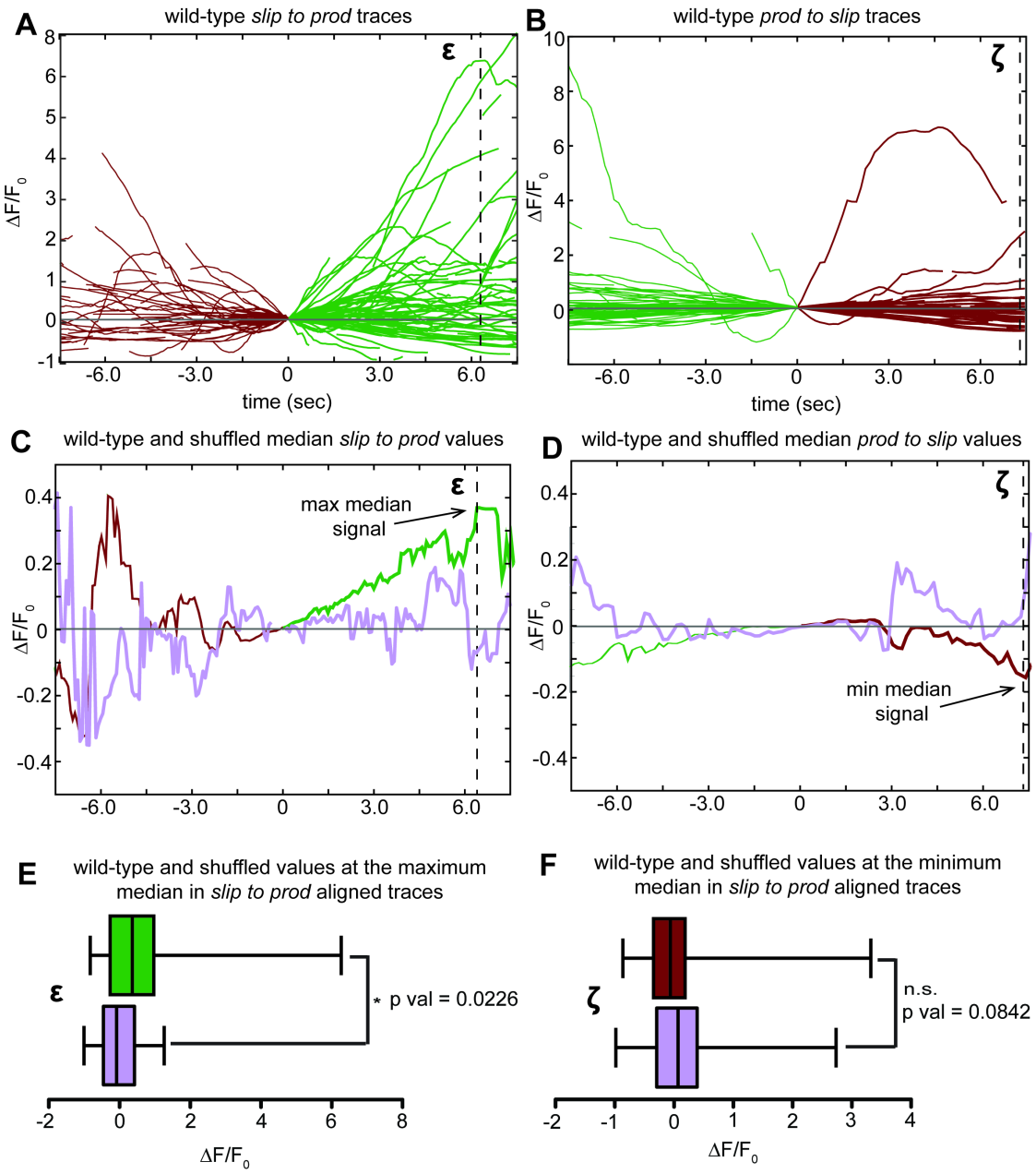

Figure 5.3: DVA activity increases at the *slip to prod* transition in wild-type males. A: Individual calcium traces for wild-type males *slipping* (*maroon*), aligned by the onset of *prodding* (*green*). *x-axis*: time before and after the event onset. *y-axis*: fold change in fluorescence where '0' is defined as the fluorescence at the onset of the event. **B**: Individual calcium traces for wild-type males *prodding*, aligned by the onset of *slipping*. *Middle*: Graphs of the median values for the *slip to prod* (**C**) and *prod to slip* (D) data at all timepoints. Shuffled control data medians graphed in *purple*. **E**: box and whiskers plots for the signal distribution for wild-type and shuffled data at the at timepoint of the

maximum median value (ε) of the wild-type data. **F**: box and whiskers plots for the signal distribution for wild-type and shuffled data at the at timepoint of the minimum median value of the wild-type data (ζ). Whiskers show minimum and maximum values of the distribution. P values calculated by the Mann Whitney Test.

To ensure that the significant rise in signal is unique to *prodding* behavior, and not just any behavior, I also analyzed the calcium signal at the *prod to slip* transition in the same manner (**Figure 5.3**, **B, D,** and **F**). Traces that began with *prodding* and transitioned to *slipping* were aligned at the onset of slipping (**Figure 5.3**, **B**) and the median of all the traces was graphed (**Figure 5.3**, **D**). The trend at the onset of *slipping* was to decrease in signal, not to increase in signal, so the minimum median value was determined to be at timepoint ζ, approximately 7.5 seconds after the onset of *slipping*. A control data set was generated by shuffling the ethograms and thereby randomly triggering *slipping* events in the calcium traces. The signals of these two data sets were compared at timepoint ζ with a Mann-Whitney test (**Figure 5.3**, **F**) and determined to be not statistically significant, with a p value of 0.0842. This demonstrates that not every sub-behavior of mating correlates with a coordinated change in DVA activity, but that this feature is unique to the onset of *prodding* and the *prodding* behavior that directly precedes *sperm transfer*.

Dopamine-deficient animals do not have coordinated changes in DVA activity at prodding or slipping transitions

While none of the dopamine-deficient animals successfully mated in this assay, they did undergo a number of *slip to prod* and *prod to slip* transitions (**Figure 5.4**). **Figure 5.4**, **A** that begins in the *slipping* sub-behavior and transitions to the *prodding* sub-behavior.

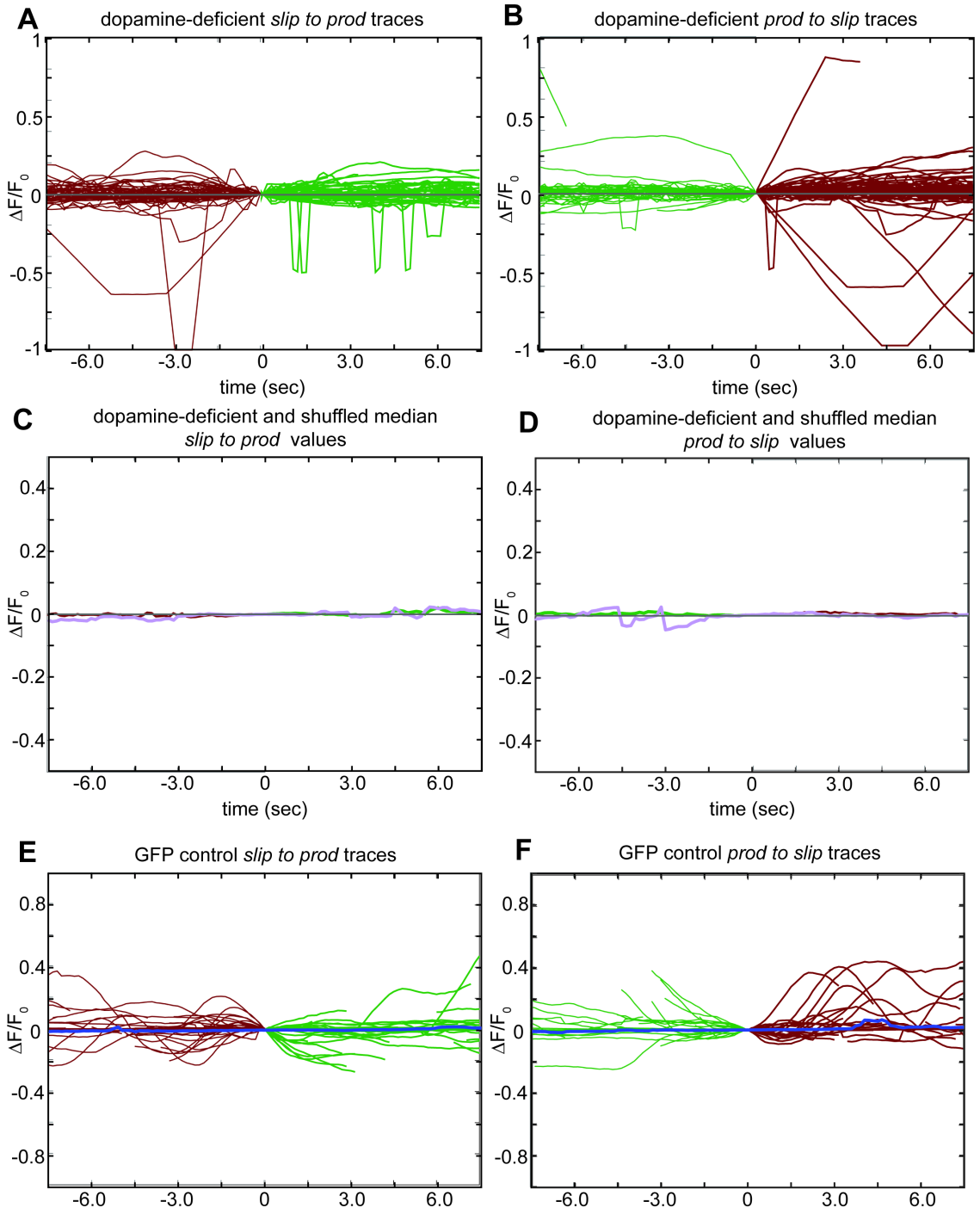

Figure 5.4: DVA activity does not significantly increase at the *slip to prod* transition in dopamine-deficient males. A: Individual calcium traces for dopamine-deficient males *slipping* (*maroon*), aligned by the onset of *prodding* (*green*). *x-axis*: time before and after the event onset. *y-axis*: fold change in fluorescence where '0' is defined as the fluorescence at the onset of the event. **B**: Individual calcium traces for dopamine-deficient males

prodding, aligned by the onset of *slipping*. *Middle*: Graphs of the median values for the *slip to prod* (**C**) and *prod to slip* (**D**) data at all timepoints. Shuffled control data medians graphed in *purple*. *Bottom*: Individual *slip to prod* (**E**) and *prod to slip* (**F**) traces for males expressing GFP in DVA. Median of traces graphed in *blue*.

The median signal for these traces is graphed in **Figure 5.4, C**. The median signal for a dopamine-deficient, ethogram-shuffled control data set is graphed in **Figure 5.4, C** in *purple*. No clear change in GCaMP signal is observed, so no minimum or maximums in the median signal could be identified. Dopamine-deficient and ethogram shuffled control data set medians largely overlap and do not veer far from the F_0 value. To compare, the signal traces for males expressing GFP in DVA were also graphed (**Figure 5.4**, **E**) with their median (*blue*). In these controls, I also do not see significant changes in signal at the onset of *prodding*, and these look similar to the dopamine-deficient male data.

The analysis was repeated for events that began with *prodding* and transitioned to *slipping.* No significant change was observed here either, nor were the dopamine-deficient traces significantly different from the ethogram-shuffled data nor the GFP control data (**Figure 5.4**, **B, D,** and **F**).

Discussion

DVA, the neuron releasing the neuropeptide nematocin, has activity at behavioral transitions that correspond to those previously identified by genetic and pharmacogenetic evidence. Either silencing DVA or genetically knocking out the nematocin gene resulted in a diminution of the *prod to sperm transfer* and the *slip to prod* transition probabilities during mating behavior. Similar defects were present in dopamine-deficient males, which I postulate mate poorly due to a dysregulation of nematocin.

Here I show a potential mechanism for DVA dysregulation. In the case of *prod to sperm transfer* I see a clear drop in GCaMP signal just prior to the transition. I suggest that dopamine-deficient animals do not carry out this transition because they do not achieve a signal rise significant enough support a drop. In the case of the *slip to prod* transition, where I do have dopamine-deficient traces to analyze, I see a clear increase in signal upon the onset of *prodding* in wild-type animals, and no such trend in dopamine-deficient animals.

The emerging model suggests a number of conclusions. For one, it indicates that the *dynamics* of nematocin release and not the absolute levels are important to mating regulation. To trigger *sperm transfer*, it is not that nematocin be present or absent, but that the levels drop. To signal the onset of *prodding*, I suggest that nematocin release increases with DVA activity, is not merely present, otherwise this transition would be preserved in dopamine-deficient animals.

Secondly, because DVA activity suggests a directionality, I propose that the role of nematocin is to assist the animal in productive persistence in the *prodding* state. If DVA activity corresponds to nematocin release, then it would follow that nematocin levels increase at the onset of *prodding* in the *slip to prod* transition. In nematocin-deficient animals, I observe an increased tendency to persist in the *prodding* state compared to their wild-type counterparts. Without nematocin, they are less likely to make the *prod to sperm transfer* transition. DVA activity at the *slip to prod* and *prod to sperm transfer* transitions is partially preserved (**Figure 5.2**), but these animals lack the neuropeptide presumably released with the changes in neuronal activity. Thus, it cannot be the dynamics of DVA

independent of nematocin responsible for the behavioral transitions, but the dynamics of the neuropeptide's action in DVA itself.

In the next chapter, I will explore how dopamine communicates with DVA to tightly couple its activity with the mating behavior.

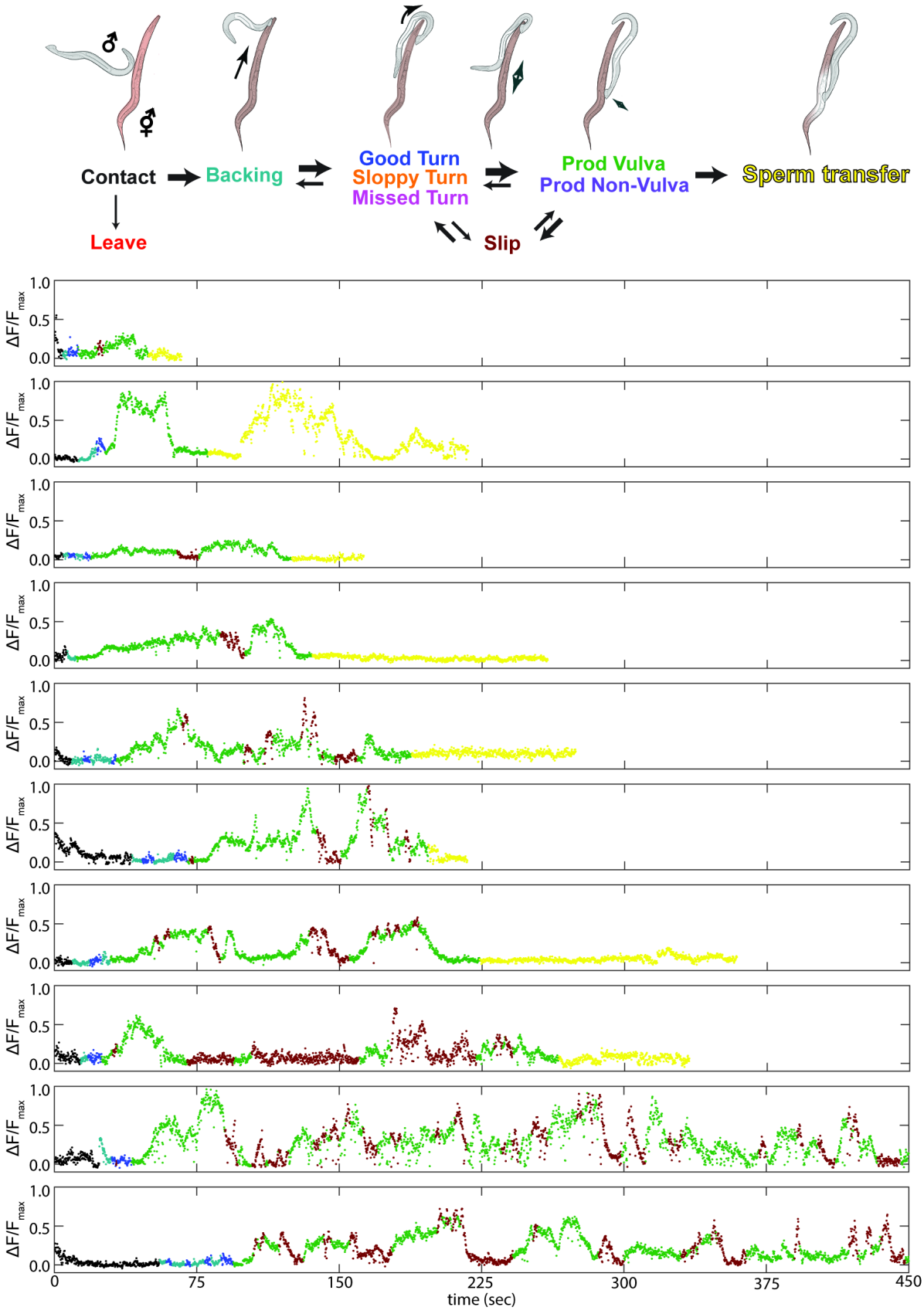

Figure 5.5: Raw traces of DVA activity in wild-type, mating males.

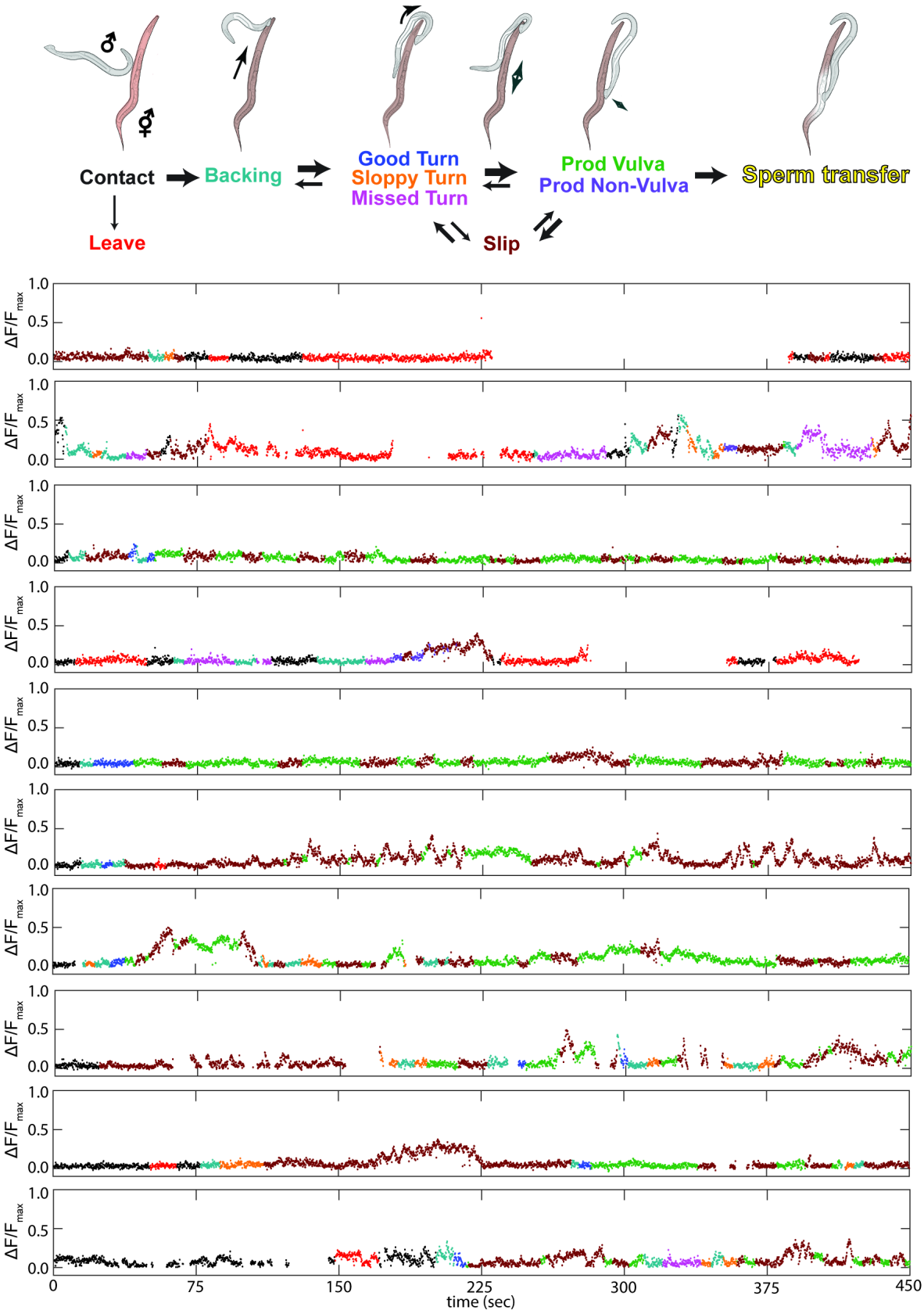

Figure 5.6: Raw traces of DVA activity in dopamine-deficient, mating males.

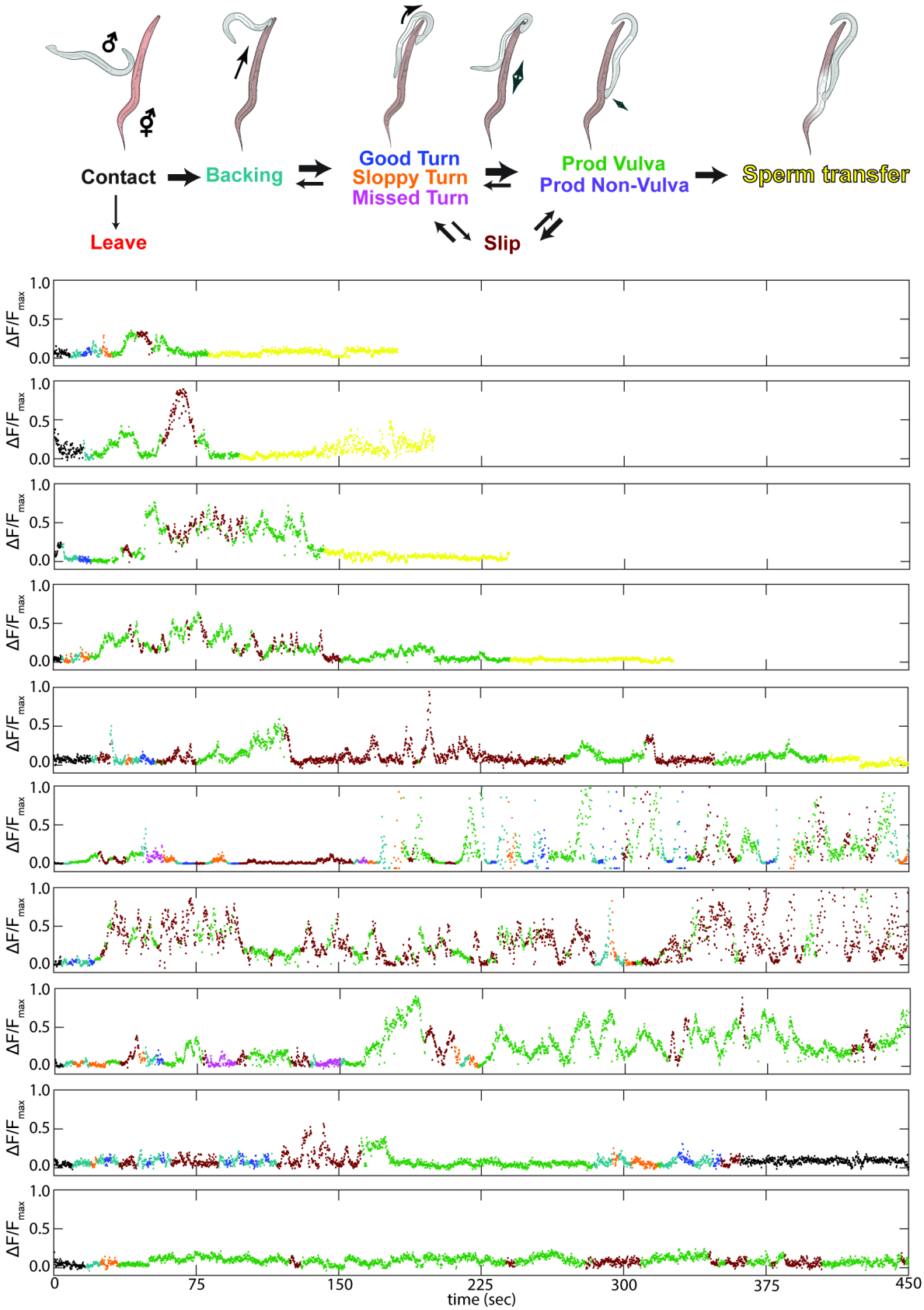

Figure 5.7: Raw traces of DVA activity in nematocin-deficient, mating males.

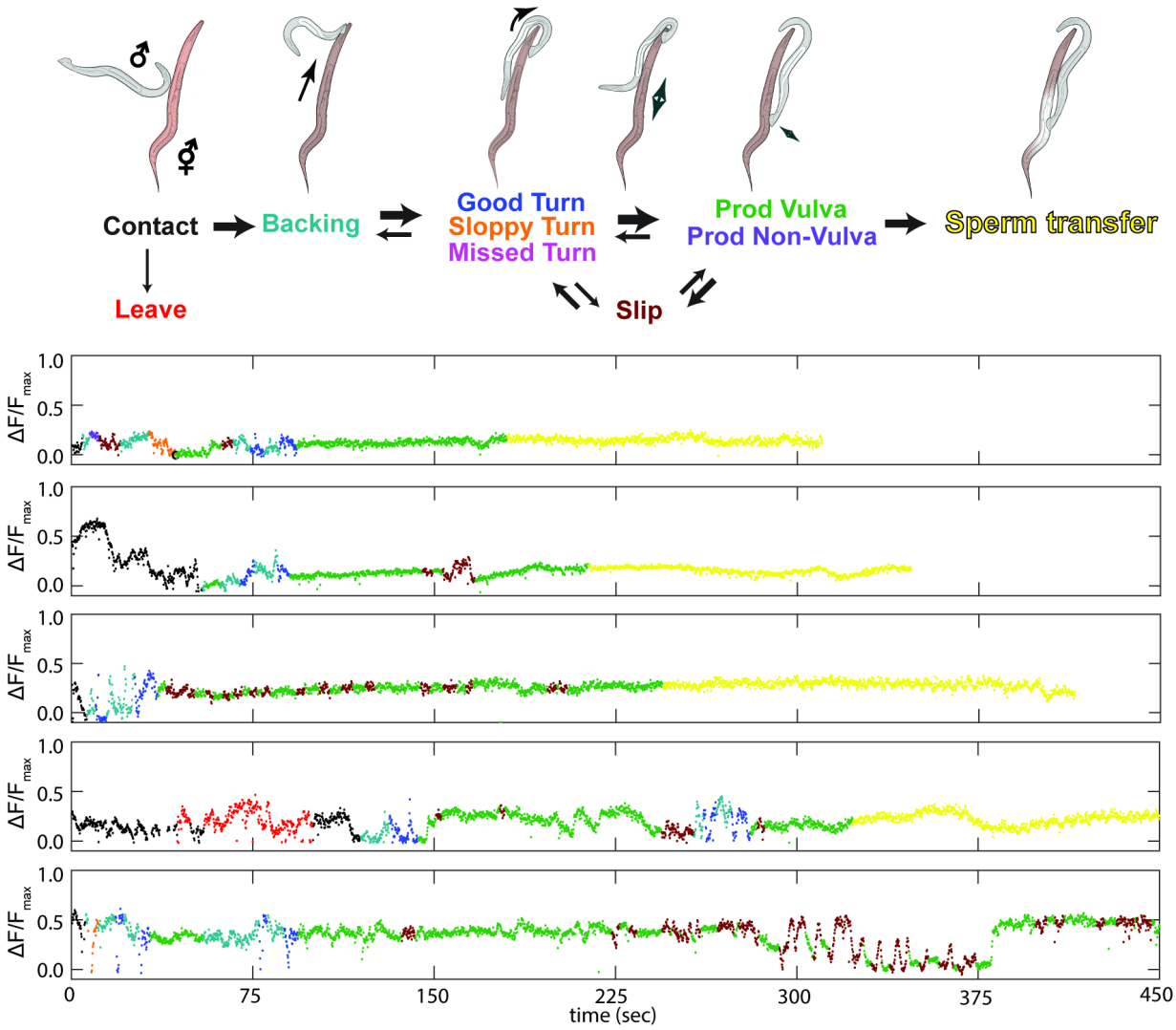

Figure 5.8: Raw traces of wild-type mating males expressing GFP in DVA.

CHAPTER VI: HOW DOPAMINE COMMUNICATES WITH DVA

The following chapter presents many experiments in which the data has not been completed entirely at the time of writing this thesis. However, it is my opinion that the work here presented is an important addition to the thesis as a whole, and that these preliminary results will hold up as the n values are increased to the numbers determined by the power calculation. It is not my intention to overstate the findings. I try to present the data, and its limitations, as authentically as possible, for your consideration.

Screening dopamine receptors for mating defects

How does dopamine communicate with DVA? At the onset of this investigation, there was no evidence for any dopamine receptor expression in DVA. Attempts to express GFP driven by receptor promoter fragments or GFP labeled fosmids further did not yield any tangible evidence. This could be a false negative for a number of reasons: incomplete fragment, expression level below the detection threshold, and so on. In their 2017 paper, Cao, J., *et al.* report *dop-1, dop-2, dop-4,* and *lgc-53* transcription in DVA (Cao et al., 2017). This was conducted in L2 hermaphrodites, and may not be relevant to adults or males.

Due to the lack of conclusive data, I decided to screen all known dopamine receptor mutants for mating defects comparable to nematocin-deficient males. **Figure 6.1** presents the mating efficiency results from this screen. *dop-3* and *dop-4* males each had significant mating defects comparable to nematocin-deficient animals. 3/10 *dop-3(vs106)* males mated within the five-minute assay (30%), as did 6/20 of the *dop-4(ok1321)* males (**Figure 6.1**). Second alleles tested for these mutants mated at similar efficiency, 9/20 for *dop-3(ok295)*

males (45%) and 4/10 males for *dop-4(tm1392*) (**Figure 6.1**). When combined, the *dop-3;dop-4* double mutant males recapitulated the dopamine-deficient mating efficiency (**Figure 6.1**). 1/10 males mated in the five-minute assay, or 10%, suggesting that the two receptor mutants together can entirely account for dopamine's regulation of DVA.

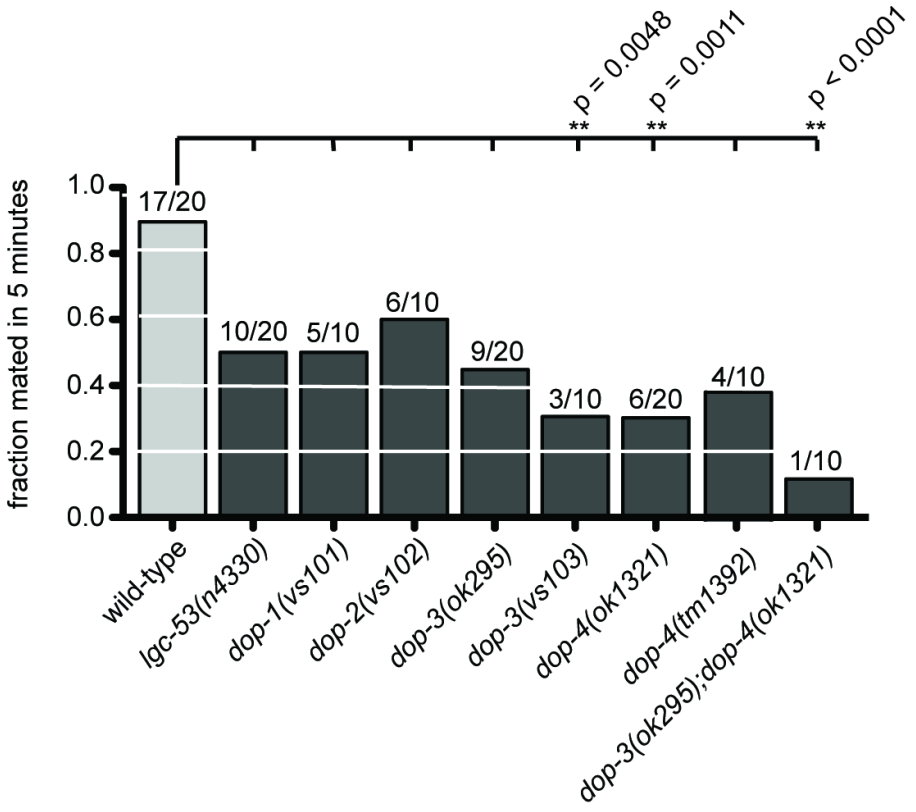

Figure 6.1: Dopamine receptor mutant screen for mating efficiency. *Light gray*: mating efficiency of wild-type males. *Dark gray*, mutant test males. *Y-axis*: fraction of males that mated in a five-minute assay. Actual mating fraction is labelled above its respective bar graph. P values were calculated with a Fisher Exact Test, and a False Discovery Rate to correct for multiple comparisons.

To validate DOP-3 and DOP-4's role in dopamine signaling in DVA, I performed cell-specific rescues under the DVA specific *nlp-12* promoter fragment (Hu et al., 2011). Both *dop-3* and *dop-4* cDNA partially restored mating to wild-type levels (**Figure 6.2**). The *nlp-12* promoter fragment was tested on its own in both the wild-type and mutant

backgrounds to ensure that the rescue phenotype was not due to promoter interaction. In the case of *dop-3,* mating was restored from 3/10 or 30% to 15/20 or 75% (**Figure 6.2** *left*) when cDNA was specifically expressed in DVA. Similarly, when *dop-4* was specifically expressed in DVA, mating was restored from 3/10 or 30% to 7/10 or 70% (**Figure 6.2**, *right*). This fell just shy of achieving statistical significance (p = 0.0562), even in the absence of the False Discovery Rate threshold, but it is also the case that the data sets are not complete, containing fewer mating trials than the power calculation dictated for the experiment (*see* EXPERIMENTAL PROCEDURES). It is my belief that, with the appropriate number of trials, this result will achieve statistical significance.

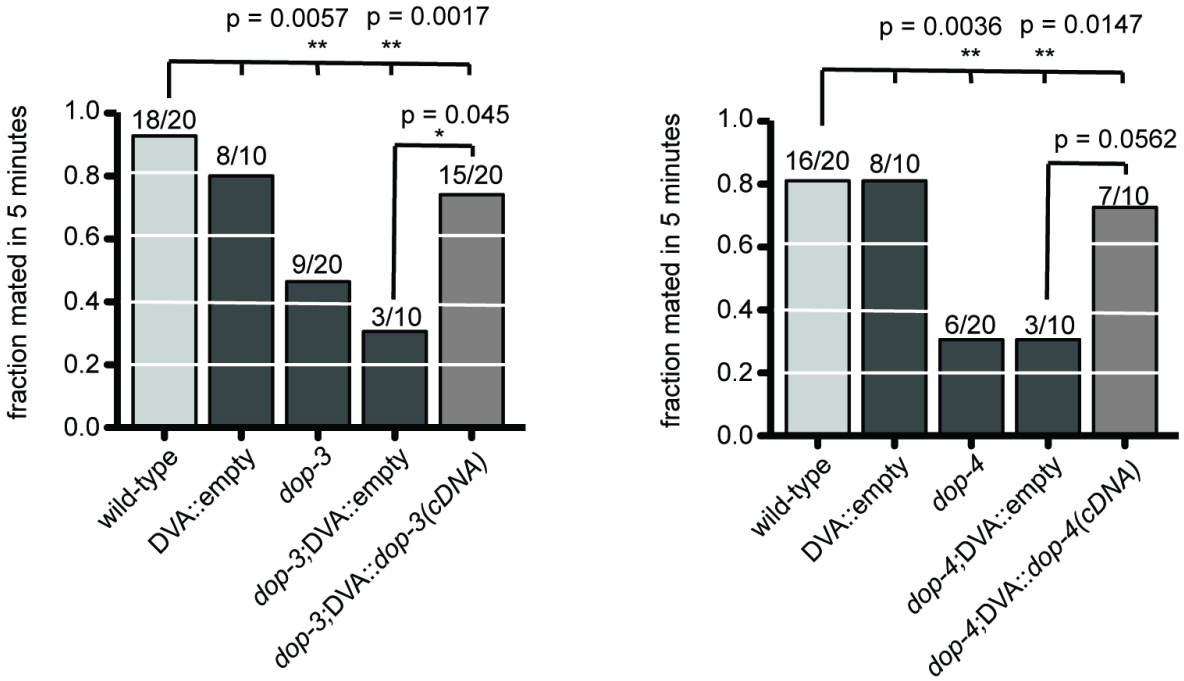

Figure 6.2: DVA-specific cell rescues for *dop-3* and *dop-4* restore mating. *Light gray*: mating efficiency of wild-type males; *dark gray*: mutant test males and transgene controls*; medium gray:* males expressing cDNA of rescue construct in DVA specifically. *Y-axis*: fraction of males mated in 5-minute assay. Actual mating fraction is labelled above its respective bar graph. P values were calculated with a Fisher Exact Test and a False Discovery Rate to correct for multiple comparisons.

A dynamic model of mating for dop-3 and dop-4 animals

I next decided to model the mating behavior of *dop-3, dop-4*, and double receptor mutant males using the same approach as before (*see* EXPERIMENTAL PROCEDURES). p values were calculated by comparing the experiment-to experiment variability of wild-type males (**Table 15**) using an unpaired, two-tailed Student's t test, just as before, and corrected for multiple comparisons using a False Discovery Rate threshold. These values are published in **Table 13** and the histograms from the bootstrapping analysis is presented in **Figure 6.4**, both at the end of the chapter**.** Significant results are summarized in **Table 12** below.

Table 12: Summary of significant results from Table 13. Mean transition probabilities for wild-type (*w.t.*), DOP-3 mutant (*dop-3*), DOP-4 mutant (*dop-4*), and double mutant (*dop-3;dop-4*) are shown. Mean values significantly higher than wild-type controls are in **bold**. Mean values significantly lower than wild-type controls are in *red*. Interesting examples where *dop-3* and *dop-4* have reciprocal phenotypes are indicated with an asterisk (*).

transition probability	w.t.	*dop-3*	*dop-4*	*dop-3;dop-4*
vulva search to vulva search	91.36	94.07	93.77	85.21
vulva search to prod*	5.51	5.59	3.08	**9.68**
vulva search to slip	**3.13**	0.34	**2.86**	**4.37**
prod to vulva search*	0	**1.11**	0	**0.49**
prod to prod*	93.05	92.58	87.33	**95.29**
prod to slip*	5.37	5.93	**12.32**	4.07
prod to sperm transfer	0.96	0.38	0.34	0.16
slip to prod*	15.1	5.92	15.15	5.82
slip to slip*	84.05	**93.3**	82.95	**92.32**

Nine out of ten of the transition probabilities have significantly altered values in the mating of either *dop-3, dop-4,* or *dop-3;dop-4* males. Despite the complexity of these phenotypes, patterns do emerge. All genotypes are defective in the *prod to sperm transfer*

transition probability. *dop-3* and *dop-4* mutants have approximately the same transition probability, 0.38+/-0.03% and 0.34+/-0.01 respectively (**Table 12, Figure 6.3)**. *dop-3;dop-4* males exhibited a *prod to sperm transfer* transition probability of 0.16+/-0.01% (**Table 12, Figure 6.3)**, approximately the product of the two individual receptor mutant probabilities. One transition probability, *vulva search to vulva search* was defective only in the double receptor mutant, falling from 91.36+/-0.19% to 85.21+/-0.20% (**Table 12, Figure 6.3)**. *vulva search to slipping* was defective in the wild-type control males of this experiment, making this transition probability difficult to interpret.

All other changes in transition probability have reciprocal phenotypes between *dop-3* and *dop-4* mutants. *prod to vulva search* transition probabilities were elevated in *dop-3* and the double receptor mutant, but not *dop-4* males (1.11+/-0.03% and 0.49+/-0.02% vs. 0.00+/-0.00%, **Table 12, Figure 6.3**). The converse transition probability, *vulva search to prod*, was significantly lower in *dop-4* males but not in *dop-3* or double receptor mutant males (3.08+/-0.04% vs 5.59+/-0.04% and 9.68+/-0.24%, **Table 12, Figure 6.3**). A similar pattern was observed at the *slip to prod* and *prod to slip* transitions. *dop-3* and *dop-3;dop-4* males had decreased probabilities in the *slip to prod* transition, 5.92+/-0.10% and 5.82+/-0.21%, and increased tendency to persist in *slipping*, 93.30+/-0.11% and 92.32+/-0.21% respectively (**Table 12, Figure 6.3**). *dop-4* males, conversely, had elevated *prod to slip* transition probability, 12.32+/-0.26%, up from 5.37+/-0.09% in wild-type males (**Table 12, Figure 6.3**), and a decreased tendency to persist in *prodding*, 87.33+/-0.26% vs wild-type's 93.05+/-0.06% (**Table 13, Figure 6.3**). The double receptor mutant more closely resembled *dop-3* than *dop-4*.

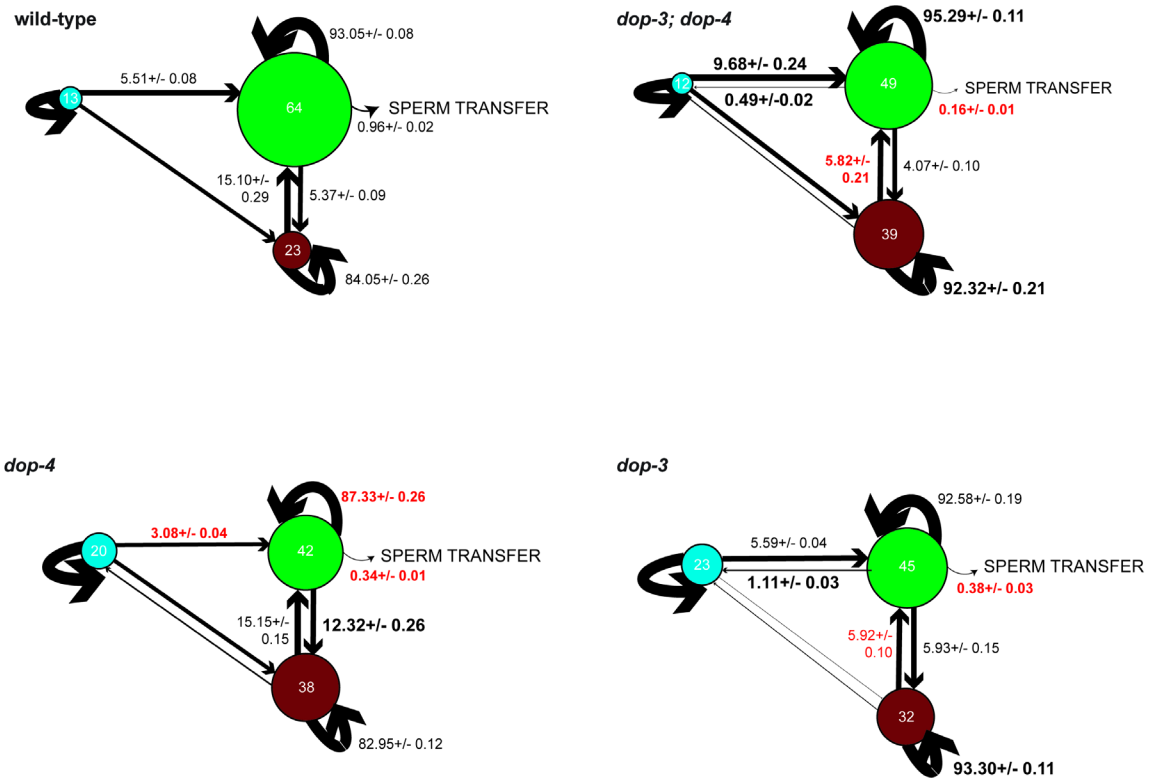

Figure 6.3: Dynamic modeling of the mating behavior of *dop-3*, *dop-4*, and *dop-3;dop-4* males. *Vulva search* represented with blue circles, *prodding* with green circles, and *slipping* with maroon circles. Numbers within a circle are the percent time in which the animals engage in that sub-behavior when mating. Arrow weights represent the probability in a given second that the animal will transition between behaviors. Curved arrows pointing back toward the circle indicate the probability per second that the animal will persist in the sub-behavior. Genotypes are labeled.

Discussion: D1-like and D2-like receptors antagonize each other to attenuate DVA activity

Here, I have identified two dopamine receptors responsible for communicating dopamine signaling to DVA by screening genetic candidates for behavioral defects in mating, and also by rescuing these behavioral defects by expressing the genes for these receptors specifically in DVA. Ethomic analysis of the mating defects of these receptor

mutants reveals equivalent and reciprocal mating defects. These results are particularly interesting given the molecular biology of DOP-3 and DOP-4. DOP-4 is a G_s-coupled, cAMP activating D1-like receptor (Suo et al., 2004), while DOP-3 is G_o-coupled, cAMP inhibiting D2-like receptor (Suo et al., 2004). Their antagonistic effects are reflected in the general reciprocal relationship of the behavioral phenotypes of the receptor mutants. Where *dop-3* will exhibit an alteration in one transition frequency, for example, a decrease in *slip to prod* transition frequency, *dop-4* will exhibit the converse and opposite alteration, for example an increase in *prod to slip* transition frequencies. Notably, the double receptor mutant more closely resembles DOP-3, the cAMP inhibitory receptor. This is consistent with my hypothesis that dopamine signaling regulates DVA by "quieting" its activity, until the balance is disrupted by a triggering event (**Chapter V**).

Table 13: Means, standard deviations, p values, and effect sizes for *dop-3*, *dop-4* receptors and their double knockout p values were determined by an unpaired, two-tailed Student's t test with the mean and s.d. from dopamine-deficient controls calculated in **Table 17** (*see* EXPERIMENTAL PROCEDURES). Statistical significance was determined by the p value and a False Discovery Rate multiple comparison correction. Statistically significant results are depicted in **bold**.

index	genotype	probability	mean	sd	p val	sig?
1	wild-type	searchtosearch	91.36	0.19	0.1604	
2	wild-type	searchtoprod	5.51	0.08	0.5034	
3	**wild-type**	**searchtoslip**	**3.13**	**0.16**	**0.0083**	**
4	wild-type	prodtosearch	0.00	0.00	0.3434	
5	wild-type	prodtoprod	93.05	0.06	0.6849	
6	wild-type	prodtoslip	5.37	0.09	0.8847	
7	wild-type	prodtosperm	0.96	0.02	1.000	
8	wild-type	sliptosearch	0.00	0.00	0.0155	
9	wild-type	sliptoprod	15.10	0.29	0.8937	
10	wild-type	sliptoslip	84.05	0.26	0.3986	
11	*dop-3*	searchtosearch	94.07	0.04	0.1783	
12	*dop-3*	searchtoprod	5.59	0.04	0.4295	
13	*dop-3*	searchtoslip	0.34	0.01	0.1759	
14	*dop-3*	**prodtosearch**	**1.11**	**0.03**	**<0.0001**	***
15	*dop-3*	prodtoprod	92.58	0.19	0.2750	
16	*dop-3*	prodtoslip	5.93	0.15	**0.4507**	
17	*dop-3*	**prodtosperm**	**0.38**	**0.03**	**0.0011**	**
18	*dop-3*	sliptosearch	0.78	0.02	.7151	
19	*dop-3*	**sliptoprod**	**5.92**	**0.10**	**<0.0001**	***
20	*dop-3*	**sliptoslip**	**93.30**	**0.11**	**0.0034**	**
21	*dop-4*	searchtosearch	93.77	0.02	0.2871	
22	*dop-4*	**searchtoprod**	**3.08**	**0.04**	**0.0115**	*
23	*dop-4*	**searchtoslip**	**2.86**	**0.03**	**0.0165**	*
24	*dop-4*	prodtosearch	0.00	0.00	0.3434	
25	*dop-4*	**prodtoprod**	**87.33**	**0.26**	**<0.0001**	***
26	*dop-4*	**prodtoslip**	**12.32**	**0.26**	**<0.0001**	***
27	*dop-4*	**prodtosperm**	**0.34**	**0.01**	**0.0007**	***
28	*dop-4*	sliptosearch	1.18	0.03	0.3482	
29	*dop-4*	sliptoprod	15.15	0.15	0.9412	
30	*dop-4*	sliptoslip	82.95	0.12	0.1750	
31	***dop-3;dop-4***	**searchtosearch**	**85.21**	**0.20**	**<0.0001**	***
32	***dop-3;dop-4***	**searchtoprod**	**9.68**	**0.24**	**<0.0001**	***

33	***dop-3;dop-4***	**searchtoslip**	**4.37**	**0.10**	**0.0005**	***
34	***dop-3;dop-4***	**prodtosearch**	**0.49**	**0.02**	**<0.0001**	***
35	***dop-3;dop-4***	**prodtoprod**	**95.29**	**0.11**	**0.0126**	*
36	***dop-3;dop-4***	prodtoslip	4.07	0.10	0.2150	
37	***dop-3;dop-4***	**prodtosperm**	**0.16**	**0.01**	**<0.0001**	***
38	***dop-3;dop-4***	sliptosearch	0.74	0.02	0.6200	
39	***dop-3;dop-4***	**sliptoprod**	**5.82**	**0.21**	**<0.0001**	***
40	***dop-3;dop-4***	**sliptoslip**	**92.32**	**0.21**	**0.0072**	**

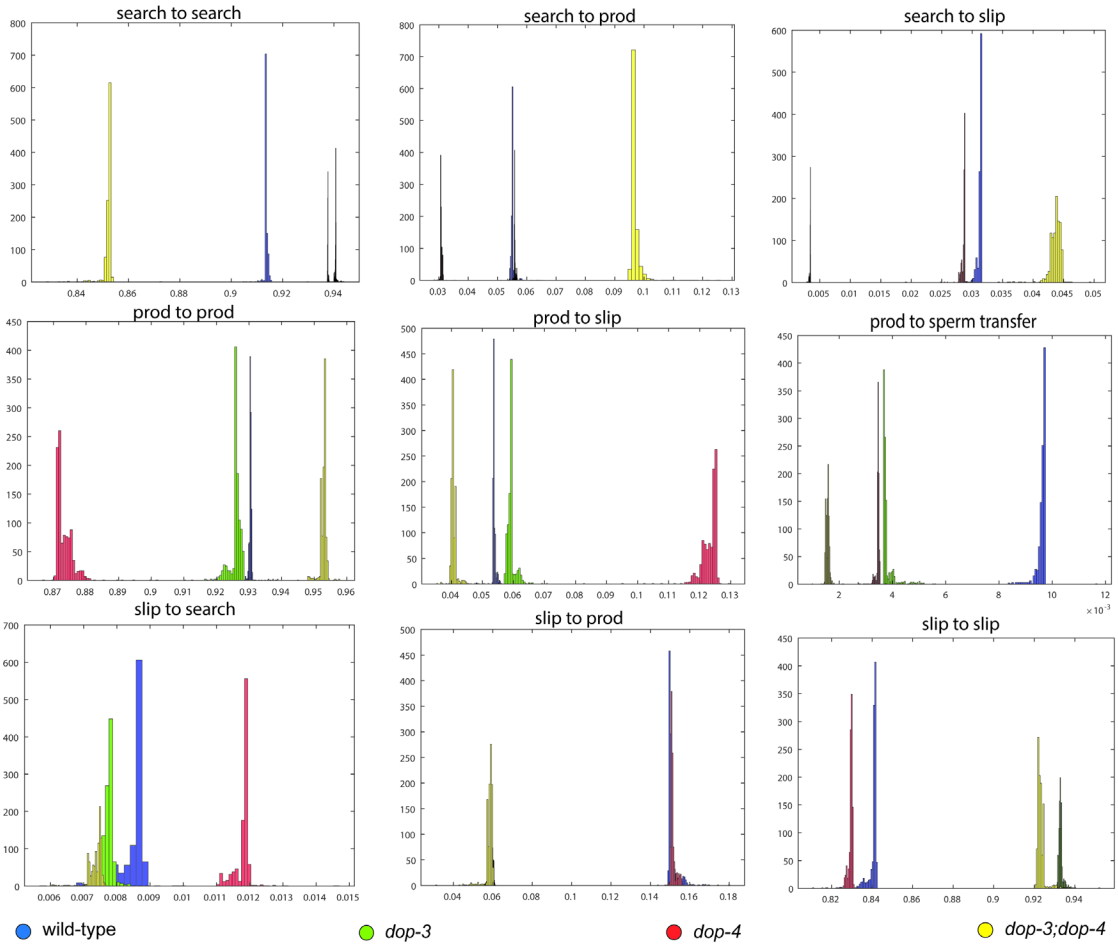

Figure 6.4: Bootstrap data distributions for all sub-behaviors of *dop-3*, *dop-4*, and *dop-3;dop-4* mating males.

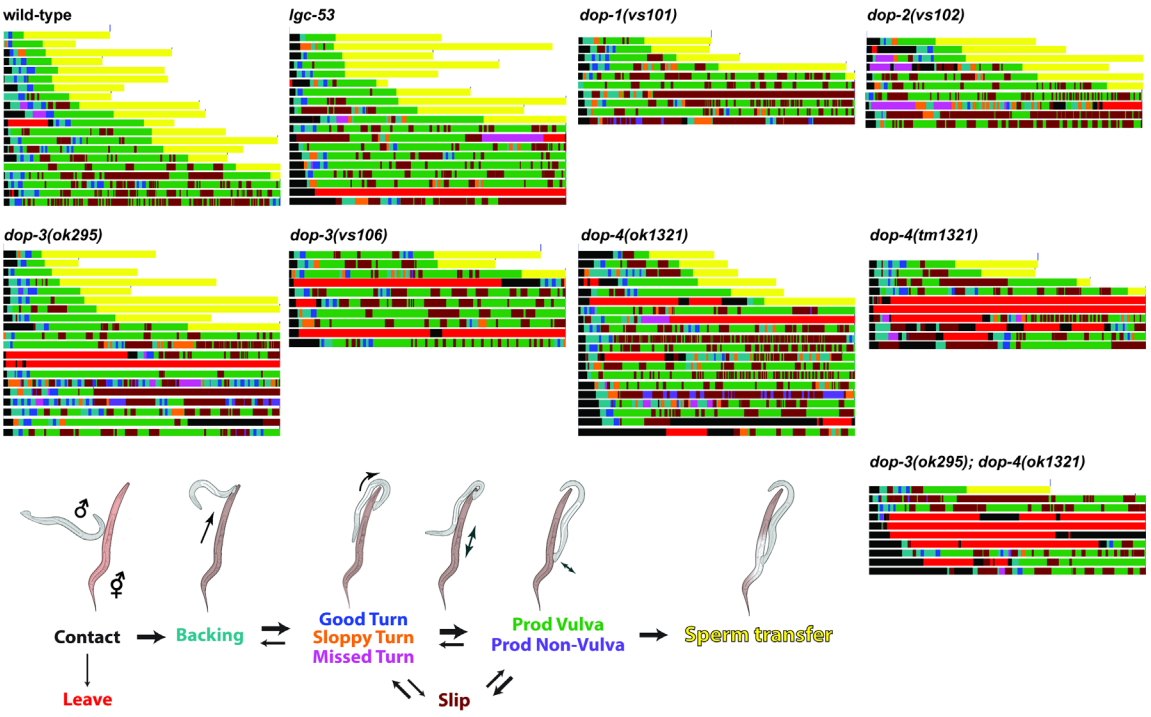

Figure 6.5: Raw mating traces from dopamine receptor genetic screen. *Top*, raw mating traces for dopamine receptor screens, including wild-type, ligand chloride channel *lgc-53*, receptors *dop-1, dop-2, dop-3 (alleles ok295* and *vs106), dop-4 (alleles ok1321* and *tm1392),* and the *dop-3;dop-4* double mutant. *Bottom*, colorized mating schema indicating the color code for the behavioral traces.

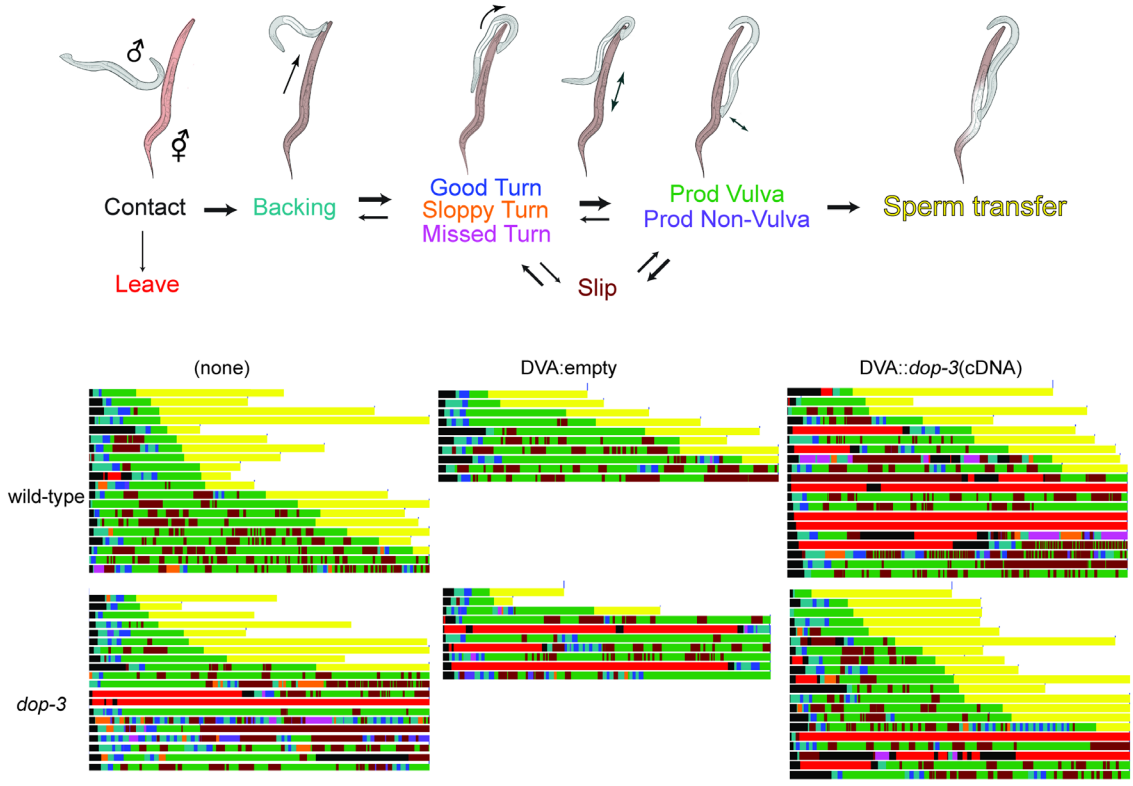

Figure 6.6: Raw mating traces from DVA-specific rescue of *dop-3*. *Top*, colorized mating schema indicating the color code for the behavioral traces. *Bottom*, raw mating traces for *dop-3* rescue in DVA and controls. *Top row* are all wild-type males. *Bottom row* are all *dop-3* males. *Left column* have no transgene. *Middle column* has only the DVA-specific promoter fragment. *Right column* expresses *dop-3* cDNA under the DVA-specific promoter.

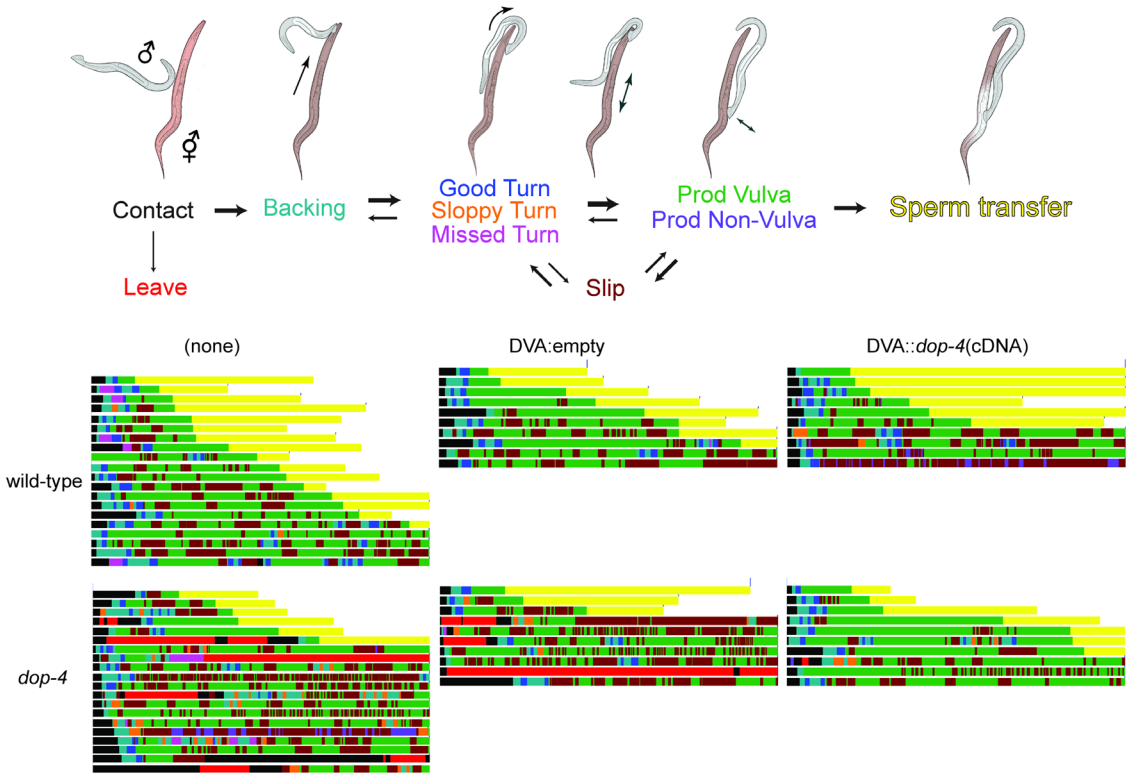

Figure 6.7: Raw mating traces from DVA-specific rescue of *dop-4*. *Top*, colorized mating schema indicating the color code for the behavioral traces. *Bottom*, raw mating traces for *dop-4* rescue in DVA and controls. *Top row* are all wild-type males. *Bottom row* are all *dop-4* males. *Left column* have no transgene. *Middle column* has only the DVA-specific promoter fragment. *Right column* expresses *dop-4* cDNA under the DVA-specific promoter.

CHAPTER VII: CONCLUDING REMARKS

Nematocin regulates mating behavior largely by acute release from DVA

In Chapter III, I recapitulated the nematocin knockout mating defect by acutely silencing DVA with HisCl in fully mature adult males just prior to mating. I was able to restore mating in the same animals by allowing them to recover off histamine before attempting to mate again. By modeling the dynamic behavior of these animals, I was able to identify a constellation of mating sub-behavior state transitions affected by DVA silencing. I then repeated the DVA silencing experiment in nematocin-deficient animals, which allowed me to differentiate which of the affected state transitions were nematocin-mediated, and which were likely the result of DVA's other functions. *prod to sperm transfer*, *slip to prod*, and persistence in the *slipping* state were identified as state transitions mediated by acute nematocin release from DVA.

Dopamine regulates nematocin action

With a candidate gene screen, I identified and characterized the genetic epistasis relationship between genes required for dopamine and nematocin signalling. By knocking out nematocin in dopamine-deficient males, I was able to rescue the mating phenotype to nematocin-deficient mating levels. Dynamic behavioral analysis of these mutants revealed a constellation of state transition changes that overlapped with those seen in the DVA silencing experiment in Chapter III: *slip to prod*, and persistence in the *slipping* state. *prod to sperm transfer* was more defective in dopamine-deficient animals than in other tested groups. I then orthogonally recapitulated the genetic epistasis result with a neural circuit manipulation: by pharmacogenetically silencing DVA in the dopamine-deficient animals. Dynamic behavioral analysis revealed that all state transitions were ameliorated by this

manipulation except *slip to prod,* persistence in the *slipping* state, and, partially, *prod to sperm transfer,* once again presenting me with the same anchors of behavioral evidence as the previous experiments.

Dopamine regulates the coordination of DVA activity with mating behavior

By expressing GCaMP in DVA, I was able to visualize changes in cellular calcium levels while the animals were mating. In wild-type males, I established patterns where specific dynamics corresponded to the onset of behaviors or behavioral transitions. Two examples are the drop in GCaMP signal just prior to *sperm transfer*, and the rise in GCaMP signal at the *slip to prod* transition. In dopamine-deficient animals, GCaMP signal was observed, but had less robust dynamics that were not coordinated as in the wild-type animals. Nematocin-deficient animals were also tested, showing a less severe loss of robustness and coordination than the dopamine-deficient animals, which suggests that nematocin signaling itself feeds back onto DVA activity through some mechanism. The presence of the nematocin receptor NTR-1 in R1B, which is presynaptic to DVA, provides a readily available hypothesis to investigate for this feedback.

The drop prior to *sperm transfer* was characterized and statistically tested using a randomly shuffled ethogram of the same mating/neuronal imaging traces. It was determined to be a statistically significant change in the calcium dynamics, coupled with the behavior. The same analysis could not be performed on dopamine-deficient males because none of the animals successfully transferred sperm during the assay. One can presume that completion of mating is rare in dopamine-deficient males because DVA

rarely achieves a calcium level sufficiently high enough from which to drop, so as to signal the onset of *sperm transfer*.

Calcium activity at *slip to prod* state transitions were analyzed in both wild-type and dopamine-deficient males. Wild-type males exhibited a statistically significant increase upon the onset of *prodding*, which was not present in the dopamine-deficient animals. This result reinforces the genetic result, where *slip to prod* transition probabilities decrease in dopamine-deficient animals. Combined, the data suggest that the ramping up of nematocin release induces the mating animal to enter and persist in the *prodding* state, and, when it ramps down, leave the *prodding* state to carry out consummation.

Both D1 and D2-like receptors communicate dopamine signals to DVA

A candidate gene screen based firstly on male mating behavior and secondly on DVA-specific rescue identified the D1-like receptor DOP-4 and the D2-like receptor DOP-3 (Suo et al., 2004) as necessary for dopamine signaling to DVA. By knocking out both receptors, I was able to recapitulate the severe mating defect observed in dopamine-deficient animals. Dynamic behavioral analysis once again identified the *prod to sperm transfer* transition probability and the transition probabilities between *prodding* and *slipping* to be affected by the genetic perturbations. Knocking out *dop-4* caused an increase in *prod to slip* transitions and a decrease in *prodding* persistence. Knocking out *dop-3* caused a decrease in *slip to prod* transition probabilities and an increase in *slipping* persistence. In each case, knocking out one receptor resulted in a similar transition probability of *slip to prod* and *prod to slip* behaviors within the genotype, either by elevating the probability (*dop-4*) or lowering it (*dop-3*).

DOP-4, a G_s-coupled D1-like receptor (Suo et al., 2004), likely antagonizes the response of DOP-3, a G_o-coupled D2-like receptor (Suo et al., 2004) to tightly couple nematocin action with a specific conditions. Many models have been proposed for this antagonism, from regulation of cAMP levels (Neve, et al., 2004), to Akt/PP2A signaling (Beaulieu, et al., 2005), to PLCβ activation Allen, et al. 2011) to direct regulation of the synaptic machinery (Dong, et al. 2018). It has been demonstrated in *C. elegans* (Harris et al., 2010), in other invertebrates (Berry et al., 2012; Kim et al., 2007), and in mammals (Tritsch and Sabatini, 2012) that having dual activating/inhibiting receptors of different affinities for the same ligand is a common motif when trying to lock a neural response with another signal. The higher-affinity receptor generates the baseline response to lower concentrations of the ligand. Once a threshold is crossed, the lower-affinity receptor is activated, thereby terminating or otherwise altering the ligand response in the receptor-expressing neuron. DOP-3 is reported as having a higher affinity for dopamine than DOP-4 when expressed in heterologous cell culture (Suo et al., 2003). I suggest that basal levels of dopamine assist in "quieting" DVA by activating its inhibitory, D2-like receptor, until it receives a specific signal ushered in by a rapid increase in dopamine levels. At this point, the activating D1-like receptor precipitates G_s signaling and neuropeptide release. I use calcium activity as a proxy for neuropeptide release, and it is indeed the case that calcium activity is disrupted at the behavioral transitions consistent with the dopamine and dopamine receptor genetic evidence, but this may not be entirely accurate. Costa *et al*. showed that cAMP levels evoke dense core vesicle release independent of calcium activity (Costa et al., 2017). Perhaps the calcium activity I observe experimentally is not the release

of nematocin alone, but the co-release of nematocin and DVA's neurotransmitter acetylcholine (Pereira, L., et al., 2015).

Nematocin release dynamics, not absolute levels, are important for mating behavior

In **Chapter IV** and **V**, I show how dopamine regulates the release of nematocin by regulating DVA activity at specific behavioral state transitions during mating behavior. What remains to be understood, however, is whether the dopamine-deficient defect is due to a general excess of nematocin, nematocin release at the wrong time, or some combination of the two. Basal GCaMP signal in DVA for dopamine-deficient males qualitatively appeared to be elevated compared to wild-type, but this could be due to a variety of direct or indirect effects. To satisfactorily address the mechanism, one would have to perform a calibration experiment, possibly lowering DVA activity artificially and in a controlled manner in both genotypes with a tool like HisCl, which is titratable at different levels, and measuring the decrease in signal.

My results indicate that the dynamics of nematocin release drive mating behavior, and not its presence/absence or absolute levels. A similar mechanism has been demonstrated in other kinds of oxytocin-related physiology, specifically osteogenesis and maternal skeletal restructuring during parturition (Colaianni et al., 2014a). Osteoblasts express the oxytocin receptor OXTR, for which oxytocin has high affinity as well as two of the three arginine-vasopressin receptors (Avpr1α and Avpr2), for which oxytocin has low affinity (Sun et al., 2016). As oxytocin slowly ramps from low levels to high levels during the late stages of pregnancy, it activates the OXTR and promotes the dissolution of bone calcium in the service of promoting osteogenesis in the fetus (Colaianni et al., 2014b).

During childbirth, and during lactation post-partum, the mother receives surges of oxytocin, invoking activation of the lower affinity vasopressin receptors, which promote osteogenesis and the rebuilding of the bone mass lost during pregnancy (Di Benedetto et al., 2014; Sun et al., 2016). Much more remains to be learned about how the dynamics of neuromodulators govern behavior within the "central" nervous systems of animals.

Nematocin induces persistence in the prodding state, possibly analogous to anxiolytic properties of other oxytocin homologs

By manipulating DVA both genetically and pharmacologically, I was able to demonstrate that nematocin regulates a male's transitions into the *prodding* state from the *slipping* state and out of the *prodding* state into *sperm transfer*. In the first case, the mating male must stop performing the repetitive forward and reverse movements of *slipping* and "pause" at the vulva in order to probe its spicules. Something analogous is described in hermaphrodite *C. elegans* in Hums, *et al.* 2016. DVA activity is routinely seen coupled with "pausing" in the animal locomotion when oxygen levels are reduced from 21% to 10%. Low oxygen is a favorable condition for laboratory *C. elegans*, often signaling the thickening of their food patches. It would be interesting if this more general, perhaps more primal circuit of DVA-induced pausing in response to desirable stimuli was related to for the purposes of mating modulation.

Nematocin-deficient males and dopamine-deficient males have lower *slip to prod* transition probabilities, similar in magnitude to the *prod to slip* probabilities. It appears as if, by knocking out these genes, the animal is no longer driven into the *prodding* state, but rather *prod to slip* and *slip to prod* are more "at equilibrium" with one another. We see

these transitions balance both by an increase in the *prod to slip* transition probability (DOP-4) and by a decrease in the *slip to prod* transition probability (DOP-3) in behavioral ethomics for the dopamine receptors.

Slipping can be a "high arousal" behavioral state, or a low one. Males move back and forth vigorously or slowly and languidly along the body. From the analysis I performed, it is not clear if there is a qualitative difference in nematocin-deficient *slipping* vs. dopamine-deficient *slipping*. The dopamine receptor data gives us some insight, however. Males lacking DOP-3, the D2-like inhibitory dopamine receptor, have a phenotype similar to nematocin-deficient and dopamine-deficient males: a lowering of *slip to prod* transition probability to its *prod to slip* transition probability. Males lacking DOP-4, the D1-like excitatory receptor, on the other hand, equilibrate between the two behavioral states by raising the *prod to slip* transition probability to the *slip to prod* level. This is a condition of higher arousal, where in the same amount of time, the *dop-4* male moves from one state to the next with a higher frequency than its *dop-3* mutant counterpart. If DOP-4 coordinates nematocin release with dopamine signaling, then it follows that *dop-4* males do not release nematocin at *prod* transition to hold them in the *prodding* state, thereby failing to move from the "high arousal" state-switching to the "low arousal" pausing and persistence in *prodding*. Perhaps this response is analogous to the anxiolytic properties of other oxytocin homologs (Waldherr, M., et al. 2007; Yoshida, M,. et al., 2009). The lack of mating motivation of the dopamine-deficient animals, depicted by their significant increase in aborted mating attempts, could be consistent with this hypothesis, in which nematocin released in excess or at the wrong time during mating could "pause"

the mating behavior unproductively, thereby demotivating the male, or breaking up the coherence of the behavior pattern.

Is this example of dopamine "goal oriented behavior" or "motivation/reward signaling?"

In vertebrate biology, two distinct paradigms for dopamine signaling exist for the two dopaminergic systems of the brain: the goal-oriented movement function of the substantia nigra dopaminergic circuit and the motivation and reward function of the ventral tegmental area dopaminergic circuit (Cooper, S., et al., 2017; Rizzi and Tan, 2017). Both kinds of functionality have also been described in invertebrates (Guo et al., 2018; Lowenstein and Velazquez-Ulloa, 2018). In previous studies, dopamine's role in *C. elegans* male mating has been previously described with the "goal oriented behavior" paradigm, due it its antagonistic relationship with acetylcholine in carrying out intromission and ejaculation (Correa et al., 2012).

While these models are useful for discussion, they are not entirely distinct at the biological level. It has been suggested that these two functions are not distinguishable in dopaminergic systems of invertebrates (Zhang et al., 2018), based on studies of mating and courtship behavior in other model animals, specifically *Drosophila melanogaster.* In this present study also it seems that both "goal oriented behavior" or "motivation/reward signaling" are equally applicable to describe the functionality of dopamine's regulation of DVA and nematocin release. On the one hand, dopamine can be seen as directing the *prodding* motor activity in a goal-oriented fashion. DVA itself is a cholinergic neuron (Liu et al., 2011), perhaps analogous to the dopamine/acetylcholine movement circuit of

mammalian brains (Rizzi and Tan, 2017) . On the other hand, dopamine can also be described as signaling a "reward" for finding the vulva, motivating the animal to exit its high arousal state and "pause" at the stimulus. Understanding circuits like these more deeply may aid us in understanding the fundamental functionality of dopaminergic circuitry.

The coupling of oxytocin and dopamine is conserved in complex reproductive behavior

Dopamine and oxytocin have been implicated in complex reproductive behavior time and again in mammals, from mate search and sexual exploration (Smith et al., 2015), to pair bonding and mating (Johnson and Young, 2015) to parental behavior and provisioning for offspring (Dulac et al., 2014). Here also I describe how the two overlapping systems cooperate to govern the mating behavior of an invertebrate nematode with 600 million years of evolutionary divergence from its mammalian counterparts. Nematocin and dopamine show anatomical convergence in their circuitry in the male. NTR-1 is expressed in rays R5B, R7B, and R9B, where the A Ray equivalents are dopaminergic (Garrison, J.G. et al., 2012: Serrano-Saiz, E., 2017b). NTR-2 is present in the spicule motor neuron SPC, which has been shown to receive dopamine signals from the surrounding socket cells during copulation (LeBoeuf et al., 2014).

Why do dopamine and oxytocin share this deep evolutionary connection? In *C. elegans*, dopamine is the regulator of nematocin release. Disregulation of nematocin, the dopamine-deficient phenotype, is far worse for mating that having no nematocin at all. One might speculate that the dopaminergic system, a synthesized biogenic amine known to tightly control its levels of secretion, was coopted to ensure precision in the regulation

of nematocin, a translated peptide with that is perhaps less precise but more flexible in its secretion. This fundamental combination may have been so successful that it was either conserved, or paralogously acquired time and again during metazoan evolution. It would be interesting to see what dopamine's role is, if any, in other species' oxytocin mediated behavior, whether related or unrelated to reproduction.

Broader implications of the work

In her recent book *The Opposite of Hate*, political scientist Sally Kohn examines one of the greatest atrocities of my living memory: the Rwandan genocide. She is particularly interested in its aftermath and how the country healed from the massacre, in examples of "the opposite of hate." It is easy to imagine atrocities like this committed by anonymous guerilla groups that come charging into villages and towns and commit the acts. What Kohn describes from her research of Rwanda, however, is that most of the murdering of the Tutsis was done by Hutu members of the same community, their neighbors with whom they cooperatively farmed the land, and in many cases, immediate family members of Hutu and Tutsi intermarriages, which was very common. In the genocide's aftermath, as Kohn tells it, it was not foreign aid and NGOs that rebuilt the country and its communities, but the very same people who picked up machetes and slaughtered their neighbors and kin. These same individuals took in the now orphans of their villages, helped rebuild Tutsi homes, and went on living with each other as they did before. How does this happen? How do we become one thing overnight, and then another?

In his book *On Aggression*, Konrad Lorenz describes "…the Bond… the way we distinguish friend from stranger…" as one of the strongest and most profound forces in

nature. He hypothesizes that it is an evolutionary adaptation to overcome aggression in the most aggressive species so that they can mate and raise offspring. The "Bond" is stronger than aggression, but is also inextricably intertwined with it. It is the fundamental builder of societies, and simultaneously one of its greatest threats. It is how we come together as families, as collectives, but also how we form in-groups and out-groups, how we identify "the Other," and why we see "the Other" as a threat to our own tribe. This is a story that plays out over and over in our history, and is even playing out in today's politics and the attitudes surrounding different political parties, immigrants, and refugees in our country and others.

The "Bond" is not a natural force reserved for humans, or even just mammals. It can be found in many bird species (graylag geese) and fish species (convict cichlids). While it is unlikely that nematodes "bond," nematodes do in fact have the same neuromodulators, oxytocin and dopamine, working together in analogous ways to regulate their complex reproductive behavior. Perhaps the difference in their mating behavior and our "bonding" is not a difference of kind but a difference of degree. It is my hope that studies of the nature that this thesis presents will shed light on how these circuits fundamentally work, aid us in better understanding of both how we form social attachments, and inform us about how those attachments are manipulated by our external environment.

EXPERIMENTAL PROCEDURES

Nematode growth and molecular biology

All strains were maintained at room temperature (22-23°C) on nematode growth medium (NGM) plates (51.3 mM NaCl, 1.7% agar, 0.25% peptone, 1 mM $CaCl_2$, 12.9 µM cholesterol, 1 mM $MgSO_4$, 25 mM KPO_4, pH 6), seeded with *E. coli* OP50 bacteria as a food source. Wild-type animals were the Bristol strain N2 (Brenner, 1974). Standard cloning and molecular biology methods were used. Generation of extrachromosomal array transgenes was carried out using standard procedures (Mello and Fire, 1995). Generation of integrated transgenic lines was carried out using the protocols described in Mello and Fire as well.

Mating assay

The mating assay was adapted from the standard mating assay (Liu and Sternberg, 1995). 5 cm petri plates were filled with 10ml of NGM and allowed to cool at 4°C. 72 hours prior to the assay, the plates were placed at room temperature (22-24°C) unstacked, lid side down, and allowed to dry. 24 hours prior to the assay, plates were seeded with a small lawn OP50 *E. coli*, freshly grown to 1 O.D., and allowed to incubate at room temperature overnight.

unc-64(e246) hermaphrodites were picked at the L4 stage 24 hours prior to the assay, moved to a plate with only other L4 *unc-64(e246)* hermaphrodites, and placed at 15°C. These standard partners were used for each male genotype or condition being tested: ~10 L3/L4males were placed on plates with only other L3/L4 males of their kind. Test strains were then blinded and placed at 15°C. overnight.

Table 14: *Caenorhabditis elegans* strain list

Strain	Description	Notes	Figure(s)
CB246	*unc-64(e246) III*	Animals lacking the ortholog to syntaxin 1A. Defect in synaptic fusion. Extremely sluggish.	All mating behavior experiments
CX17123	*kyIs713* [*pnlp-12*::HisCl_2A_mCherry]	Wild-type with integrated HisCl in DVA with mCherry expression reporter. Initially injected at 30ng/ul.	3.2, 3.4, 3.7, 3.8, 3.10
CX8634	*ntc-1(tm2385) X*	Nematocin-deficient animals. Male mating defect. backcrossed into lab N2 strain 6X.	3.5, 3.6, 3.9, 3.11, 4.2, 4.3, 4.4, 4.5, 4.6, 4.11, 4.13, 4.14, 4.15
CX17704	*ntc-1(tm2385) X*; *kyIs713*	Integrated HisCl in DVA with mCherry expression reporter crossed into the *ntc-1* genetic background	3.5, 3.6, 3.9
CX15799	*nlp-12(ok335) I*	Deletion in the neuropeptide *nlp-12*. Aldicarb resistant. Postural defect. Locomotive defect. Backcrossed with lab N2 6X.	4.2, 4.11
CX15929	*nlp-12(ok335) I; ntc-1(tm2385) X*	Nematocin-deficient and *nlp-12* double mutant. Aldicarb resistant. Postural defect. Locomotive defect. Male mating defect	4.2, 4.11
TQ296	*trp-4(sy695) I*	Type-N TRP channel expressed in DVA and the dopaminergic neurons (ADE, CEPs, PDE, R5A, R7A, R9A). Postural defect. locomotive defect. mating defect.	4.3, 4.12
Need to deposit	*trp-4(sy695) I; ntc-1(tm2385) X*	Type-N TRP channel and Nematocin-deficient double mutant. Postural defect. Locomotive defect. Male mating defect.	4.3, 4.12
CX11078	*cat-2(e1112) II*	Nonsense mutation in a coding exon of tyrosine hydroxolase, rate limiting enzyme in dopamine synthesis. Expressed in dopaminergic neurons. Postural	4.4, 4.5, 4.6, 4.7, 4.8, 4.9, 4.11, 4.12,

		defect. Locomotive defect (hyperactive). Basal slowing response defect. Crawl to swim transition defect. Severe male mating defect. Backcrossed 6X.	4.15, 4.16
CX17708	*cat-2(e1112) II; ntc-1(tm2385) X*	Dopamine-deficient and nematocin-deficient animals. Male mating defect akin to nematocin-deficient animals, less severe than dopamine-deficient animals.	4.4, 4.5, 4.6, 4.11, 4.15
CX17709	*cat-2(e1112) II; ntc-1(tm2385) X; kyEx6239* [*pntc-1::ntc-1*_SL2_GFP]	Dopamine and nematocin double mutant with nematocin rescued on an extrachromosomal array under its endogeneous reporter. Severe male mating defect. Injected at 20ng/ul.	4.4, 4.5, 4.6, 4.11, 4.15
Need to deposit	*cat-2(e1112) II*; *kyIs713*	Dopamine deficient animals expressing *kyIs713*	4.7, 4.8, 4.9, 4.12, 4.16
CX17707	*unc-64(e246) III; lite-1(ce314) X*	Blue light insensitive animals lacking ortholog to syntaxin 1A. Extreme sluggishness. Defect in synaptic fusion.	5.1, 5.2, 5.3, 5.4, 5.5, 5.6, 5.7, 5.8
CX16553	*lite-1(ce314) X*; *kyIs686* [*pnlp-12*::GCaMP5A]	Blue light insensitive animals expressing the genetically encoded GFP-based calcium indicator GCaMP5A in DVA. Initially injected at 30ng/ul	5.1, 5.2, 5.3, 5.5
Need to deposit	*lite-1(ce314) X; ntc-1(tm2385) X*; *kyIs686*	Nematocin deficient, blue light insensitive animals expressing *kyIs686*. Crossed from CX16553.	5.1, 5.7
CX17706	*cat-2(e1112) II*; *lite-1(ce314) X; kyIs686*	Dopamine deficient, blue light insensitive animals expressing GCaMP5A in DVA. Crossed from CX16553.	5.1, 5.4, 5.6
CX17712	*lite-1(ce314) X*; *kyEx6238* [*pnlp-12*::GFP]	DVA labelled with GFP injected at 2ng/ul for calcium imaging control	5.4, 5.8
LX645	*dop-1(vs101) X*	D1-like dopamine receptor, $G_{\alpha s}$, tap habituation defective.	6.1, 6.5
LX702	*dop-2(vs105) V*	D2-like dopamine receptor, G_0/G_i, expressed in dopaminergic neurons ADE, PDE, CEPs, R5A, R7A, R9A, and other sites. Dopamine auto-regulation defective.	6.1, 6.5

BZ873	*dop-3(ok295) X*	D2-like dopamine receptor, G_0/G_i, moderate male mating defect. Postural defect.	6.1, 6.2, 6.3, 6.4, 6.5, 6.6
LX703	*dop-3(vs106) X*	D2-like dopamine receptor, G_0/G_i, moderate male mating defect. Postural defect. Deletion of first exon.	6.1, 6.5
CX11751	*dop-4(ok1321) X*	D1-like dopamine receptor, $G_{\alpha s}$, moderate male mating defect.	6.1, 6.2, 6.3, 6.4, 6.5, 6.7
FG58	*dop-4(tm1392) X*	D1-like dopamine receptor, $G_{\alpha s}$, moderate male mating defect. Large deletion in 1^{st}-3^{rd} exons.	6.1, 6.5
CX17710	*dop-3(ok295) dop-4(ok1321) X*	DOP-3/DOP-4 double mutant. Severe mating defect.	6.1, 6.2, 6.3, 6.4, 6.5
CX11500	*lgc-53(n4330) X*	Dopamine ligand gated chloride channel. Slight male mating defect.	6.1, 6.5
CX17625	*kyEx6024* [*pnlp-12*:: SL2_mCherry]	Rescue experiment control animals expressing an empty coding vector with *nlp-12* promoter and SL2_mCherry reporter. Injected at 5ng/ul	6.2, 6.6, 6.7
Need to deposit	*dop-3(ok295) X*; *kyEx6024*	DOP-3 deficient rescue experiment control animals expressing an empty coding vector with *nlp-12* promoter and SL2_mCherry reporter. Crossed from CX17625.	6.2, 6.6
CX17563	*kyEx6180* [*pnlp-12*:: *dop-3*(cDNA)_SL2_mCherry]	Wild-type animals expressing the DVA specific *dop-3* cDNA rescue construct with mCherry reporter. Injected at 5ng/ul.	6.2, 6.6
CX17562	*dop-3(ok295) X*; *kyEx6180*	*dop-3* animals expressing the DVA specific *dop-3* cDNA rescue construct with mCherry reporter. Crossed from CX17563.	6.2, 6.6
CX17627	*dop-4(ok1321) X*; *kyEx6024*	DOP-4 deficient Rescue experiment control animals expressing an empty coding vector with *nlp-12* promoter and SL2_mCherry reporter. Crossed from CX17625.	6.2, 6.7
Need to deposit	*kyEx6184* [*pnlp-12*:: *dop-4*(cDNA)_SL2_mCherry]	Wild-type animals expressing the DVA specific *dop-4* cDNA rescue	6.2, 6.7

		construct with mCherry reporter. Injected at 5ng/ul.	
CX17573	*dop-4(ok1321) X*; *kyEx6184*	*dop-4* animals expressing the DVA specific *dop-4* cDNA rescue construct with mCherry reporter. Crossed from NEED TO DEPOSIT	6.2, 6.7

Prior to the assay, *unc-64(e246)* hermaphrodites were picked onto the assay plates, one animal per plate, and allowed to settle at room temperature for 30-45 minutes. Individual test males were then picked onto the assay plates with the *unc-64(e246)* mates, and recorded for 350 seconds at 10 fps at 10X magnification under bright field illumination on the Arena Imaging Microscope (Larsch et al., 2013). Recording began right before the male made first contact with the hermaphrodite. Once complete, males were removed from the assay plate, and it was annotated and stored at room temperature. 48 hours later, the plates were examined for male progeny to confirm successful mating behavior observed in the video recordings.

Five animals for each test strain were assayed at a time, so each data set of 20 animals consists of four distinct assay days. One test strain per assay day was always a wild-type control. If the wild-type animals did not mate at an efficiency of 60% (3/5 successful), the results of the day were discarded.

Ethograms and mating analysis

Mating videos were cued up to frame where males make first contact with the hermaphrodite, and trimmed to 3000 frames, or 300 seconds, in ImageJ (https://imagej.nih.gov/ij/). Videos were then tracked manually in a Graphical User Interface (GUI) customized in MATLAB (Mathworks®). Frames were assigned one of the ten sub-behaviors of mating: contact, backing, good turn, sloppy turn, missed turn, vulva prod, slip, non-vulva prod, leaving, and sperm transfer. Catagories were later simplified into “vulva search” (backing, all turning), “prodding” (at vulva and non-vulva locations), and “slipping.” Sub-behaviors “Contact,” “Leaving,” and “Sperm Transfer” were deemed

to be categorical (yes/no) measurements. Genotypes/conditions were unblinded post-tracking.

Effective sample size was determined based on a power calculation for the χ^2-test. A sample size of 20 with an effect size of 0.8 (wild-type mating % success) to a significance of 0.05 was calculated to accept the alternative hypothesis with 95% accuracy. (https://www.anzmtg.org/stats/PowerCalculator/PowerChiSquare). Mating success p values were then calculated using a Fisher's Exact test, with a False Discovery Rate multiple comparison correction.

Markov modeling was done with a customized script in MATLAB. State durations are calculated based on the fraction time of all the animals in a given genotype/condition spend engaged in that specific sub-behavior. A one second time unit was chosen for determining percent likelihood of behavioral state transitions because it is an appropriate time vector for mating behavior. Probabilities were calculated over 10 frames with the following general equation:

$$P_{1->2 \text{ over n frames}} = P_{1->2}*(1 + P_{1->1} + P_{1->1}^2 + \ldots + P_{1->1}^{n-1})$$

This was calculated for the 10 transition probabilities: *vulva search to vulva search*, *vulva search to prodding*, *vulva search to slipping*, *prodding to vulva search*, *prodding to prodding, prodding to sperm transfer, prodding to slipping*, *slipping to vulva search, slipping to prodding,* and *slipping to slipping*.

In many ethomic studies of *C. elegans*, behaviors can be assumed to be independent of one another, and multiple repetitions can be considered as data sets per animal. For example, a pulse of odor may elicit a number of reversals from a worm, as does a similar pulse a minute later. These odor responses then may be pooled into a data set for the given

animal, with a mean, median, standard deviation and error, and so on. In the instance of mating, however, the investigator cannot assume independence of the sub-behaviors. The behavioral "unit" is the entire mating event, and the sub-behaviors (*vulva search, prodding, slipping*) are quantitatively descriptive components of the more complex unit of behavior. This means that, in order to make meaningful statistical comparisons between genotypes and conditions, a different approach is needed to statistically quantify the variability in the data.

To these ends, I performed a bootstrapping analysis on each of my 20-member data sets. I allowed the program to randomly generate a new set of 20 mating traces from my original, allowing for the program to select traces multiple times (resampling). I then performed the Markov modelling on the randomized set, generating my ten transition probability values (*vulva search to prodding, etc.*) for the new, randomized set of 20 mating traces. I then repeated this 1,000 times, generating a new, randomized set of 20 mating traces with each loop. This gave me a normal distribution with a mean and standard deviation representative of the variability in my data set, which I could then compare to other data sets with statistical tests. To ensure the mean and standard deviations the program made sense given my experimental results, I compared them to the transition probability values calculated with the original 20 mating traces. In every case, the calculated experimental value fell well within one standard deviation of the bootstrapped mean, even in instances where the standard deviation was relatively small, as did newly calculated means and standard deviations when the bootstrapping analysis was repeated. Below is a flow chart of how the bootstrapping analysis was conducted for the ethomic data sets (**Figure EP1**).

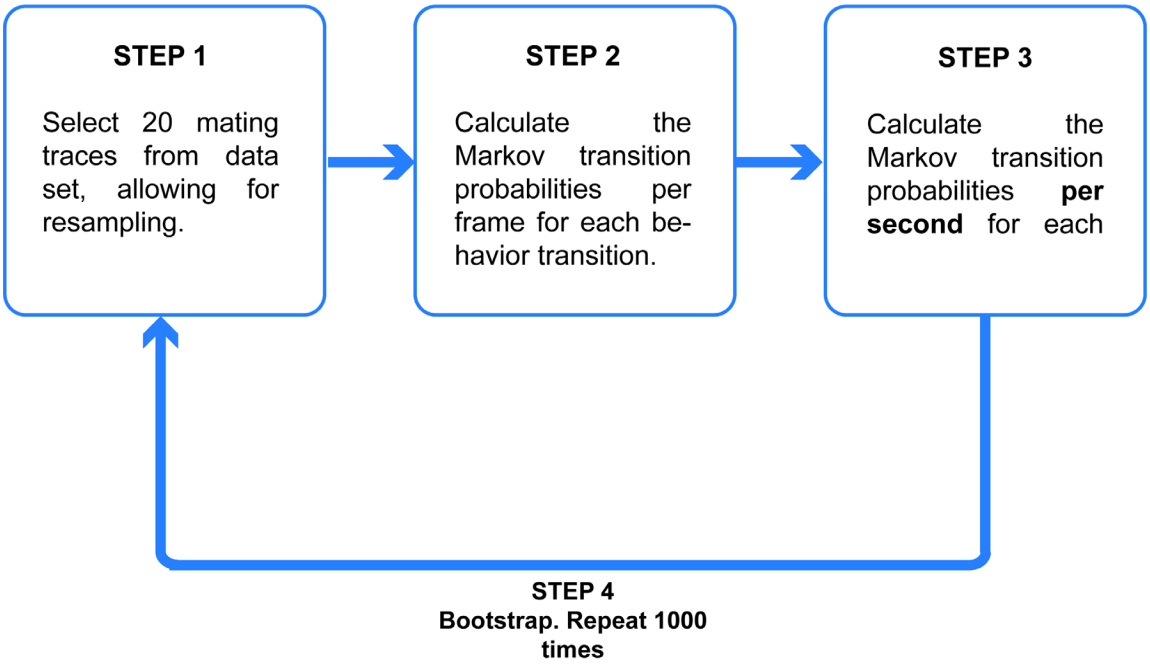

Figure E.P.1: Flow chart for steps taken to build Markov model of mating behavioral dynamics.

When comparing data sets, I wanted to not only address statistical significance, but also relative effect size. A small change in a transition probability, say from adding 10 mM of histamine to the assay plate, may be statistically significant from the control set from that day, but is not meaningful for my inquiry. The means and standard deviations calculated from the bootstrapping analysis allow me to calculate statistical significance, but do not address effect size.

To determine a meaningful effect size, I looked at the variability in the control data from all of my experimental data sets for the thesis. I had five sets of wild-type traces that I assayed in tandem with my experiments as controls. I compared the means and standard deviations of the ten transition probabilities for these five data sets. There was more variability between experiments than there was within experiments, and these means fell

Table 15: Means for transition frequencies for wild-type animals over 5 experiments.

Index	transition probability	mean #1	mean #2	mean #3	mean #4	mean #5	adj. mean	s.d.
1	vulva search to vulva search	95.07	92.94	90.19	94.18	91.36	**92.75**	**2.00**
2	vulva search to prod	2.00	6.73	4.70	5.47	5.51	**5.08**	**1.37**
3	vulva search to slip	1.73	0.34	0.30	0.35	3.13	**1.17**	**1.25**
4	prod to vulva search	0.20	0.00	0.00	0.00	0.00	**0.04**	**0.09**
5	prod to prod	95.07	92.17	94.37	91.89	93.05	**93.31**	**1.38**
6	prod to slip	4.04	7.01	2.64	7.17	5.37	**5.24**	**1.94**
7	prod to sperm transfer	0.69	0.78	1.37	1.00	0.96	**0.96**	**0.26**
8	slip to vulva search	1.70	1.09	1.14	0.54	0.00	**0.89**	**0.65**
9	slip to prod	17.29	16.62	13.15	13.88	15.10	**15.21**	**1.76**
10	slip to slip	81.01	92.29	85.46	85.71	84.05	**85.70**	**4.13**

Table 16: Means for transition frequencies for nematocin-deficient animals over 4 experiments.

Index	transition probability	mean #1	mean #2	mean #3	mean #4	adj. mean	s.d.
1	vulva search to vulva search	93.36	94.84	93.22	93.92	**93.99**	**0.66**
2	vulva search to prod	4.07	2.65	3.13	5.12	**3.74**	**1.09**
3	vulva search to slip	1.29	1.52	1.08	0.33	**1.06**	**0.52**
4	prod to vulva search	0.73	0.40	0.64	0.79	**0.64**	**0.17**
5	prod to prod	96.95	95.33	96.83	96.01	**96.28**	**0.76**
6	prod to slip	2.04	3.91	2.03	2.94	**2.73**	**0.89**
7	prod to sperm transfer	0.27	0.36	0.51	0.26	**0.35**	**0.12**
8	slip to vulva serarch	0.59	0.78	0.47	0.89	**0.68**	**0.19**
9	slip to prod	11.33	9.46	11.01	9.52	**10.33**	**0.98**
10	slip to slip	87.99	89.76	88.85	89.59	**89.05**	**0.81**

well outside the distributions of one another. Thus, I decided to take one of the more conservative approaches to my data analysis, and say by definition that I was interested in effect sizes LARGER than the experiment-to-experiment variability of my control data. I calculated means and standard deviations of the ten transition frequencies for the distribution of these five wild-type data sets (**Table 15**), and used those values to calculate p values and determine statistical significance for my data.

The same was done for the nematocin-deficient male control data sets, of which I had four sets and not five. In instances where it was appropriate to calculate the p value from the nematocin-deficient data (*e.g.* the *ntc-1* HisCl silencing experiments), I used this adjusted mean and standard deviation **Table 16**).

Table 17: Means for transition frequencies for dopamine-deficient animals.

Index	transition probability	mean #1	mean #2	mean #3	mean #4	adj. mean	s.d.
1	vulva search to vulva search	92.09	90.33	90.84	92.62	**91.47**	**1.07**
2	vulva search to prod	6.04	4.07	2.70	1.07	**3.47**	**2.11**
3	vulva search to slip	0.86	3.93	5.41	4.40	**3.65**	**1.96**
4	prod to vulva search	0.05	0.00	0.08	0.10	**0.058**	**0.043**
5	prod to prod	93.65	93.85	95.73	97.09	**95.08**	**1.64**
6	prod to slip	6.20	6.02	4.04	2.62	**4.72**	**1.71**
7	prod to sperm transfer	0.09	0.13	0.15	0.20	**0.14**	**0.05**
8	slip to vulva serarch	0.33	0.49	0.42	0.97	**0.55**	**0.29**
9	slip to prod	12.65	2.12	7.5	4.23	**6.63**	**4.59**
10	slip to slip	87.57	97.18	91.56	93.44	**92.44**	**4.00**

Finally, for the dopamine-deficient, HisCl silencing experiment, I needed a dopamine-deficient effect size. I only had two data sets of dopamine-deficient mating traces from my entire data repertoire, so I used the *cat-2*, histamine alone and *cat-2*, transgene alone data to supplement this data distribution. The approach felt justified for

two reasons. One, I was only performing this analysis on data from the HisCl silencing experiment, and two, I was also, by definition, looking for effect sizes larger than the effect of either reagent alone. This adjusted mean and standard deviation is presented in **Table 15**. **Figure EP2** shows dot plots for the distributions of means for wild-type, nematocin-deficient, and dopamine-deficient control sets.

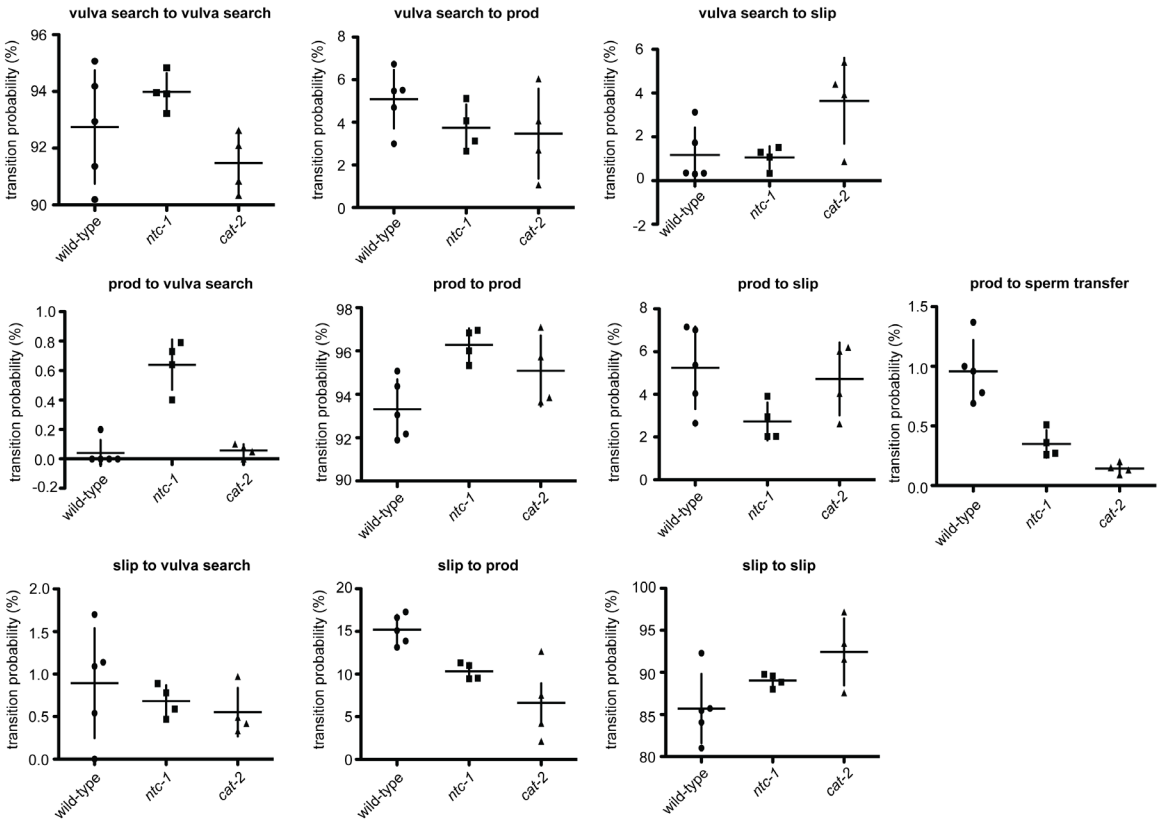

EP2: Distribution of all transition probabilities for experiment-to-experiment variability of wild-type, nematocin-deficient, and dopamine-deficient males. Horizontal lines indicate the mean of the distributions, vertical lines indicate the standard deviation. *circles* are calculated mean values from an experimental day for wild-type males, *squares* are calculated mean values from an experimental day for nematocin-deficient (*ntc-1*) males, and *triangles* are calculated mean values from an experimental day for dopamine-deficient (*cat-2*) males.

Histamine-gated chloride channel silencing of DVA

1 M histamine-dihydrochloride (Sigma-Aldrich) stock was made with M9 buffer (0.022 M KH_2PO_4, 0.042 M Na_2HPO_4, 0.086 M NaCl, 1m M $MgSO_4$), sterile filtered, and diluted into NGM agar that had cooled to 55°C at 10mM. Half of the NGM agar was reserved to pour control plates without histamine. All plates were stored at 4°C and used within one month.

In addition to the mating assay plates, "incubation plates" both with and without 10 mM histamine were seeded with 50 µL of 1 OD OP50 24 hours prior to the assay. Additional plates without histamine were seeded in the same manner at this time as "recovery plates." Males with and without an integrated DVA::HisCl_2A_mCherry transgene, blinded from the night before, were placed on the incubation plates, half the animals in the histamine free condition and half in the 10 mM histamine condition for 2 hours before beginning mating. Mating assays were conducted on plates with conditions consistent with the males' incubation plate.

Males on histamine that did not mate were placed on a recovery plate after being assayed and incubated at room temperature for two hours. These males were then re-assayed off histamine with new hermaphrodites, and their behavior was recorded.

DVA activity imaging protocol

Mating assays were prepared as previously described, selecting L4 males for strong expression of the integrated DVA::GCaMP5A transgene in the *lite-1(ce314)* genetic background and incubating them at 15°C 24 hours prior to the assay. The lawns of mating assay plates were cut out of the 5 cm plates and placed in customized mating chips made

with a 3D Printer (MakerBot Replicator Plus). When a coverslip is placed over the chip, a chamber is created on the surface of the NGM agar that stabilizes the environment for the mating animal and allows it to be imaged with epi-flourescent microscopy.

3500 frame movies of mating attempts were taken with the AIM setup (Larsch et al., 2013) under 488 nm fluorescent illumination with a 10X objective and at an exposure time of 15 ms/frame to increase the light collected. Light was pulsed at the frame rate to reduce photosensitivity and phototoxicity. 10 videos were recorded of 10 separate mating attempts of different animals for each phenotype. Control animals expressing GFP in DVA at a low level were also assayed.

DVA calcium signal tracking and analysis

Calcium imaging videos were first processed and behaviorally tracked as previously described. The videos were then uploaded into a second customized MATLAB GUI, and the DVA neuron was hand-tracked for the video, selected by the user in each frame. The program then finds the 9 brightest pixels in the frame, segments them, and averages their fluorescence to calculate a raw signal. The pixels in the selected area that surround the segmented neuron are also averaged and recorded as a local background. In frames where the neuron was obscured or not visible, no region was selected.

$\Delta F/F_{background}$ was calculated by subtracting the calculated local background at any given point from the calculated signal, and then dividing the difference by that same local background. Traces were then normalized onto a 0 to 1 scale by subtracting the 5^{th} percentile of the data as a baseline and dividing by the 98^{th} percentile to generate a $\Delta F/F_{max}$. Event triggered analysis was also conducted in MATLAB with custom scripts. Traces were

smoothed with the "smoothdata" function in MATLAB. F_0 was defined as the $\Delta F/F_{max}$ at the onset of the event being analyzed, *e.g. sperm transfer*, and $\Delta F/F_0$ was calculated as $(\Delta F/F_{max} - F_0)/F_0$. For *prod to sperm transfer*, the control data set was generated by fragmenting the ethograms into 300 ten-frame sections and randomly reassembling. The calcium imaging analysis was then conducted on the 10, randomized ethogram traces, triggering the event at random points in the calcium trace instead of moment coordinated with the behavioral event. The number of "event-triggered" traces was then pared down to equal the number of data "event-triggered" traces, so the statistics would be on equivalent data sets. All values that did not correspond to designated sub-behavior were assigned "nan." Graph window were determined by the length of time before 25% of the traces "dropped out," meaning that animal began engaging in another sub-behavior other than the designated one. Box and whiskers graphs were generated and analyzed in Prism® statistical software (https://www.graphpad.com/scientific-software/prism/).

REFERENCES

Ahier, A., Jarriault, S., 2014. Simultaneous expression of multiple proteins under a single promoter in Caenorhabditis elegans via a versatile 2A-based toolkit. Genetics 196, 605-613.

Albertin, C.B., Simakov, O., Mitros, T., Wang, Z.Y., Pungor, J.R., Edsinger-Gonzales, E., Brenner, S., Ragsdale, C.W., Rokhsar, D.S., 2015. The octopus genome and the evolution of cephalopod neural and morphological novelties. Nature 524, 220-224.

Allen, A.T., Maher, K.N., Wani, K.A., Betts, K.E., Chase, D.L., 2011. Coexpressed D1- and D2-Like Dopamine Receptors Antagonistically Modulate Acetylcholine Release in *Caenorhabditis elegans.* Genetics 188(3), 579–590.

Anderson, D.J., Perona, P., 2014. Toward a science of computational ethology. Neuron 84, 18-31.

Anderson, J.L., Morran, L.T., Phillips, P.C., 2010. Outcrossing and the maintenance of males within C. elegans populations. The Journal of heredity 101 Suppl 1, S62-74.

Aponte, Y., Atasoy, D., Sternson, S.M., 2011. AGRP neurons are sufficient to orchestrate feeding behavior rapidly and without training. Nature neuroscience 14, 351-355.

Appleby, P.A., 2012. A model of chemotaxis and associative learning in C. elegans. Biological cybernetics 106, 373-387.

Aristotle, 1970. Aristotle's Physics. Books 1 & 2. Oxford : Clarendon P., 1970.

Avery, L., Wasserman, S., 1992. Ordering gene function: the interpretation of epistasis in regulatory hierarchies. Trends in Genetics 8(9), 312-316.

Bae, Y.K., Barr, M.M., 2008. Sensory roles of neuronal cilia: cilia development, morphogenesis, and function in C. elegans. Frontiers in bioscience : a journal and virtual library 13, 5959-5974.

Bardou, I., Leprince, J., Chichery, R., Vaudry, H., Agin, V., 2010a. Vasopressin/oxytocin-related peptides influence long-term memory of a passive avoidance task in the cuttlefish, Sepia officinalis. Neurobiology of learning and memory 93, 240-247.

Bardou, I., Maubert, E., Leprince, J., Chichery, R., Cocquerelle, C., Launay, S., Vivien, D., Vaudry, H., Agin, V., 2009. Distribution of oxytocin-like and vasopressin-like immunoreactivities within the central nervous system of the cuttlefish, Sepia officinalis. Cell and tissue research 336, 249-266.

Bardou, I., Maubert, E., Leprince, J., Chichery, R., Dallerac, G., Vaudry, H., Agin, V., 2010b. Ontogeny of oxytocin-like immunoreactivity in the cuttlefish, Sepia officinalis, central nervous system. Developmental neuroscience 32, 19-32.

Bargmann, C.I., Avery, L., 1995. Laser killing of cells in Caenorhabditis elegans. Methods in cell biology 48, 225-250.

Barr, M.M., Garcia, L.R., Male mating behavior (June 19, 2006), WormBook, ed. The *C. elegans* Research Community, WormBook, doi/10.1895/wormbook.1.7.1, http://www.wormbook.org.

Barrios, A., Ghosh, R., Fang, C., Emmons, S.W., Barr, M.M., 2012. PDF-1 neuropeptide signaling modulates a neural circuit for mate-searching behavior in C. elegans. Nature neuroscience 15, 1675-1682.

Barrios, A., Nurrish, S., Emmons, S.W., 2008. Sensory regulation of C. elegans male mate-searching behavior. Current biology 18, 1865-1871.

Beaulieu, J.M., Sotnikova, T., Marion, S., Lefkowitz, R.J., Gainetdinov, R.R., Caron, M.G., 2005. An Akt/β-Arrestin 2/PP2A Signaling Complex Mediates Dopaminergic Neurotransmission and Behavior. Cell 122(2), 261-273.

Beets, I., Janssen, T., Meelkop, E., Temmerman, L., Suetens, N., Rademakers, S., Jansen, G., Schoofs, L., 2012. Vasopressin/oxytocin-related signaling regulates gustatory associative learning in C. elegans. Science 338, 543-545.

Berry, J.A., Cervantes-Sandoval, I., Nicholas, E.P., Davis, R.L., 2012. Dopamine is required for learning and forgetting in Drosophila. Neuron 74, 530-542.

Brenner, S., 1974. The genetics of Caenorhabditis elegans. Genetics 77, 71-94.

Brenner, S., 2009. In the beginning was the worm. Genetics 182, 413-415.

Cao, J., Packer, J.S., Ramani, V., Cusanovich, D.A., Huynh, C., Daza, R., Qiu, X., Lee, C., Furlan, S.N., Steemers, F.J., Adey, A., Waterston, R.H., Trapnell, C., Shendure, J., 2017. Comprehensive single-cell transcriptional profiling of a multicellular organism. Science 357, 661-667.

Chasnov, J.R., 2010. The evolution from females to hermaphrodites results in a sexual conflict over mating in androdioecious nematode worms and clam shrimp. Journal of evolutionary biology 23, 539-556.

Chelur, D.S., Chalfie, M., 2007. Targeted cell killing by reconstituted caspases. Proceedings of the National Academy of Sciences of the United States of America 104, 2283-2288.

Christ-Crain, M., Fenske, W., 2016. Copeptin in the diagnosis of vasopressin-dependent disorders of fluid homeostasis. Nature reviews endocrinology 12, 168-176.

Colaianni, G., Sun, L., Zaidi, M., Zallone, A., 2014a. Oxytocin and bone. American journal of physiology. Regulatory, integrative and comparative physiology 307, R970-977.

Colaianni, G., Tamma, R., Di Benedetto, A., Yuen, T., Sun, L., Zaidi, M., Zallone, A., 2014b. The oxytocin-bone axis. Journal of neuroendocrinology 26, 53-57.

Cooper, S., Robison, A.J., Mazei-Robison, M.S., 2017. Reward Circuitry in Addiction. Neurotherapeutics 14(3), 687-697.

Coria-Avila, G.A., Manzo, J., Garcia, L.I., Carrillo, P., Miquel, M., Pfaus, J.G., 2014. Neurobiology of social attachments. Neuroscience and biobehavioral reviews 43C, 173-182.

Correa, P., LeBoeuf, B., Garcia, L.R., 2012. C. elegans dopaminergic D2-like receptors delimit recurrent cholinergic-mediated motor programs during a goal-oriented behavior. PLoS genetics 8, e1003015.

Correa, P.A., Gruninger, T., Garcia, L.R., 2015. DOP-2 D2-Like Receptor Regulates UNC-7 Innexins to Attenuate Recurrent Sensory Motor Neurons during C. elegans Copulation. The Journal of neuroscience : the official journal of the Society for Neuroscience 35, 9990-10004.

Costa, W.S., Yu, S., Liewald, J.F., Gottshalk, A., 2017 Fast cAMP Modulation of Neurotransmission via Neuropeptide Signals and Vesicle Loading. Current Biology, CB: 27(4), 495-507.

D'Souza, T.G., Michiels, N.K., 2008. Correlations between sex rate estimates and fitness across predominantly parthenogenetic flatworm populations. Journal of evolutionary biology 21, 276-286.

Darwin, C., 1871. On the origin of species. New York: D. Appleton and Co., 1871.

De Boer, P.A., Ter Maat, A., Pieneman, A.W., Croll, R.P., Kurokawa, M., Jansen, R.F., 1997. Functional role of peptidergic anterior lobe neurons in male sexual behavior of the snail Lymnaea stagnalis. Journal of neurophysiology 78, 2823-2833.

De Bree, F.M., 2000. Trafficking of the vasopressin and oxytocin prohormone through the regulated secretory pathway. Journal of neuroendocrinology 12, 589-594.

De Lange, R.P., Joosse, J., Van Minnen, J., 1998. Multi-messenger innervation of the male sexual system of Lymnaea stagnalis. The Journal of comparative neurology 390, 564-577.

Di Benedetto, A., Sun, L., Zambonin, C.G., Tamma, R., Nico, B., Calvano, C.D., Colaianni, G., Ji, Y., Mori, G., Grano, M., Lu, P., Colucci, S., Yuen, T., New, M.I., Zallone, A., Zaidi, M., 2014. Osteoblast regulation via ligand-activated nuclear trafficking of the oxytocin receptor. Proceedings of the National Academy of Sciences of the United States of America 111, 16502-16507.

Dickel, L., Chichery, M.P., Chichery, R., 2001. Increase of learning abilities and maturation of the vertical lobe complex during postembryonic development in the cuttlefish, Sepia. Developmental psychobiology 39, 92-98.

Donaldson, Z.R., Young, L.J., 2008. Oxytocin, vasopressin, and the neurogenetics of sociality. Science 322, 900-904.

Dong, N., Lee, D.W.K., Sun, H., Feng, Z., 2018. Dopamine-mediated calcium channel regulation in synaptic suppression in L. stagnalis interneurons. Channels 12(1), 153-173.

Dulac, C., O'Connell, L.A., Wu, Z., 2014. Neural control of maternal and paternal behaviors. Science 345, 765-770.

Dutertre, S., Croker, D., Daly, N.L., Andersson, A., Muttenthaler, M., Lumsden, N.G., Craik, D.J., Alewood, P.F., Guillon, G., Lewis, R.J., 2008. Conopressin-T from Conus tulipa reveals an antagonist switch in vasopressin-like peptides. The Journal of biological chemistry 283, 7100-7108.

Egekwu, N., Sonenshine, D.E., Bissinger, B.W., Roe, R.M., 2014. Transcriptome of the female synganglion of the black-legged tick Ixodes scapularis (Acari: Ixodidae) with comparison between Illumina and 454 systems. PloS one 9, e102667.

Ellis, R., Schedl, T., Sex determination in the germ line (January 30, 2007), WormBook, ed. The *C. elegans* Research Community, WormBook, doi/10.1895/wormbook.1.7.1, http://www.wormbook.org.

Elphick, M.R., 2012. The protein precursors of peptides that affect the mechanics of connective tissue and/or muscle in the echinoderm Apostichopus japonicus. PloS one 7, e44492.

Elphick, M.R., Rowe, M.L., 2009. NGFFFamide and echinotocin: structurally unrelated myoactive neuropeptides derived from neurophysin-containing precursors in sea urchins. The Journal of experimental biology 212, 1067-1077.

Emmons, S.W., Lipton, J., 2003. Genetic basis of male sexual behavior. Journal of neurobiology 54, 93-110.

Fitch, D.H.A., Introduction to nematode evolution and ecology (August 31, 2005), WormBook, ed. The *C. elegans* Research Community, WormBook, doi/10.1895/wormbook.1.19.1, http://www.wormbook.org.

Flavell, S.W., Pokala, N., Macosko, E.Z., Albrecht, D.R., Larsch, J., Bargmann, C.I., 2013. Serotonin and the neuropeptide PDF initiate and extend opposing behavioral states in C. elegans. Cell 154, 1023-1035.

Fujino, Y., Nagahama, T., Oumi, T., Ukena, K., Morishita, F., Furukawa, Y., Matsushima, O., Ando, M., Takahama, H., Satake, H., Minakata, H., Nomoto, K., 1999. Possible functions of oxytocin/vasopressin-superfamily peptides in annelids with special reference to reproduction and osmoregulation. The Journal of experimental zoology 284, 401-406.

Garcia, L.R., LeBoeuf, B., Koo, P., 2007. Diversity in mating behavior of hermaphroditic and male-female Caenorhabditis nematodes. Genetics 175, 1761-1771.

Garcia, L.R., Portman, D.S., 2016. Neural circuits for sexually dimorphic and sexually divergent behaviors in Caenorhabditis elegans. Current opinion in neurobiology 38, 46-52.

Garrison, J.L., Macosko, E.Z., Bernstein, S., Pokala, N., Albrecht, D.R., Bargmann, C.I., 2012. Oxytocin/vasopressin-related peptides have an ancient role in reproductive behavior. Science 338, 540-543.

Gladyshev, E.A., Arkhipova, I.R., 2010. Genome structure of bdelloid rotifers: shaped by asexuality or desiccation? The Journal of heredity 101 Suppl 1, S85-93.

Godwin, J., Thompson, R., 2012. Nonapeptides and social behavior in fishes. Hormones and behavior 61, 230-238.

Gruber, C.W., 2014. Physiology of invertebrate oxytocin and vasopressin neuropeptides. Experimental physiology 99, 55-61.

Gruber, C.W., Muttenthaler, M., 2012. Discovery of defense- and neuropeptides in social ants by genome-mining. PloS one 7, e32559.

Guo, J.F., Zhang, L., Li, K., Mei, J.P., Xue, J., Chen, J., Tang, X., Shen, L., Jiang, H., Chen, C., Guo, H., Wu, X.L., Sun, S.L., Xu, Q., Sun, Q.Y., Chan, P., Shang, H.F., Wang, T., Zhao, G.H., Liu, J.Y., Xie, X.F., Jiang, Y.Q., Liu, Z.H., Zhao, Y.W., Zhu, Z.B., Li, J.D., Hu, Z.M., Yan, X.X., Fang, X.D., Wang, G.H., Zhang, F.Y., Xia, K., Liu, C.Y., Zhu, X.W., Yue, Z.Y., Li, S.C., Cai, H.B., Zhang, Z.H., Duan, R.H., Tang, B.S., 2018. Coding mutations in NUS1 contribute to Parkinson's disease. Proceedings of the National Academy of Sciences of the United States of America. 115(45) 11567-11572.

Gwee, P.C., Tay, B.H., Brenner, S., Venkatesh, B., 2009. Characterization of the neurohypophysial hormone gene loci in elephant shark and the Japanese lamprey: origin of the vertebrate neurohypophysial hormone genes. BMC evolutionary biology 9, 47.

Haag, E. S. The evolution of nematode sex determination: *C. elegans* as a reference point for comparative biology (December 29, 2005), WormBook, ed. The *C. elegans* Research Community, WormBook, doi/10.1895/wormbook.1.120.1, http://www.wormbook.org.

Han, B., Dong, Y., Zhang, L., Liu, Y., Rabinowitch, I., Bai, J., 2017. Dopamine signaling tunes spatial pattern selectivity in C. elegans. eLife 6, e22896.

Harris, G., Mills, H., Wragg, R., Hapiak, V., Castelletto, M., Korchnak, A., Komuniecki, R.W., 2010. The monoaminergic modulation of sensory-mediated aversive responses in Caenorhabditis elegans requires glutamatergic/peptidergic cotransmission. The Journal of neuroscience : the official journal of the Society for Neuroscience 30, 7889-7899.

Henry, J., Cornet, V., Bernay, B., Zatylny-Gaudin, C., 2013. Identification and expression of two oxytocin/vasopressin-related peptides in the cuttlefish Sepia officinalis. Peptides 46, 159-166.

Herberstein, M.E., Wignall, A.E., Hebets, E.A., Schneider, J.M., 2014. Dangerous mating systems: signal complexity, signal content and neural capacity in spiders. Neuroscience and biobehavioral reviews 46 Pt 4, 509-518.

Hille, B., 1994. Modulation of ion-channel function by G-protein-coupled receptors. Trends in neurosciences 17, 531-536.

Hochner, B., 2010. Functional and comparative assessments of the octopus learning and memory system. Frontiers in bioscience (Scholar edition) 2, 764-771.

Hodgkin, A.L., Huxley, A.F., 1990. A quantitative description of membrane current and its application to conduction and excitation in nerve. 1952. Bulletin of mathematical biology 52, 25-71.

Hu, Z., Pym, E.C., Babu, K., Vashlishan Murray, A.B., Kaplan, J.M., 2011. A neuropeptide-mediated stretch response links muscle contraction to changes in neurotransmitter release. Neuron 71, 92-102.

Hudson, A.E., 2018. Genetic Reporters of Neuronal Activity: c-Fos and G-CaMP6. Methods in enzymology 603, 197-220.

Huffman, L.S., Hinz, F.I., Wojcik, S., Aubin-Horth, N., Hofmann, H.A., 2015. Arginine vasotocin regulates social ascent in the African cichlid fish Astatotilapia burtoni. General and comparative endocrinology 212, 106-113.

Hums, I., Riedl, J., Mende, F., Kato, S., Kaplan, H.S., Latham, R., Sonntag, M., Traunmuller, L., Zimmer, M., 2016. Regulation of two motor patterns enables the gradual adjustment of locomotion strategy in Caenorhabditis elegans. eLife 5, e14116.

Husson, S.J., Gottschalk, A., Leifer, A.M., 2013. Optogenetic manipulation of neural activity in C. elegans: From synapse to circuits and behaviour. Biology of the cell / under the auspices of the European Cell Biology Organization. 105(6), 235-50

Insel, T.R., Winslow, J.T., Wang, Z., Young, L.J., 1998. Oxytocin, vasopressin, and the neuroendocrine basis of pair bond formation. Advances in experimental medicine and biology 449, 215-224.

Jang, H., Kim, K., Neal, S.J., Macosko, E., Kim, D., Butcher, R.A., Zeiger, D.M., Bargmann, C.I., Sengupta, P., 2012. Neuromodulatory state and sex specify alternative behaviors through antagonistic synaptic pathways in C. elegans. Neuron 75, 585-592.

Jarrell, T.A., Wang, Y., Bloniarz, A.E., Brittin, C.A., Xu, M., Thomson, J.N., Albertson, D.G., Hall, D.H., Emmons, S.W., 2012. The connectome of a decision-making neural network. Science 337, 437-444.

Jing, J., Sweedler, J.V., Cropper, E.C., Alexeeva, V., Park, J.-H., Romanova, E.V., Xie, F., Dembrow, N.C., Ludwar, B.C., Weiss, K.R., Vilim, F.S., 2010. Feedforward compensation mediated by the central and peripheral actions of a single neuropeptide discovered using representational difference analysis. The Journal of Neuroscience 30, 16545-16558.

Kabelik, D., Magruder, D.S., 2014. Involvement of different mesotocin (oxytocin homologue) populations in sexual and aggressive behaviours of the brown anole. Biology letters 10(8), 20140566. http://dx.doi.org/10.1098/rsbl.2014.0566

Johnson, Z.V., Young, L.J., 2015. Neurobiological mechanisms of social attachment and pair bonding. Current opinion in behavioral sciences 3, 38-44.

Kanda, A., Satake, H., Kawada, T., Minakata, H., 2005. Novel evolutionary lineages of the invertebrate oxytocin/vasopressin superfamily peptides and their receptors in the common octopus (Octopus vulgaris). The Biochemical journal 387, 85-91.

Kanda, A., Takuwa-Kuroda, K., Iwakoshi-Ukena, E., Furukawa, Y., Matsushima, O., Minakata, H., 2003. Cloning of Octopus cephalotocin receptor, a member of the oxytocin/vasopressin superfamily. The Journal of endocrinology 179, 281-291.

Kawada, T., Sekiguchi, T., Itoh, Y., Ogasawara, M., Satake, H., 2008. Characterization of a novel vasopressin/oxytocin superfamily peptide and its receptor from an ascidian, Ciona intestinalis. Peptides 29, 1672-1678.

Kawazu, I., Kino, M., Maeda, K., Yamaguchi, Y., Sawamukai, Y., 2014. Induction of oviposition by the administration of oxytocin in hawksbill turtles. Zoological science 31, 831-835.

Kelly, A.M., Goodson, J.L., 2014. Hypothalamic oxytocin and vasopressin neurons exert sex-specific effects on pair bonding, gregariousness, and aggression in finches. Proceedings of the National Academy of Sciences of the United States of America 111, 6069-6074.

Kim, J., Inoue, K., Ishii, J., Vanti, W.B., Voronov, S.V., Murchison, E., Hannon, G., Abeliovich, A., 2007. A MicroRNA feedback circuit in midbrain dopamine neurons. Science 317, 1220-1224.

Knobel, K.M., Peden, E.M., Barr, M.M., 2008. Distinct protein domains regulate ciliary targeting and function of C. elegans PKD-2. Experimental cell research 314, 825-833.

Koene, J.M., 2010. Neuro-Endocrine control of reproduction in hermaphroditic freshwater snails: mechanisms and evolution. Frontiers in behavioral neuroscience 4, 167.

Konopka, R.J., Benzer, S., 1971. Clock mutants of Drosophila melanogaster. Proceedings of the National Academy of Sciences of the United States of America 68, 2112-2116.

Larsch, J., Ventimiglia, D., Bargmann, C.I., Albrecht, D.R., 2013. High-throughput imaging of neuronal activity in Caenorhabditis elegans. Proceedings of the National Academy of Sciences of the United States of America 110, E4266-4273.

Lazaro, E.M., Harrath, A.H., Stocchino, G.A., Pala, M., Baguna, J., Riutort, M., 2011. Schmidtea mediterranea phylogeography: an old species surviving on a few Mediterranean islands? BMC evolutionary biology 11, 274.

LeBoeuf, B., Correa, P., Jee, C., Garcia, L.R., 2014. Caenorhabditis elegans male sensory-motor neurons and dopaminergic support cells couple ejaculation and post-ejaculatory behaviors. eLife 3, e02938.

Leypold, B.G., Yu, C.R., Leinders-Zufall, T., Kim, M.M., Zufall, F., Axel, R., 2002. Altered sexual and social behaviors in trp2 mutant mice. Proceedings of the National Academy of Sciences of the United States of America 99, 6376-6381.

Li, W., Feng, Z., Sternberg, P.W., Xu, X.Z., 2006. A C. elegans stretch receptor neuron revealed by a mechanosensitive TRP channel homologue. Nature 440, 684-687.

Lints, R., Jia, L., Kim, K., Li, C., Emmons, S.W., 2004. Axial patterning of C. elegans male sensilla identities by selector genes. Developmental biology 269, 137-151.

Lipton, J., Kleemann, G., Ghosh, R., Lints, R., Emmons, S.W., 2004. Mate searching in Caenorhabditis elegans: a genetic model for sex drive in a simple invertebrate. The Journal of neuroscience : the official journal of the Society for Neuroscience 24, 7427-7434.

Liu, J., Ward, A., Gao, J., Dong, Y., Nishio, N., Inada, H., Kang, L., Yu, Y., Ma, D., Xu, T., Mori, I., Xie, Z., Xu, X.Z., 2010. C. elegans phototransduction requires a G protein-dependent cGMP pathway and a taste receptor homolog. Nature neuroscience 13, 715-722.

Liu, K.S., Sternberg, P.W., 1995. Sensory regulation of male mating behavior in Caenorhabditis elegans. Neuron 14, 79-89.

Liu, T., Kim, K., Li, C., Barr, M.M., 2007. FMRFamide-like neuropeptides and mechanosensory touch receptor neurons regulate male sexual turning behavior in Caenorhabditis elegans. The Journal of neuroscience : the official journal of the Society for Neuroscience 27, 7174-7182.

Liu, Y., LeBeouf, B., Guo, X., Correa, P.A., Gualberto, D.G., Lints, R., Garcia, L.R., 2011. A cholinergic-regulated circuit coordinates the maintenance and bi-stable states of a sensory-motor behavior during Caenorhabditis elegans male copulation. PLoS genetics 7, e1001326.

Loer, C., Kenyon, C., 1993. Serotonin-deficient mutants and male mating behavior in the nematode Caenorhabditis elegans. The Journal of neuroscience : the official journal of the Society for Neuroscience 13 12, 5407-5417.

Lowenstein, E.G., Velazquez-Ulloa, N.A., 2018. A fly's eye view of natural and drug reward. Frontiers in physiology 9, 407.

Luo, Y.J., Takeuchi, T., Koyanagi, R., Yamada, L., Kanda, M., Khalturina, M., Fujie, M., Yamasaki, S., Endo, K., Satoh, N., 2015. The Lingula genome provides insights into brachiopod evolution and the origin of phosphate biomineralization. Nature communications 6, 8301.

Markert, M., Garcia, L.R., 2013. Virgin Caenorhabditis remanei females are attracted to a coital pheromone released by con-specific copulating males. Worm 2, e24448.

Marlin, B.J., Mitre, M., D'Amour J, A., Chao, M.V., Froemke, R.C., 2015. Oxytocin enables maternal behaviour by balancing cortical inhibition. Nature 520, 499-504.

Martinez-Padron, M., Gray, W.R., Lukowiak, K., 1992. Conopressin G, a molluscan vasopressin-like peptide, alters gill behaviors in Aplysia. Canadian journal of physiology and pharmacology 70, 259-267.

Melis, M.R., Argiolas, A., 2011. Central control of penile erection: a re-visitation of the role of oxytocin and its interaction with dopamine and glutamic acid in male rats. Neuroscience and biobehavioral reviews 35, 939-955.

Mello, C., Fire, A., 1995. DNA transformation. Methods in cell biology 48, 451-482.

Montejo, A.L., Llorca, G., Izquierdo, J.A., Rico-Villademoros, F., 2001. Incidence of sexual dysfunction associated with antidepressant agents: a prospective multicenter study of 1022 outpatients. Spanish Working Group for the Study of Psychotropic-Related Sexual Dysfunction. The Journal of clinical psychiatry 62 Suppl 3, 10-21.

Morran, L.T., Cappy, B.J., Anderson, J.L., Phillips, P.C., 2009. Sexual partners for the stressed: facultative outcrossing in the self-fertilizing nematode Caenorhabditis elegans. Evolution; international journal of organic evolution 63, 1473-1482.

Nadim, F., Bucher, D., 2014. Neuromodulation of neurons and synapses. Current opinion in neurobiology 29, 48-56.

Neve, K.A., Seamans, J.K.,Trantham-Davidson, H., 2004. Dopamine Receptor Signaling. Journal of receptor and signal transduction research 24(3), 165-205.

Nossa, C.W., Havlak, P., Yue, J.X., Lv, J., Vincent, K.Y., Brockmann, H.J., Putnam, N.H., 2014. Joint assembly and genetic mapping of the Atlantic horseshoe crab genome reveals ancient whole genome duplication. GigaScience 3, 9.

Nguyen, C.Q., Hall, D.H., Yang, Y., Fitch, D.H., 1999. Morphogenesis of the Caenorhabditis elegans male tail tip. Developmental biology 207, 86-106.

Oettl, L.L., Ravi, N., Schneider, M., Scheller, M.F., Schneider, P., Mitre, M., da Silva Gouveia, M., Froemke, R.C., Chao, M.V., Young, W.S., Meyer-Lindenberg, A., Grinevich, V., Shusterman, R., Kelsch, W., 2016. Oxytocin Enhances Social Recognition by Modulating Cortical Control of Early Olfactory Processing. Neuron 90, 609-621.

Oranth, A., Schultheis, C., Tolstenkov, O., Erbguth, K., Nagpal, J., Hain, D., Brauner, M., Wabnig, S., Steuer Costa, W., McWhirter, R.D., Zels, S., Palumbos, S., Miller Iii, D.M., Beets, I., Gottschalk, A., 2018. Food Sensation Modulates Locomotion by Dopamine and Neuropeptide Signaling in a Distributed Neuronal Network. Neuron S0896-6273(18)30912-7, doi: 10.1016/j.neuron.2018.10.024. Epub. ahead of print.

Oumi, T., Ukena, K., Matsushima, O., Ikeda, T., Fujita, T., Minakata, H., Nomoto, K., 1996. Annetocin, an annelid oxytocin-related peptide, induces egg-laying behavior in the earthworm, Eisenia foetida. The Journal of experimental zoology 276, 151-156.

Pereira, L., Kratsios, P., Serrano-Saiz, E., Sheftel, H., Mayo, A.E., Hall, D.H., White, J.G., LeBoeuf, B., Garcia, L.R., Alon, U., Hobert, O., 2015. A cellular and regulatory map of the cholinergic nervous system of C. elegans. eLife 4, e12432.

Pisani, A., Bernardi, G., Ding, J., Surmeier, D.J., 2007. Re-emergence of striatal cholinergic interneurons in movement disorders. Trends in neurosciences 30, 545-553.

Pokala, N., Liu, Q., Gordus, A., Bargmann, C.I., 2014. Inducible and titratable silencing of Caenorhabditis elegans neurons in vivo with histamine-gated chloride channels. Proceedings of the National Academy of Sciences of the United States of America 111, 2770-2775.

Proux, J.P., Miller, C.A., Li, J.P., Carney, R.L., Girardie, A., Delaage, M., Schooley, D.A., 1987. Identification of an arginine vasopressin-like diuretic hormone from Locusta migratoria. Biochemical and biophysical research communications 149, 180-186.

Ragnauth, A.K., Goodwillie, A., Brewer, C., Muglia, L.J., Pfaff, D.W., Kow, L.M., 2004. Vasopressin stimulates ventromedial hypothalamic neurons via oxytocin receptors in oxytocin gene knockout male and female mice. Neuroendocrinology 80, 92-99.

Riddiford, N., Olson, P.D., 2011. Wnt gene loss in flatworms. Development genes and evolution 221, 187-197.

Rizzi, G., Tan, K.R., 2017. Dopamine andAcetylcholine, a Circuit Point of View in Parkinson's Disease. Frontiers in Neural Circuits. 11(110), eCollection 2017.

Sanggaard, K.W., Bechsgaard, J.S., Fang, X., Duan, J., Dyrlund, T.F., Gupta, V., Jiang, X., Cheng, L., Fan, D., Feng, Y., Han, L., Huang, Z., Wu, Z., Liao, L., Settepani, V., Thogersen, I.B., Vanthournout, B., Wang, T., Zhu, Y., Funch, P., Enghild, J.J., Schauser, L., Andersen, S.U., Villesen, P., Schierup, M.H., Bilde, T., Wang, J., 2014. Spider genomes provide insight into composition and evolution of venom and silk. Nature communications 5, 3765.

Sarnyai, Z., Kovacs, G.L., 2014. Oxytocin in learning and addiction: From early discoveries to the present. Pharmacology, biochemistry, and behavior 119, 3-9.

Scott, E., Hudson, A., Feist, E., Calahorro, F., Dillon, J., de Freitas, R., Wand, M., Schoofs, L., O'Connor, V., Holden-Dye, L., 2017. An oxytocin-dependent social interaction between larvae and adult C. elegans. Scientific reports 7, 10122.

Searcy, B.T., Bradford, C.S., Thompson, R.R., Filtz, T.M., Moore, F.L., 2011. Identification and characterization of mesotocin and V1a-like vasotocin receptors in a urodele amphibian, Taricha granulosa. General and comparative endocrinology 170, 131-143.

Semmens, D.C., Beets, I., Rowe, M.L., Blowes, L.M., Oliveri, P., Elphick, M.R., 2015. Discovery of sea urchin NGFFFamide receptor unites a bilaterian neuropeptide family. Open biology 5, 150030.

Semmens, D.C., Mirabeau, O., Moghul, I., Pancholi, M.R., Wurm, Y., Elphick, M.R., 2016. Transcriptomic identification of starfish neuropeptide precursors yields new insights into neuropeptide evolution. Open biology 6, 150224.

Senior, A.M., Nat Lim, J., Nakagawa, S., 2012. The fitness consequences of environmental sex reversal in fish: a quantitative review. Biological reviews of the Cambridge Philosophical Society 87, 900-911.

Serrano-Saiz, E., Oren-Suissa, M., Bayer, E.A., Hobert, O., 2017a. Sexually Dimorphic Differentiation of a C. elegans Hub Neuron Is Cell Autonomously Controlled by a Conserved Transcription Factor. Current Biology 27, 199-209.

Serrano-Saiz, E., Pereira, L., Gendrel, M., Aghayeva, U., Bhattacharya, A., Howell, K., Garcia, L.R., Hobert, O., 2017b. A Neurotransmitter Atlas of the Caenorhabditis elegans Male Nervous System Reveals Sexually Dimorphic Neurotransmitter Usage. Genetics 206, 1251-1269.

Sulston, J.E., Albertson, D.G., Thomson, J.N., 1980. The Caenorhabditis elegans male: postembryonic development of nongonadal structures. Developmental biology 78, 542-576.

Shawn Xu, X.Z., Barr, M.M., 2007. TRP Channel Functioning in Mating and Fertilization
TRP Ion Channel Function in Sensory Transduction and Cellular Signaling Cascades. Taylor & Francis Group, LLC.,: Boca Raton FL. 2007.

Smith, C.J., Wilkins, K.B., Mogavero, J.N., Veenema, A.H., 2015. Social Novelty Investigation in the Juvenile Rat: Modulation by the mu-Opioid System. Journal of neuroendocrinology 27, 752-764.

Sofroniew, M.V., 1983. Morphology of vasopressin and oxytocin neurones and their central and vascular projections. Progress in brain research 60, 101-114.

Stafflinger, E., Hansen, K.K., Hauser, F., Schneider, M., Cazzamali, G., Williamson, M., Grimmelikhuijzen, C.J., 2008. Cloning and identification of an oxytocin/vasopressin-like receptor and its ligand from insects. Proceedings of the National Academy of Sciences of the United States of America 105, 3262-3267.

Stelzer, C.-P., Schmidt, J., Wiedlroither, A., Riss, S., 2010. Loss of Sexual Reproduction and Dwarfing in a Small Metazoan. PloS one 5, e12854.

Stoop, R., 2014. Neuromodulation by oxytocin and vasopressin in the central nervous system as a basis for their rapid behavioral effects. Current opinion in neurobiology 29, 187-193.

Sun, L., Tamma, R., Yuen, T., Colaianni, G., Ji, Y., Cuscito, C., Bailey, J., Dhawan, S., Lu, P., Calvano, C.D., Zhu, L.-L., Zambonin, C.G., Di Benedetto, A., Stachnik, A., Liu,

P., Grano, M., Colucci, S., Davies, T.F., New, M.I., Zallone, A., Zaidi, M., 2016. Functions of vasopressin and oxytocin in bone mass regulation. Proceedings of the National Academy of Sciences of the United States of America 113, 164-169.

Suo, S., Ishiura, S., Van Tol, H.H., 2004. Dopamine receptors in C. elegans. European journal of pharmacology 500, 159-166.

Suo, S., Sasagawa, N., Ishiura, S., 2003. Cloning and characterization of a Caenorhabditis elegans D2-like dopamine receptor. Journal of neurochemistry 86, 869-878.

Takuwa-Kuroda, K., Iwakoshi-Ukena, E., Kanda, A., Minakata, H., 2003. Octopus, which owns the most advanced brain in invertebrates, has two members of vasopressin/oxytocin superfamily as in vertebrates. Regulatory peptides 115, 139-149.

Ter Maat, A., 1992. Egg laying in the hermaphrodite pond snail Lymnaea stagnalis. Progress in brain research 92, 345-360.

Tinbergen, N., 1951. The study of instinct. Clarendon Press, Oxford [Eng.]. 1951.

Tritsch, N.X., Sabatini, B.L., 2012. Dopaminergic modulation of synaptic transmission in cortex and striatum. Neuron 76, 33-50.

Van Golen, F.A., Li, K.W., De Lange, R.P., Van Kesteren, R.E., Van Der Schors, R.C., Geraerts, W.P., 1995. Co-localized neuropeptides conopressin and ALA-PRO-GLY-TRP-NH2 have antagonistic effects on the vas deferens of Lymnaea. Neuroscience 69, 1275-1287.

Van Kesteren, R.E., Smit, A.B., De Lange, R.P., Kits, K.S., Van Golen, F.A., Van Der Schors, R.C., De With, N.D., Burke, J.F., Geraerts, W.P., 1995a. Structural and functional evolution of the vasopressin/oxytocin superfamily: vasopressin-related conopressin is the only member present in Lymnaea, and is involved in the control of sexual behavior. The Journal of neuroscience : the official journal of the Society for Neuroscience 15, 5989-5998.

Van Kesteren, R.E., Tensen, C.P., Smit, A.B., van Minnen, J., van Soest, P.F., Kits, K.S., Meyerhof, W., Richter, D., van Heerikhuizen, H., Vreugdenhil, E., et al., 1995b. A novel G protein-coupled receptor mediating both vasopressin- and oxytocin-like functions of Lys-conopressin in Lymnaea stagnalis. Neuron 15, 897-908.

Van Soest, P.F., Lodder, J.C., Kits, K.S., 2000. Activation of protein kinase C by oxytocin-related conopressin underlies pacemaker current in Lymnaea central neurons. Journal of neurophysiology 84, 2541-2551.

Von Boletzky, S., 2003. Biology of early life stages in cephalopod molluscs. Advances in marine biology 44, 143-203.

Von de Wall, W., 1963. Bewegungsstudien an Anatiden. Journal of Ornithology 104, 1-14.

Wagenaar, D.A., Hamilton, M.S., Huang, T., Kristan, W.B., French, K.A., 2010. A hormone-activated central pattern generator for courtship. Current biology : CB 20, 487-495.

Waldherr, M., Neumann, I.D., 2007. Centrally released oxytocin mediated mating-induced anxiolysis in male rats. Proceedings of the National Academy of Sciences. 104(42) 16681-4.

Wang, Z.X., Liu, Y., Young, L.J., Insel, T.R., 2000. Hypothalamic vasopressin gene expression increases in both males and females postpartum in a biparental rodent. Journal of neuroendocrinology 12, 111-120.

White, J.G., Southgate, E., Thomson, J.N., Brenner, S., 1986. The structure of the nervous system of the nematode Caenorhabditis elegans. Philosophical transactions of the Royal Society of London. Series B, Biological sciences 314, 1-340.

Whitfield, P.J., Evans, N.A., 1983. Parthenogenesis and asexual multiplication among parasitic platyhelminths. Parasitology 86 (Pt 4), 121-160.

Wilson, E.O., Holldobler, B., 2005. Eusociality: origin and consequences. Proceedings of the National Academy of Sciences of the United States of America 102, 13367-13371.

Winslow, J.T., Hastings, N., Carter, C.S., Harbaugh, C.R., Insel, T.R., 1993. A role for central vasopressin in pair bonding in monogamous prairie voles. Nature 365, 545-548.

Xu, S., 2015. The Application of CRISPR-Cas9 Genome Editing in Caenorhabditis elegans. Journal of genetics and genomics 42, 413-421.

Yamamoto, D., Koganezawa, M., 2013. Genes and circuits of courtship behaviour in Drosophila males. Nature reviews. Neuroscience 14, 681-692.

Yizhar, O., Fenno, L.E., Davidson, T.J., Mogri, M., Deisseroth, K., 2011. Optogenetics in neural systems. Neuron 71, 9-34.

Yoshida, M., Takayanagi, Y., Inoue, K., Kimura, T.,Young, L.J., Onaka, T., Nishimori, K., 2009. Evidence that oxytocin exerts its anaxiolytic effects via oxytocin receptor expressed in serotonergic neurons in mice. Journal of Neuroscience 29(7), 2259-71.

Young, W.S., 3rd, Gainer, H., 2003. Transgenesis and the study of expression, cellular targeting and function of oxytocin, vasopressin and their receptors. Neuroendocrinology 78, 185-203.

Zarrella, I., Ponte, G., Baldascino, E., Fiorito, G., 2015. Learning and memory in Octopus vulgaris: a case of biological plasticity. Current opinion in neurobiology 35, 74-79.

Zhang, S.X., Miner, L.E., Boutros, C.L., Rogulja, D., Crickmore, M.A., 2018. Motivation, Perception, and Chance Converge to Make a Binary Decision. Neuron 99, 376-388 e376.

Zitnan, D., Kingan, T.G., Hermesman, J.L., Adams, M.E., 1996. Identification of ecdysis-triggering hormone from an epitracheal endocrine system. Science 271, 88-91.